Chapter 2
Attempts to Improve Axonal Pathfinding and Quality of Target Reinnervation

Numerous experiments were grouped into three major sets.

In the first major set, we report our attempts to improve axonal pathfinding by reduction of collateral axonal branching at the lesion site by means of (1) local trophic factor neutralization or (2) application of established pharmacological agents to perturb microtubule assembly.

In the second major set, we describe several experiments in which we tried to reduce intramuscular axonal sprouting in denervated muscles by (1) modification of microtubule dynamics, (2) intraoperative electrical stimulation (IOES) of the transected facial nerve before its surgical reconstruction, (3) postoperative electrical stimulation (POES) of denervated vibrissal muscles, (4) manual mechanical stimulation of denervated vibrissal muscles after varying facial nerve reconstruction strategies, (5) manual mechanical stimulation of denervated orbicularis oculi muscle (OOM), (6) manual mechanical stimulation of denervated tongue muscles, and (7) manual mechanical stimulation of denervated forearm muscles.

In the third major set, we summarize the results from experiments in which we tried to reveal the mechanism of action of the manual mechanical stimulation by means of experiments with permanent abolishment of the trigeminal afferents from the whisker pad. Before and after the experiments, all animals were kept on standard laboratory food (Altromin, 32791 Lage, Germany) and tap water ad libitum with an artificial light–dark cycle of 12 h light on, 12 h off. We used female young adult (175–200 g) Wistar rats (strain HsdCpb:WU, Harlan-Winkelmann, Borchen, Germany), because testosterone has been shown to beneficially affect peripheral nerve regeneration (Yu and Yu 1983).

All experiments were conducted in accordance with the "German Law for Animals Protection" and were approved by the local animal care committee (Bezirksregierung Köln).

For a given parameter, data from all relevant experimental groups were tested in one-way analysis of variance (one-way ANOVA) procedure for overall experimental effects. If significant effects were detected ($p < 0.05$), comparisons of all groups with one control group were performed using the post hoc test of Dunnett

at a significance level of 0.05. For analysis, Statistica 6.0 software (StatSoft, Tulsa, OK, USA) was used.

2.1 Efforts to Reduce Collateral Axonal Branching at the Lesion Site

2.1.1 Neutralization of Trophic Factors at the Lesion Site Reduced Collateral Axonal Branching, but Did Not Improve Recovery of Function

Within an earlier experimental set, Streppel et al. (2002) tested the hypothesis that neutralization of diffusable neurotrophic factors (NGF, BDNF, FGF-2, IGF-1, CNTF, GDNF) at the lesion site could reduce collateral branching of transected axons and thus improve quality of reinnervation. Neutralizing concentrations of anti-NGF, anti-BDNF, and anti-IGF-I significantly reduced branching. These results appeared very promising with regard to the feasibility of the method for treatment of patients, on one side, and to the presumed dominant contribution of axonal misguidance to the failure of recovery, on the other. However, experimental data proving that suppressed branching would enhance precision of target reinnervation and favor functional recovery were required. In other words, before considering this treatment as of potential value in clinical situations it should be known whether reduced collateral axonal branching at the lesion site would be associated with improved recovery of motor function.

The results from all counts in this chapter were obtained in a manner that was absolutely identical (rat strain, sex, weight, surgical treatment, postoperative survival period, tracers, etc.) to that used in an earlier set of experiments (Streppel et al. 2002; Angelov et al. 2005). This permits pooling of the present and earlier data. The larger sample size in each group (17 instead of eight animals) allowed a more powerful statistical analysis and more reliable conclusions.

2.1.1.1 Animals

Seventy-two Wistar rats were distributed in nine groups (group 1 of intact controls and groups 2–8 of surgically treated) each consisting of eight animals.

In addition, 12 female young adult Sprague-Dawley (SD) rats were divided into two groups. Half of the animals were with normal visual perception (purchased from Charles River, Germany) and the other group consisted of blind rats (substrain Royal College of Surgeons, RCS, generously supplied by U. Schraermeyer). The SD/RCS rats lose their photoreceptor cells 2 months after birth due to a genetic defect of the retinal pigment epithelium (D'Cruz et al. 2000; Sheedlo et al. 1991). Thus, these animals can obtain spatial information only by their mystacial vibrissae (Brecht et al. 1997).

2.1.1.2 Overview of Experiments

Two months after surgery on the facial nerve, the recovery of vibrissal motor performance was assessed in all surgically treated rats (84 animals) using video-based motion analysis (VBMA) of explorative whisking. Thereafter, the animals of groups 1–9 were used to analyze the degree of posttransectional collateral axonal branching by retrograde labeling with three different fluorescent dyes applied simultaneously to three different branches of the facial nerve. All Sprague-Dawley rats (group SD and group SD/RCS) were not subjected to tracer applications, but used to study qualitative and quantitative aspects of muscle reinnervation by means of immunocytochemistry for neuronal class III β-tubulin and histochemistry with alpha bungarotoxin.

2.1.1.3 Facial–Facial Anastomosis

Transection and end-to-end suture of the right facial nerve (facial–facial anastomosis, FFA) were performed in group 2 of the Wistar rats and in all Sprague-Dawley animals (group SD and group SD/RCS). Following an intraperitoneal injection of ketamin/xylazin, the main trunk of the facial nerve was exposed and transected close to its emergence out of the foramen stylomastoideum (Fig. 2.1a). The proximal stump was then microsurgically reconnected to the distal stump with two 11–0 atraumatic sutures (Ethicon, Norderstedt, Germany). Finally the wound was closed by three 4–0 skin sutures (Ethicon).

2.1.1.4 Entubulation of the Facial Nerve Trunk

Under anesthesia, the right facial nerve in groups 3–9 of the Wistar rats was transected and both stumps were inserted into a silicone precision tube (Fig. 2.1b). The tube had an inner diameter of 1.47 mm and outer diameter of 1.96 mm (Aromando Medizintechnik, Düsseldorf, Germany). The space between the proximal and distal nerve stumps with a volume of approximately 8 μl (5 mm $\times$ 0.735 mm $\times$ 0.735 mm $\times$ π) was filled with collagen type I (group 3) or with collagen gel containing antibodies to trophic factors in the following neutralizing concentrations (Fig. 2.1b):

Group 4: mouse monoclonal anti-NGF (40 μg/ml; Roche, Mannheim, Germany; Bedi et al. 1992; Diamond et al. 1992; Ro et al. 1996)

Group 5: mouse monoclonal anti-BDNF (160 μg/ml; R&D Systems, Wiesbaden, Germany; Tonra et al. 1998)

Group 6: mouse monoclonal anti-bFGF (100 μg/ml; UBI/Biomol, Hamburg, Germany; Tuttle et al. 1994; Murai et al. 1996)

Group 7: mouse monoclonal anti-IGF-I (30 μg/ml; UBI/Biomol, Zheng et al. 1997)

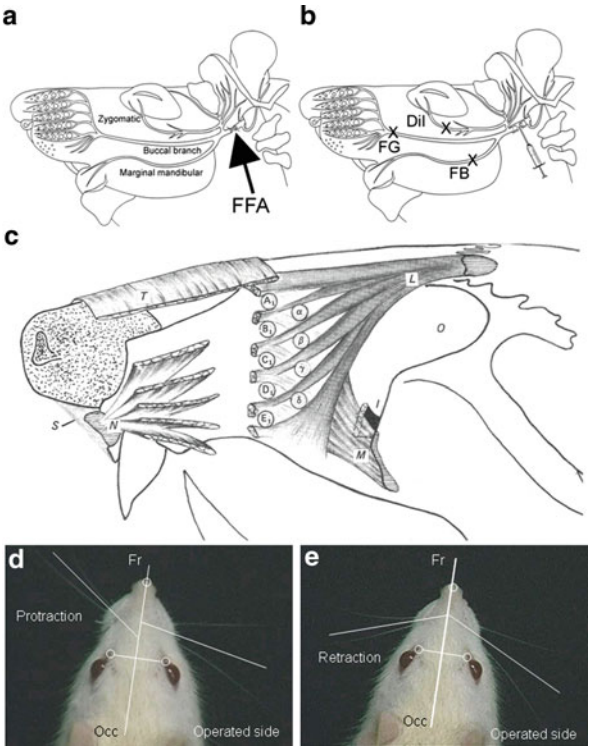

Fig. 2.1 (**a**–**e**) Schematic drawings of the infratemporal portion of the rat facial nerve. The site of transection and end-to-end suture of the facial nerve trunk, i.e., facial–facial anastomosis (FFA) is indicated by an *arrow* (**a**). The site of entubulation and the tracer application are indicated by abbreviations of the three different labels applied, i.e., DiI, FG, and FB, respectively (**b**). Schematic drawing of the extrinsic vibrissae muscles according to Dörfl (1982): α-δ: the four caudal hair follicles, the muscles slings of which "straddle" the five vibrissae rows (**a**–**e**); T – m. transversus nasi; L – m. levator labii superioris; N – m. nasalis; M – m. maxillolabialis; O – orbit; S – septum intermusculare (**c**). Analysis of the vibrissae motor performance with precise measurement of angles, angular velocity, and angular acceleration of the intact and operated side during protraction (**d**) and retraction (**e**) of the vibrissae. Note the significant change in angle between the sagittal line **Fr-Occ** during protraction and retraction on the intact side. The vibrissae on the operated side remain stiff. Adopted from Guntinas-Lichius et al. 2002

Group 8: mouse monoclonal anti-GDNF (3 μg/ml; R&D Systems, Wiesbaden; Vega et al. 1996)

Group 9: goat polyclonal anti-CNTF (100 μg/ml; R&D Systems; Ding et al. 1994; Tokiwa et al. 1994)

Since, except for anti-CNTF, all neutralizing antibodies were raised in mice, an entubulation of the facial nerve in a gel containing mouse nonimmune IgG would

be a necessary control. However, previous own experiments have shown that the application of mouse nonimmune IgG (160 μg/ml; Sigma) has no reducing effect on axonal sprouting (Streppel et al. 2002). Therefore, such a control group was not included in this study.

2.1.1.5

Observations on the Function of Mystacial Vibrissae

The ability to observe postoperative paralysis of vibrissae and the subsequent gradual recovery of rhythmical whisking is one of the major advantages of the "facial-nerve transection model." Under normal physiological conditions, the mystacial vibrissae of the rat are erect with anterior orientation. Their simultaneous sweeps known as "whisking" or "sniffing" (Semba et al. 1980; Welker 1964) occur 5–11 times per second (Bermejo et al. 1996; Komisaruk 1970; Carvell and Simons 1990). The key movements of this motor activity are the protraction and retraction of the vibrissal hairs by the piloerector (follicular) muscles. The striated muscle fibers mediating protraction form a sling around the rostral aspect of each hair follicle: contraction of these muscles pulls the base of the follicle caudally, moving the distal aspects of the whisker hair forward. By contrast, retraction of the vibrissae depends primarily upon passive elastic properties of the deep connective tissue (Dörfl 1985; Wineski 1985). All muscles are innervated by the buccal and marginal mandibular branches of the facial nerve (Dörfl 1985).

As a result of muscle denervation after nerve transection, the whiskers acquired a caudal orientation and remained motionless within the first 10 days after surgery. At 10–14 days postoperation (DPO), the vibrissae rose to the level of the mouth with a posterior orientation in all animals irrespective of treatment. An overall poor restoration of rhythmical whisking was observed in all experimental groups.

2.1.1.6

Analysis of Vibrissae Motor Performance

The method of VBMA of vibrissae motor performance has been thoroughly established and tested in a series of experiments (Tomov et al. 2002). Two months after surgery on the facial nerve, all animals (of the strains Wistar, SD and SD/RCS) were videotaped for 3–5 min during active exploration using a digital camcorder (Panasonic NV DX-110 EG). Selected sequences containing the most pronounced movements of the intact contralateral vibrissal hairs were captured by a 2D/Manual Advanced Video System (PEAK Motus 2000, PEAK Performance Technologies, Inc., Englewood, CO, USA). The geometrical model consisted of three reference points (1) a point in the medial sagittal line close to the end of the nose, (2) a point corresponding to the medial angle of the left orbita, and (3) a

point corresponding to the medial angle of the right orbita (Fig. 2.1d, e). Using this model, we collected and evaluated data on the following parameters:

- Whisking frequency: cycles of protraction (forward movement) and retraction (backward movement) per second
- Angle at maximal protraction: the rostrally open angle between the mid-sagittal plane and the hair shaft (in degrees)
- Amplitude: the difference between maximal retraction and maximal protraction (in degrees)
- Angular velocity during protraction (in degrees per second)
- Angular acceleration during protraction (in degrees per second^2)

2.1.1.7

Intact Rats

During exploration the mystacial vibrissae swept back and forth with a frequency of about 6 Hz. The maximal protraction (a rostrally open angle between the vibrissa shaft and the median sagittal plane) was about 70°. The mean amplitude of whisking (the difference between maximal retraction and maximal protraction in degrees) measured about 50°. These movements were performed at a sagittal angular velocity of about 500°/s and a sagittal angular acceleration of 20,000°/s^2 (Table 2.1, group intact). These results are consistent with our previous observations (Tomov et al. 2002).

2.1.1.8

Operated Rats

Also consistent with previous data are the results obtained from animals with facial nerve anastomosis (Table 2.1, group 2; Tomov et al. 2002). As compared with intact animals, large functional deficiency was evident from the significantly larger angle at maximal protraction (+28% vs. the *Intact* group), the smaller amplitude of vibrissae movement (−72%), as well as the lower angular velocity and acceleration during protraction (−75% and 87%, respectively). These postoperative changes were due to inadequate muscle function during the active protraction phase (see above). The frequency of movements was similar to intact animals which is explainable by the roughly similar reduction of both range and speed of movement, as well as by the influence of passive elastic tissue properties on this parameter.

Taken together, these findings show that the range and velocity of movements remained severely impaired even 2 months after facial anastomosis. As compared with the FFA group, application to the transected and entubulated facial nerve of collagen alone or collagen plus neutralizing antibodies did not produce any

Table 2.1 Motor recovery after entubulation of the facial nerve into silicone tubes containing neutralizing antibodies against neurotrophic factors

Group of animals	Frequency (in Hz)	Angle at maximal protraction (in degrees)	Amplitude (in degrees)	Angular velocity during protraction (in degrees/s)	Angular acceleration during protraction (in degrees/s^2)
1. Intact	6.4 ± 1.1	71 ± 15*	50 ± 15*	530 ± 330*	19,293 ± 13,514*
2. FFA	6.3 ± 0.5	91 ± 12	19 ± 6	135 ± 54	2,485 ± 792
3. Collagen	5.0 ± 0.9	91 ± 12	15 ± 5	146 ± 37	3,036 ± 1,576
4. NGF	5.3 ± 0.9	94 ± 13	16 ± 5	113 ± 64	2,648 ± 2,202
5. BDNF	5.9 ± 0.5	93 ± 12	17 ± 6	152 ± 77	3,176 ± 2,109
6. bFGF	5.8 ± 1.3	103 ± 16	18 ± 9	193 ± 50	3,417 ± 1,643
7. IGF-I	5.8 ± 1.7	93 ± 18	17 ± 8	283 ± 140	2,322 ± 1,381
8. GDNF	5.4 ± 1.4	99 ± 22	16 ± 6	245 ± 122	2,600 ± 1,350
9. CNTF	4.6 ± 0.7*	113 ± 6*	8 ± 2*	164 ± 20	816 ± 294

Biometrics of vibrissae motor performance in intact rats (group *Intact*), in rats after transection and suture of the right facial nerve (*FFA*), and after entubulation of the facial nerve into a silicone tube containing collagen Type I alone (collagen) or collagen plus antibodies against neurotrophic factors (NGF, BDNF, bFGF, IGF-I, GDNF, or CNTF) in neutralizing concentrations (see Material and Methods). Each group consisted of eight animals (Wistar rats, strain HsdCpb:WU). Shown are group mean values ± SD. Group mean values significantly different from the control group (2. FFA, ANOVA and post hoc Dunnett's test, $p < 0.05$) are indicated by asterisks

positive functional effects (Table 2.1, groups *Collagen, NGF, BDNF, IGF-I and GDNF*). Since treatment with some antibodies, however, significantly reduced axonal branching (Table 2.2), we suggested that the excessive collaterals at the lesion site may not be a critical factor in the recovery of coordinated muscle activity. As an attempt to search for this critical factor, we decided to estimate the quality of target muscle reinnervation.

2.1.1.9

Simultaneous Application of Three Fluorescent Tracers (DiI, FG, and FB)

One day after videotaping, the animals received an intraperitoneal injection of ketamin/xylazin. The zygomatic, buccal, and marginal mandibular ramus of eight intact (group 1) and 64 operated (groups 2–9) animals were transected and instilled with crystals of DiI (1,1′-dioctadecyl-3,3,3′,3′-tetramethylindocarbocyanine perchlorate, Molecular Probes, Leiden, The Netherlands), Fluoro-Gold (FG; Fluorochrome Inc., Denver, CO, USA), and Fast Blue (FB; EMS-Chemie GmbH, Groß-Umstadt, Germany), respectively (Fig. 2.1b). To avoid the mingling of FG and FB (both water soluble) and DiI, all crystals were left in situ only for 30 min. Thereafter, the application site was carefully rinsed and dried and the wound was closed.

Table 2.2 Degree of collateral axonal branching after treatment of the transected facial nerve with neutralizing antibodies against neurotrophic factors

Group of animals	Neurons projecting only into the zygomatic nerve (DiI-only)	Neurons projecting into the zygomatic and buccal nerves (DiI + FG)	Neurons projecting into zygomatic and marginal mandibular nerves (DiI + FB)	All DiI labeled neurons projecting into the zygomatic nerve (DiI, DiI + FG, DiI + FB)	Neurons projecting only into the buccal nerve (FG-only)	Neurons projecting only into the marginal mandibular nerve (FB-only)
1. Intact	364 ± 47*	–*	–*	364 ± 47*	1,441 ± 101*	379 ± 94*
	100%	0%	0%	100%		
2. FFA	213 ± 53	239 ± 52	257 ± 56	709 ± 178	1,908 ± 289	1,488 ± 356
	30%	34%	36%	100%		
3. Collagen	194 ± 89	334 ± 74*	227 ± 74	755 ± 125	1,966 ± 203	1,543 ± 348
	26%	44%	30%	100%		
4. NGF	343 ± 78*	74 ± 32*	63 ± 59*	465 ± 133*	1,408 ± 562*	546 ± 156*
	70%	16%	14%	100%		
5. BDNF	360 ± 73*	79 ± 71*	49 ± 40*	488 ± 125*	1,538 ± 610	565 ± 204*
	74%	16%	10%	100%		
6. bFGF	321 ± 95*	50 ± 47*	30 ± 28*	401 ± 76*	1,200 ± 672*	580 ± 148*
	79%	13%	8%	100%		
7. IGF-I	361 ± 81*	118 ± 92*	98 ± 42*	578 ± 140*	1,635 ± 616	652 ± 143*
	64%	20%	16%	100%		
8. GDNF	361 ± 98*	131 ± 66*	49 ± 30*	541 ± 127*	1,633 ± 575	668 ± 135*
	67%	24%	9%	100%		
9. CNTF	348 ± 69*	109 ± 22*	29 ± 10*	482 ± 70*	1,425 ± 312	701 ± 141*
	71%	23%	6%	100%		

Number of retrogradely labeled motoneurons with projection axons in the zygomatic, buccal, or marginal mandibular branches of the facial nerve of intact rats (group Intact), after transection and suture of the facial nerve (FFA), and after entubulation with collagen Type I (collagen) or collagen plus antibodies against NGF, BDNF, bFGF, IGF-I, or GDNF. Seventeen animals (Wistar rats, strain HsdCpb:WU) were studied per group. Shown are group mean values ± SD. Group mean values significantly different from the control group (FFA, ANOVA and post hoc Dunnett's test, $p < 0.05$) are indicated by asterisks. The percentage values below the absolute numbers in columns 2–5 indicate the proportions of motoneurons projecting through the zygomatic nerve with branched axons (DiI + FG or DiI + FB, column 3 and 4) and unbranched axons (DiI-only, column 2) are indicated as percentages of all neurons carrying DiI label (column 5)

2.1.1.10

Tissue Preparation

Ten days after triple labeling, all animals were fixed by perfusion with 4% paraformaldehyde in 0.1 M phosphate buffer pH 7.4. Their brainstems were cut in 50 μm thick vibratome serial sections.

2.1.1.11

Fluorescence Microscopy After Triple Retrograde Labeling

Sections were observed with a Zeiss Axioskop 50 epifluorescence microscope through a custom-made band pass-filter set (no. F31-000; excitation D 436/10; beam splitter 450 DCLP; barrier filter D470/40), which allows recognition only of FB-labeled (appearing blue). Observations through a custom-made HQ-Schmal-band-filter set (no. F36-050; excitation D 369/40; beam splitter 400DCLP; barrier filter HQ 635/30) and a HQ-Schmalband-filter set for Fluoro-Gold visualized all motoneurons containing FG. Observations through a filter set 15 of Carl Zeiss (Excitation BP 546/12, Emission LP 590) revealed the red fluorescence of those motoneurons retrogradely labeled by DiI. The fluorescence crosstalk between the tracers was restricted with this filter combination *ad maximum*:

2.1.1.12

Image Analysis After Triple Retrograde Labeling

Employing a CCD Video Camera System combined with the image analyzing software Optimas 6.5. (Optimas Corporation, Bothell, Washington, DC, USA), separate color images of retrogradely labeled facial motoneurons were created through the different filter sets, and all cells stained by DiI_{only}, FG_{only}, FB_{only} and all cells double stained by DiI + FG or DiI + FB were identified and manually counted on the computer screen as described by Dohm et al. (2000).

2.1.1.13

Qualitative and Quantitative Estimates in the Facial Nucleus of Intact Rats

Motoneurons innervating muscles through the zygomatic, buccal, or marginal mandibular branches are localized in three distinct subnuclei of the facial nucleus – the dorsal, lateral, and intermediate subnucleus, respectively (Hinrichsen and Watson 1984; Thomander 1984; Klein and Rhoades 1985; Aldskogius and Thomander 1986; Semba and Egger 1986; Ito and Kudo 1994; Dohm et al. 2000; Fig. 2.2a). The average size of these distinct populations, as estimated by the triple labeling in this experiment, was around 360 zygomatic, 1,440 buccal, and 380 marginal mandibular motoneurons (Table 2.2, group *Intact*). These data are consistent with previous reports (Dohm et al. 2000; Streppel et al. 2002). Double labeling of zygomatic, buccal, and marginal mandibular motoneurons was not observed (Fig. 2.2a; Table 2.2), which is consistent with the myotopic principle and indicates the consistent reproducibility of the tracing technique. The latter notion is further supported by the observation that no labeled cells were found in the medial or ventromedial facial subnuclei which contain motoneurons projecting

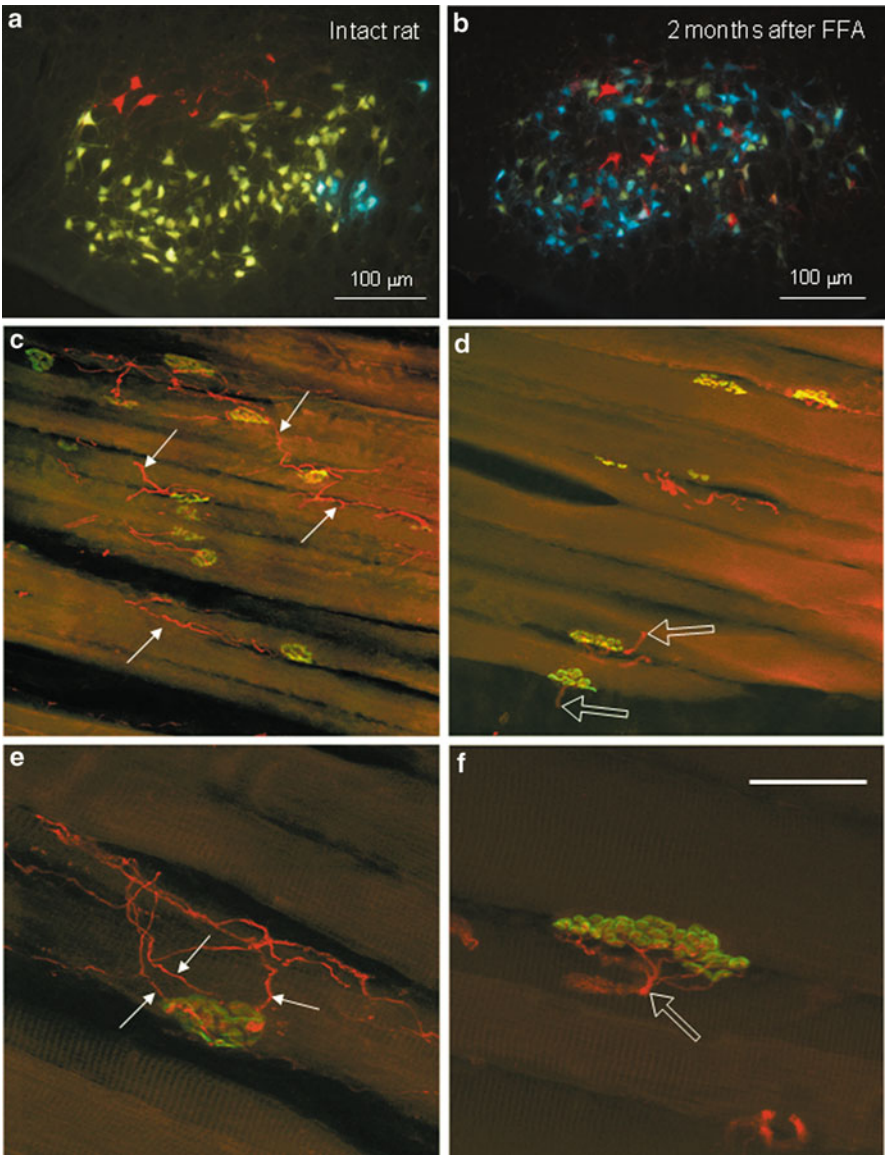

Fig. 2.2 (**a–d**) Myotopic organization of the facial nucleus and collateral axonal branching as estimated by the pattern of retrograde labeling. In intact animals, simultaneous application of DiI (*red*), FG (*yellow*), and FB (*blue*) to the zygomatic, buccal, and mandibular nerve branches, respectively, labels distinct subnuclei with no overlap (**a**). Two months after transection and suture of the facial nerve, the myotopic organization is lost irrespective whether the animals received ES (**b**). Adopted from Skouras et al. 2009. Superimposed

through the posterior auricular and cervical branches, respectively, branches that were neither transected nor labeled (data not shown, see Dohm et al. 2000; Streppel et al. 2002; Tomov et al. 2002).

2.1.1.14

Counting of Retrogradely Labeled Motoneuronal Perikarya

Employing the fractionator principle (Gundersen 1986), all retrogradely labeled motoneurons with visible cell nucleus in the 50-μm-thick sections were counted in every third section through the facial nucleus on the operated and on the unoperated side.

Eight weeks after unilateral FFA or entubulation and another 10 days after triple retrograde labeling, three major changes were detected. First, the myotopic organization into subnuclei was no longer observed, i.e., all retrogradely labeled motoneurons were scattered throughout the facial nucleus (Fig. 2.2b). Second, as a rule there were always more retrogradely labeled motoneuronal cell somata than in unoperated animals (Table 2.2). The reason for this was the postoperative hyperinnervation of targets (Angelov et al. 1996; Streppel et al. 1998), i.e., labeling of motoneurons which, under normal conditions, do not send axons to the three facial rami under study. After transection of the facial nerve, however, these motoneurons developed collateral axonal branches which adjoined the "wrong" rami and thus reached sites of tracer application. Third, numerous double-labeled motoneurons occurred after the lesion which demonstrated that twin axons projected into more than one branch of the facial nerve (Dohm et al. 2000; Streppel et al. 2002; Tomov et al. 2002). All double- and single-labeled motoneurons were counted.

Fig. 2.2 (continued) stacks of confocal images of endplates in reinnervated LLS muscles of a SD rat with normal vision (**c**, **e**) and a blind SD/RCS rat (**d**, **f**) visualized by staining of the motor endplates with Alexa Fluor 488 α-bungarotoxin (green fluorescence) and immunostaining of the intramuscular axons for neuronal class III β-tubulin (Cy3 red fluorescence) The images shown in panel **c** and **d** are taken at low magnification to reveal the pattern of innervation. Note that abundant intramuscular axonal branches are seen among endplates in panel **c** (*arrows*) but not in panel **d**. Also, the diameters of the muscle fibers seen in **c** are apparently smaller than those seen in **d**. Panels **e** and **f** show examples of a polyinnervated and a monoinnervated endplate, respectively. Three axonal branches (*arrows* in **e**) reach the boundaries of the polyinnervated endplate delineated by the alpha-bungarotoxin staining. By contrast, the monoinnervated endplate is reached by a single axon (*empty arrow* in **f**) with several preterminal rami. In both examples, the whole endplates are within the stack of confocal images. Scale bar shown in **f** indicates 125 μm for **c**, **d** and 40 μm for **e**, **f**. Adopted from Guntinas-Lichius et al. (2005)

2.1.1.15

Quantitative Estimates of the Total Number of Neurons Projecting Through the Zygomatic, Buccal, and Marginal Mandibular Branches of the Facial Nerve

Following FFA, the number of motoneurons projecting through the zygomatic, buccal, and marginal mandibular branch was increased by about 1.9-, 1.3-, and 3.9-fold, respectively, as compared with intact animals (last three columns in Table 2.2, compare groups *Intact* and *FFA*). Application of collagen to the transected and entubulated nerve did not result in substantial differences as compared with FFA (Table 2.2, group *Collagen*). By contrast, application of neutralizing antibodies (groups NGF through CNTF in Table 2.2) efficiently reduced the overall postlesional axonal branching as indicated by lower numbers of motoneurons labeled through the zygomatic (57–81% of control FFA value), the buccal (63–86%), and marginal mandibular branch (37–47%).

2.1.1.16

Quantitative Estimates of the Number of Single-Labeled (DiI-Only) and Double-Labeled (DiI + FG and DiI + FB) Motoneurons Projecting Through the Zygomatic Branch

The zygomatic branch was selected to evaluate the degree of axonal misdirection because the number of motoneurons that project(ed) through it before and after surgery was relatively small which allowed for sophisticated quantitative analysis in reasonable time. Thus, the distribution of the tracer DiI was of special interest and we carefully differentiated the proportions of motoneurons labeled by DiI_{only}, by DiI + FG, or by DiI + FB. The relative sizes of these three populations of neurons (columns 2–4 in Table 2.2) are indicated as percentages of the total population of DiI-labeled cells (column 5 in Table 2.2) below the absolute mean numbers. In intact rats the zygomatic branch consisted entirely (100%) of unbranched axons as indicated by the presence of DiI_{only}, but not of DiI + FG or DiI + FB cells. After FFA, DiI-labeled motoneurons projected through the three branches in roughly equal proportions (around 30%) indicating unselective, random growth of reinnervating axons into the three branches (Table 2.2). Application of antibodies not only reduced the total number of motoneurons labeled by DiI application to the transected zygomatic branch (see above) but also dramatically increased specificity of reinnervation: the numbers of double-projecting and thus double-labeled neurons (DiI + FG and DiI + FB) were significantly reduced. Accordingly, the portion of single-projecting and thus single-labeled cells that were labeled by DiI_{only} (64–79%) was significantly higher when compared with that after FFA (Table 2.2).

2.1.1.17

Analysis of Target Muscle Reinnervation

The reduction in collateral axonal branching at the lesion site failed to promote restoration of coordinated muscle activity. Considering the possibility that recovery of failure might be due to polyinnervation of motor endplates, we looked for parallelism between the portion of polyinnervated motor endplates and vibrissal motor performance in animals with poor recovery of whisking (SD rats with normal vision) and in rats with perfect recovery of vibrissae motor performance (RCS/SD blind rats). As a representative of the external vibrissal muscles we selected the m. levator labii superiors (LLS; Fig. 2.1c).

Two months after unilateral FFA, the SD and the SD/RCS animals were fixed by perfusion (see above). Under a surgical microscope, LLS on both operated and unoperated side of the face was dissected. Longitudinal sections (30 μm thick) were cut on a cryostat and mounted on SUPERFROST/Plus slides (Carl Roth, Karlsruhe, Germany). To visualize intramuscular axons and motor endplates, every third section through the muscle was stained with antineuronal class III β-tubulin and alpha-bungarotoxin.

Cryosections were immunostained with the polyclonal antineuronal class III β-tubulin (Covance, Richmond, CA, USA, No. PRB-435P) and anti-rabbit IgG Cy3 conjugate. Specificity controls (omission of the primary antibody or of the secondary biotinylated antibody) yielded blank sections. To visualize the motor endplates in the same sections, we stained the postsynaptic nicotinic acetylcholine receptors (nicotinic AchRs) with Alexa Fluor 488-conjugated α-bungarotoxin (Molecular Probes, B-13422; dilution 1:1,000 for 2 h at room temperature). Sections were observed with a Zeiss Axioskop 50 epifluorescence microscope through the "rhodamine" filter (excitation BP 546/12, beamsplitter FT 580, emission LP 590) and the "fluorescein" filter (excitation BP 450–490, beamsplitter FT510, emission LP 520).

Quality of endplate reinnervation was evaluated by a simple and straightforward criterion: number of axonal branches (identified by beta-tubulin staining, Fig. 2.2c–f) that enter or, in some cases, possibly leave the boundaries of individual endplates (identified by acetylcholine receptor staining with alpha-bungarotoxin, Fig. 2.2c–f). Entries by preterminal branches of one axon were counted as single events (Fig. 2.2f). According to this criterion, the endplates were identified as "monoinnervated" (one axon), "polyinnervated" (two or more axons), or denervated (no visible axonal associated with the receptor staining). The designation "polyinnervated" endplates is used to indicate similarity to a morphological abnormality in adult skeletal muscle of mammals observed in pathological conditions such as nerve damage or intoxication, which cause axonal branching, either collateral (at nodes of Ranvier) or terminal (from endplate terminals), or both (Shawe 1954;. Brown et al. 1981; Rich and Lichtman 1989), and polyneuronal

innervation of individual muscle fibers. Individual endplates were identified by the alpha-bungarotoxin staining, after which the number of axons crossing the boundaries of the receptor staining was determined by focusing through the depth of the section. The frequencies of monoinnervated, polyinnervated, and noninnervated endplates were expressed in percentage of the total population.

Our qualitative examinations of longitudinal sections revealed two important differences between the two groups of animals: the incidence of intramuscular axonal branches was higher and diameters of muscle fibers were apparently smaller in muscles of SD rats as compared with SD/RCS animals (Fig. 2.2c, d).

The parallel assessment of vibrissal function (Fig. 2.3a) and of quality of endplate innervation (Fig. 2.3b) also revealed significant differences between the two groups of animals. Vibrissal movements were largely impaired in SD rats as indicated by the small values of the three most important functional variables

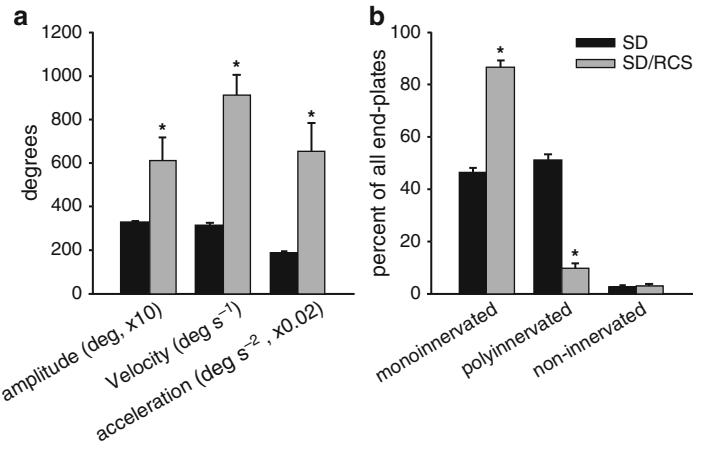

Fig. 2.3 (**a**, **b**) Results of quantitative assessment of vibrissae motor function (**a**) and evaluation of polyinnervation of muscle fibers in LLS muscles (**b**) in SD rats with normal vision (*black bars*) and blind SD/RCS rats (*gray bars*, $n = 6$ for both groups). The animals were studied 2 months after FFA anastomosis. The values for velocity and acceleration shown in **a** are for the protraction phase of the vibrissal movements (see text for further details). Endplates in the LLS muscles were classified as monoinnervated, polyinnervated, or noninnervated according to the number of beta-tubulin-immunoreactive axons that crossed the boundaries of the endplate delineated by staining for acetylcholine receptors (one, two, or more, and 0 axons for the three categories, respectively). The average number of endplates examined in every third section from the muscles was 556 $\pm$ 52 and 547 $\pm$ 79 per animal in the SD and SD/RCS group of rats, respectively. Similar numbers of endplates were examined in the contralateral intact LLS muscles of the same animals. In this case, no polyinnervated or noninnervated endplates were observed. The values shown in the graph are mean values + SEM. *Asterisks* indicate significant differences between the group mean values ($p < 0.05$, two-sided t test for independent sample). Adopted from Guntinas-Lichius et al. (2005)

estimated (Fig. 2.3a, *black bars*). By contrast, the values in the SD/RCS group were comparable with values of intact animals indicating an extraordinary high degree of recovery (Fig. 2.3a, *gray bars*, Table 2.2, Tomov et al. 2002). With regard to the differences in functional performance, the finding that muscle fibers in SD rats appear atrophic (see above) is not surprising. Poor function in the SD animals correlated with high percentage of polyinnervated endplates (>50%) in the LLS muscles (Fig. 2.3b, black bars). In the well-performing SD/RCS rats, the fraction of polyinnervated endplates was small (10%, Fig. 2.3b, *gray bars*). Analyses of endplates were also performed in sections from the intact contralateral LLS muscles of the same animals. All endplates observed in these samples were classified as monoinnervated (see Fig. 2.2 for the sample size for different groups of muscles and animals).

2.1.2 Local Stabilization of Microtubule Assembly Improved Recovery of Facial Nerve Function After Repair

To elucidate the relationship between collateral axonal branching and recovery of function, Peeva et al. (2006) analyzed the expression of cytoskeletal proteins after axotomy (Tetzlaff et al. 1988a) and determined the immunoreactivity for f-actin and neuronal class III β-tubulin, two cytoskeletal components responsible for cytomechanical forces in the leading edge of elongating axons (Challacombe et al. 1996). Using a stereological approach, Peeva et al. (2006) also estimated axonal growth cone densities in order to correlate degrees of axonal sprouting with protein expression levels. The results of this study provided experimental evidence for a possible relationship between functional outcome of facial nerve repair, on one side, and amounts of neurite growth-related proteins and numbers of outgrowing sprouts, on the other side. Better restoration of vibrissae motor performance appeared to be associated with a more vigorous early regenerative response. However, were these large amounts of tubulin due to an increased synthesis, to a slower transport, or to delayed turnover of tubulin? To prove perturbance of the microtubule assembly (polymerization and depolymerization), we applied established pharmacological agents (nocodazole, vinblastine, taxol) locally to the tips of the regrowing axons.

2.1.2.1 Animal Groups and Overview of Evaluation Methods

A total of 102 rats were divided into ten groups (1–10) (Table 2.3). Group 1 consisted of 12 intact control animals and groups 2–10 of surgically treated rats.

Two months after surgery on the buccal branch of the facial nerve (BBFN) and various treatments, the recovery of vibrissal motor performance was assessed in all rats using VBMA of explorative whisking. Thereafter in the experiments with altered local microenvironment at the lesion site (groups 2–7, all of 12 rats), half of

Table 2.3 Experimental design chart depicting animal grouping, treatments and parameters investigated

Group of animals	Video-based motion analysis of vibrissae motor performance (VBMA)	Degree of collateral axonal branching as estimated by double retrograde labeling	Amount of tubulin in BBFN as estimated by intensity of fluorescence	Pattern of motor endplate reinnervation in the LLS muscle
1. Intact animals (12 rats)	12	6	6	6
2. Surgery for buccal–buccal anastomosis (BBA; 12 rats)	12	6	6	6
3. Tube with 0.1 M phosphate buffer pH 7.4 over the transected BBFN (12 rats)	12	6	6	6
4. Tube with collagen type I over the transected BBFN (12 rats)	12	6	6	6
5. Tube with 100 μg/ml nocodazole over the transected BBFN (12 rats)	12	6	6	6
6. Tube with 20 μg/ml vinblastine over the transected BBFN (12 rats)	12	6	6	6
7. Tube with 10 μg/ml taxol over the transected BBFN (12 rats)	12	6	6	6
8. BBA + injection of nocodazole (100 μg/ml) into the whisker pad muscles (six rats)	6	–	–	6
9. BBA + injection of vinblastine (20 μg/ml) into the whisker pad muscles (six rats)	6	–	–	6
10. BBA + injection of taxol (10 μg/ml) into the whisker pad muscles (six rats)	6	–	–	6

In groups 1–7, half of the animals that underwent video-based motion analysis (VBMA) were subsequently used to estimate the degree of collateral axonal branching and the other half to determine the amount of tubulin in the regrowing buccal branch of the facial nerve (BBFN) and the pattern of motor endplate reinnervation. In groups 8–10, the animals that were subjected to VBMA were thereafter used only for establishing the pattern of motor endplates reinnervation

the animals of each group were used to establish the degree of posttransectional collateral axonal branching using retrograde labeling with two different fluorescent dyes applied simultaneously to both peripheral divisions of BBFN. The other half of the rats were used to study possible alterations in the amount of microtubules in the regrowing BBFN (quantitative immunohistochemical analysis of the expression of neuronal class III β-tubulin) and quantitative aspects of the target muscle reinnervation by means of immunocytochemistry for neuronal class III β-tubulin and histochemistry with alpha bungarotoxin. In groups 8–10 (each consisting of six rats), only the vibrissae motor performance and reinnervation pattern were analyzed.

2.1.2.2

Transection and Suture of the Buccal Branch of the Facial Nerve (Buccal–Buccal Anastomosis)

Transection and suture of the buccal branch of the facial nerve (buccal–buccal anastomosis, BBA) was performed only in animals of major groups B. The right BBFN was transected and immediately reconnected to the distal stump. Since the subsequent evaluations included analysis of the vibrissae motor performance, we had to eliminate any additional motor nerve supply to the whisker pad muscles (Semba and Egger 1986). Therefore, the transection of the buccal branch was always accompanied by transection and proximal ligature (to prevent regeneration) of the marginal mandibular branch of the facial nerve (Fig. 2.4a).

2.1.2.3

Entubulation of the Buccal Branch of the Facial Nerve

Under anesthesia, the right BBFN in groups C–G was transected and both stumps were inserted into a silicone precision tube (Fig. 2.4b). The space between the proximal and distal nerve stumps was filled with 0.1 M phosphate buffered saline pH 7.4 (group 3), collagen type I (group 4), or with collagen gel containing nocodazole (group 5), taxol (group 6), and vinblastine (group 7).

2.1.2.4

Treatments

For the *nocodazole* treatment, each silicon tube was prefilled with a gel consisting of 66 μl collagen type I (Serva, Cat. No. 47254) and 33 μl of solution containing 10.0 μg of nocodazole (Sigma, Cat. No. M1404). Alternatively, the 800 μl collagen was obtained from 5 ml collagen stock solution. The three-dimensional collagen gel (Guidry and Grinnell 1987; Mauch et al. 1988) with the nocodazole solution was left to polymerize for 2 h at 37°C. After mixing the 400 μl nocodazole solution with 800 μl collagen solution, the therapeutic concentration of 100 μg/ml was reached (Chuckowree and Vickers 2003).

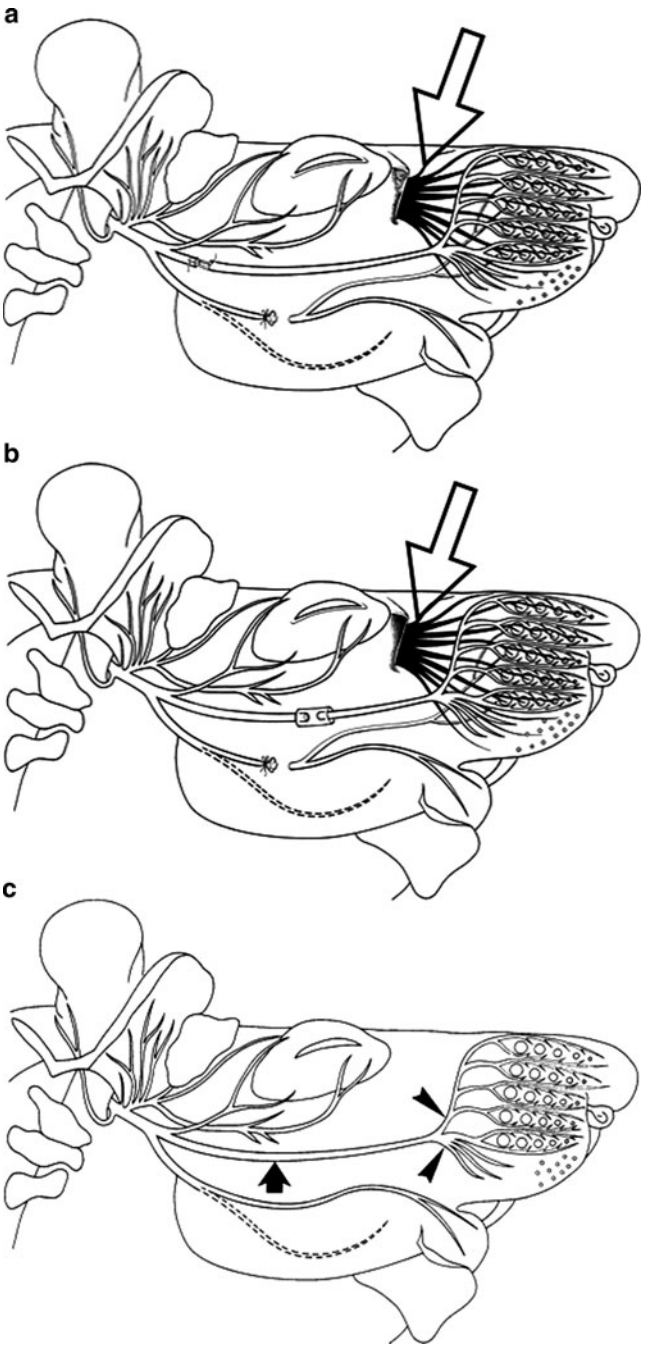

Fig. 2.4 (**a**–**c**) Surgical operations on the rat buccal branch of the facial nerve (BBFN). Schematic drawings illustrating the sites of transection and suture (**a**) and entubulation (**b**)

For the *vinblastine* treatment, the silicon tube was prefilled with a gel consisting of 67 µl collagen type I and 33 µl of 12 nM solution of vinblastine (Sigma, V1377). After mixing the 400 µl vinblastine solution with 800 µl collagen (see above), the therapeutic concentration of 4 nM or 20 µg/ml was reached (Challacombe et al. 1997).

For the *taxol* treatment, the silicon tube was prefilled with a gel consisting of 67 µl collagen type I and 33 µl of solution containing 1 µg paclitaxel (Sigma, T1912). After mixing the 400 µl paclitaxel solution with 800 µl collagen, the therapeutic concentration of 10 µg/ml was reached (Chuckowree and Vickers 2003).

2.1.2.5 Analysis of Vibrissae Motor Performance

Two months after transection and entubulation of BBFN, denervation-induced changes were found in all values (except for the frequency) selected to determine the functional state (Table 2.4). The statistical analysis revealed that only the animals in group 7 (treatment with 10 µg/ml taxol) performed significantly better than those in group 4 (entubulation in collagen; Table 2.4).

2.1.2.6 Simultaneous Application of Two Fluorescent Tracers

One day after videotaping, half of the intact rats of group A and half of the surgically treated rats from groups 2–7 received an intraperitoneal injection of ketamin/xylazin. The BBFN was exposed, and the superior and inferior buccolabial nerves on the right side of the face were transected and labeled with crystals of Fluoro-Gold (FG) and DiI, respectively (Fig. 2.4c).

2.1.2.7 Tissue Preparation, Fluorescence Microscopy, Image Analysis, and Counts

Intact Rats

Application of Fluoro-Gold crystals to the superior and DiI crystals to the inferior buccolabial nerve yielded 1,536 ± 243 FG- and 134 ± 125 DiI-labeled motoneurons (mean ± SD, $n = 6$). All retrogradely labeled cells (total of 1,682 ± 338) were localized in the lateral facial subnucleus. Thereby, the FG-labeled cells were found in its ventral and the DiI-labeled perikarya in its dorsal portion. No double-labeled motoneurons were observed (Fig. 2.5a).

Fig. 2.4 (continued) of BBFN and of the transection and ligature of the marginal mandibular branch of the facial nerve. The cervical branch of the facial nerve is indicated by a dotted line. Adopted from Skouras et al. (2002). (**c**) Schematic drawing of the infratemporal portion of the rat facial nerve. *Large arrow* indicates the transection, suture and entubulation site of BBFN. Transection and tracer application sites in the superior and inferior buccolabial nerves are indicated by *arrowheads*. Adopted from Angelov et al. (1999). The infraorbital nerve (ION) is indicated by an *arrow*

Table 2.4 Recovery of vibrissae motor performance function after buccal nerve lesion in rats

Group of animals	Frequency (in Hz)	Angle at maximal protraction (in degrees)	Amplitude (in degrees)	Angular velocity during protraction (in degrees/s)
1. Intact animals (12 rats)	6.4 ± 1.1	71 ± 15	50 ± 15	588 ± 276
2. Buccal–buccal anastomosis (BBA; 12 rats)	7.2 ± 0.8	98 ± 16	20 ± 6	326 ± 134
3. Tube with phosphate buffer (12 rats)	7.4 ± 0.6	95 ± 11	21 ± 4	404 ± 106
4. Silicon tube with collagen type I (12 rats)	7.5 ± 0.7	88 ± 18	21 ± 5	327 ± 108
5. Tube with 100 μg/ml nocodazole (12 rats)	7.4 ± 0.7	92 ± 14	22 ± 4	428 ± 116
6. Silicon tube 20 μg/ml vinblastine (12 rats)	7.2 ± 0.4	96 ± 17	20 ± 2	380 ± 187
7. Silicon tube with 10 μg/ml taxol (12 rats)	7.2 ± 0.9	84 ± 17	34 ± 8*	634 ± 164*
8. BBA with subsequent injection of nocodazole (100 μg/ml) into whisker pad muscles (six rats)	7.1 ± 1.7	71 ± 20	28 ± 7	400 ± 344
9. BBA with subsequent injection of vinblastine (20 μg/ml) into whisker pad muscles (six rats)	5.2 ± 0.9	90 ± 14	20 ± 9	340 ± 291
10. BBA with subsequent injection of taxol (10 μg/ml) into whisker pad muscles (six rats)	6.3 ± 1.1	86 ± 14	20 ± 15	216 ± 188

Shown are group mean values ± SD. Group mean values significantly different from the control group D (entubulation with collagen; ANOVA and post hoc Dunnett's test, $p < 0.05$) are indicated by asterisks. Values for intact rats are given as reference values and not included in the analysis

Operated Rats

Neuron labeling at 2 months after transection and/or entubulation of BBFN showed that all retrogradely labeled neurons were localized in the lateral facial subnucleus. However, due to a malfunctioning guidance of regrowing axons into wrong fascicles, the myotopic organization of this subnucleus into a ventral (for the superior buccolabial nerve) and a dorsal (for the inferior buccolabial nerve) portion was no longer evident (Fig. 2.5b–d). Accordingly, the number of motoneurons whose axons or axonal branches projected into the superior buccolabial nerve was lower than in the intact rats (91%). We determined that only about 28–56% of all neurons in the lateral facial subnucleus projected into the superior buccolabial nerve. On the contrary, the number of motoneurons whose axons projected into the inferior buccolabial nerve was increased in comparison with that in the intact rats: the motoneurons whose axons had regrown into the inferior buccolabial nerve comprised about 24–48% of all neurons in the lateral facial subnucleus. Compared with the values in intact rats (9%), there was a statistically significant decrease in the number of motoneurons projecting through the superior buccolabial nerve.

Another major difference to the unoperated animals was the presence of motoneurons containing both tracers. The only explanation for this may be that these double-labeled cells (approximately 21% of all motoneurons in the lateral facial

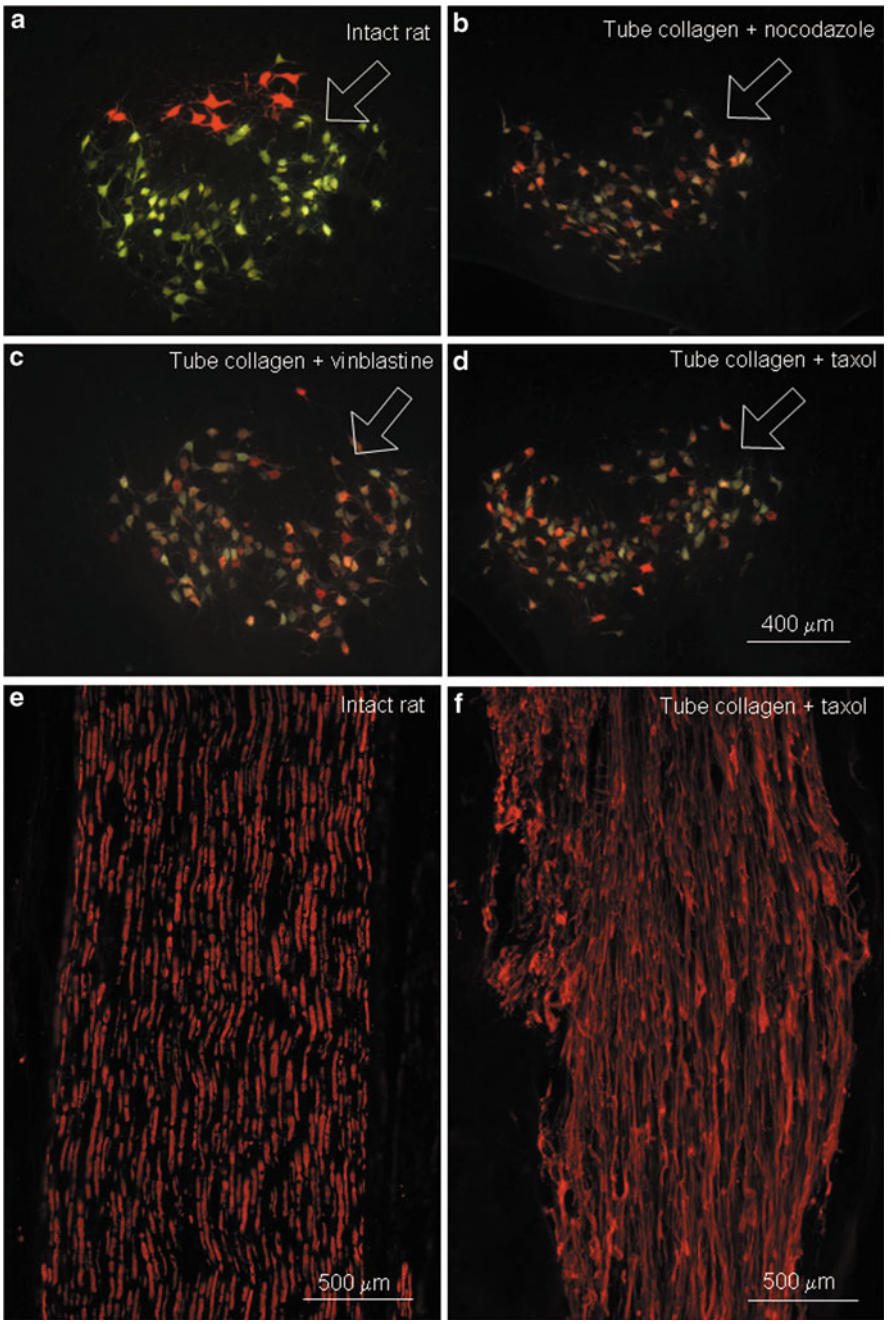

Fig. 2.5 (**a–f**) Facial nucleus after retrograde neuronal labeling in intact and operated rats. Photographs produced by double exposure. The dorsomedial border of the lateral facial

subnucleus) regrew several (but not one single) sprouts from each transected axon, which postoperatively projected simultaneously within the superior and inferior buccolabial nerves (cf. Shawe 1954). Since both rami were instilled with different tracers, the axonal branches took up and retrogradely transported two fluorescent dyes simultaneously. This in turn led to double labeling of their parent perikarya.

Two months after entubulation with collagen (group 4) we determined an index of axonal branching of 21%. None of the other entubulations (group 5 – 21%; group 6 – 21%; group 7 – 22%) had any significant influence on the projection patterns (ANOVA and post hoc Dunnett's test, $p < 0.05$). Thus, there was a complete lack of myotopic organization and a consistently elevated degree of axonal branching regardless of whether the animals were subjected to mere transection of the BBFN or to entubulation with varying agents.

2.1.2.8 Intensity of Tubulin Fluorescence

One day after videotaping, the rest of the animals from groups A–G were deeply anesthetized and transcardially perfused with 4% formaldehyde for 20 min. The masseter muscle with the transected buccal branch of the facial nerve (BBFN) on it was removed, post-fixed, cryoprotected, and cut in 20-μm-thick frozen sections (Streppel et al. 2002; Peeva et al. 2006). All sections used to compare the intensity of fluorescence between the various groups were incubated simultaneously using identical solutions.

Immunocytochemistry with 1:1,000 rabbit polyclonal antineuronal class III β-tubulin (Covance, Richmond, CA, USA) was performed as previously described.

For quantification of pixel brightness, images were captured with a slow scan CCD camera (Spot RT, Diagnostic Instruments) using the ×16 objective and the Image-Pro Plus Software Version 5.0 (Media Cybernetics, Inc., Silver Spring, MD, USA). Analysis with a threshold for tubulin that had been set at pixel gray value of 120 was performed as previously described (Peeva et al. 2006).

Reliable immunostaining with the selected antibodies as described above allowed us to readily identify Cy3-fluorescent microtubules in longitudinal sections

Fig. 2.5 (continued) subnucleus is indicated by an *arrow*. (**a**) Unlesioned lateral facial subnucleus with preserved myotopic organization of the motoneurons whose axons project into the superior buccolabial nerve (retrogradely labeled in *yellow* by Fluoro-Gold) and into the inferior buccolabial nerve (labeled in *red* by DiI). Whereas most FG-labeled motoneurons are localized in the ventral portion, those labeled with DiI are in the dorsal part of the subnucleus. (**b**)–(**d**)**:** Lesioned lateral facial subnucleus after treatment of the transected BBFN with nocodazole (**b**), vinblastine (**c**), and taxol (**d**) and application of FG to the superior and DiI to the inferior buccolabial nerve. Note the complete lack of myotopic organization: the FG-labeled (*yellow*), DiI-labeled (*red*), and DiI + FG-labeled (*shades of pink and orange*) motoneurons are scattered throughout the whole lateral facial subnucleus. 50 μm vibratome sections. Immunocytochemical demonstration of neuronal class III β-tubulin in rat BBFN axons. Representative longitudinal sections from an intact nerve (**e**) and from a fragment proximal to the silicon tube, which had been filled with 10 μg/ml taxol in collagen 2 months beforehand (**f**). Adopted from Grosheva et al. 2008

through the intact and lesioned BBFN (Fig. 2.5e, f). At least six equidistant (each second) 20-μm-thick longitudinal sections through the BBFN of each animal were measured, yielding a mean of about 40 sections per group (each experimental group consisted of six rats).

The results on the intensity of fluorescence showed that there was no significant difference in the amount of tubulin (indirectly determined by the number of pixels at the defined gray value of 120) between the intact BBFN (group 1: 5,493 ± 3,418) and the BBFN at 2 months after its transection and suture (group 2: 5,384 ± 2,145). Similar values were determined after entubulation of transected BBFN in phosphate buffer (group 3: 2,814 ± 1,873), collagen type I (group 4: 4,275 ± 924), nocodazole (group 5: 3,666 ± 957), vinblastine (group 6: 5,049 ± 2,185), and taxol (group 7: 2,158 ± 1,706). No statistically significant differences between any of the groups were detected.

2.1.2.9

Degree of Motor Endplate Polyinnervation

Degree of motor endplate polyinnervation was investigated in the m. levator labii superioris (Fig. 2.1c) as described (Sect. 2.1.1). The frequencies of monoinnervated, polyinnervated, and noninnervated endplates were expressed as percentage of the total population. Although postlesional polyinnervation of the endplates has been claimed to be transient (Hennig and Dietrichs 1994), accumulating evidence suggests that it persists after establishment of nerve–muscle contacts (Esslen 1960; Mackinnon et al. 1991; Reynolds and Woolf 1992; Madison et al. 1999; Jergovic et al. 2001; Ijkema-Paassen et al. 2002; Grant et al. 2002; Choi and Raisman 2005). Our previous work indicates that it has a deleterious effect on recovery of facial motor function (Guntinas-Lichius et al. 2005).

In intact animals, all motor endplates were monoinnervated (Fig. 2.2d, f; Table 2.5). Two months after any transection and end-to-end suture or entubulation of the BBFN (groups B–F), about 30% of the motor endplates were polyinnervated, i.e., innervated by two or more axons (Fig. 2.2c, e; Table 2.5). The only procedure that significantly reduced the degree of polyinnervated endplates (12 ± 4%) was entubulation in 10 μg/ml taxol.

2.2
Efforts to Reduce Axonal Sprouting in Denervated Muscles

2.2.1
Direct Modification of Microtubule Dynamics in Reinnervated Muscles Failed to Reduce Terminal Axonal Sprouting

Our results described in Sect. 2.1.2 showed that stabilization of microtubules with 10 μg/ml taxol reduced intramuscular axonal sprouting and polyinnervation of

Table 2.5 Reinnervation pattern of the m. levator labii superioris (LLS)

Group of animals	Monoinnervated motor endplates (%)	Polyinnervated motor endplates (%)	Noninnervated motor endplates (%)	Total number of motor endplates examined
1. Intact animals	100 ± 0	0	0	1,521 ± 111
2. Buccal–buccal anastomosis	67 ± 10	29 ± 7	4 ± 3	1,763 ± 131
3. Tube with 0.1 M phosphate buffer pH 7.4	71 ± 6	26 ± 5	3 ± 1	1,868 ± 313
4. Tube with collagen	70 ± 7	24 ± 4	2 ± 1	1,650 ± 221
5. Tube with 100 μg/ml nocodazole	69 ± 12	27 ± 5	4 ± 3	1,426 ± 73
6. Tube with 20 μg/ml vinblastine	74 ± 9	23 ± 4	3 ± 1	1,482 ± 161
7. Tube with 10 μg/ml taxol	86 ± 9*	12 ± 4*	2 ± 1	1,362 ± 149
8. BBA with subsequent injection of nocodazole (100 μg/ml) into the whisker pad muscles	59 ± 14	37 ± 5	4 ± 3	1,722 ± 312
9. BBA with subsequent injection of vinblastine (20 μg/ml) into the whisker pad muscles	51 ± 16	45 ± 5	4 ± 1	1,560 ± 212
10. BBA with subsequent injection of taxol (10 μg/ml) into the whisker pad muscles	60 ± 15	36 ± 5	4 ± 2	1,716 ± 318

Motor endplates were classified as monoinnervated, polyinnervated, or noninnervated according to the number of beta-tubulin-immunoreactive axons that crossed the boundaries of the endplate. Shown are group mean values ± SD. Group mean values significantly different from the control group D (entubulation with collagen; ANOVA and post hoc Dunnett's test, $p < 0.05$) are indicated by asterisks. Values for intact rats are given as reference values and not included in the analysis

the motor endplates which was accompanied by improved restoration of function. This led to the question whether direct modification of microtubule dynamics in reinnervated muscles by local application of nocodazole, vinblastine, and taxol would reduce the terminal axonal sprouting and thus diminish the portion of polyinnervated motor endplates.

Earlier own experience has shown that, after BBA, the first regrowing axons bridge the gap between transection site and target muscles (about 12 mm long) for 4 days (Angelov et al. 1999). This is why starting at 5 days after BBA, rats received 50 μl injections of nocodazole (10 μg/100 μl), vinblastine (2 μg/100 μl), and taxol (1 μg/100 μl) into muscles of the whisker pad once in a week.

Analysis of vibrissae motor performance and analysis of target muscle reinnervation were performed as described. Contrary to our expectation that direct modification of microtubule dynamics in reinnervated muscles would reduce the

terminal axonal sprouting and thus diminish the portion of polyinnervated motor endplates, we found an average of 35–45% polyinnervated muscle fibers after local application of nocodazole, vinblastine, and taxol and poor recovery of vibrissal motor performance (Tables 2.4 and 2.5).

2.2.2 Intraoperative Electrical Stimulation Prior to Reconstructive Surgery Did Not Improve Recovery of Function

Recently, a novel clinically feasible approach to enhance peripheral nerve regeneration after femoral nerve lesion in rats was suggested (Al-Majed et al. 2000; Brushart et al. 2005; Geremia et al. 2007; Gordon et al 2007). Briefly, low-frequency intraoperative electrical stimulation (IOES; 1 h, 20 Hz) was delivered to the proximal nerve stump of the severed nerve prior to surgical reconstruction. Stimulation led to depolarization of the motoneuron perikarya and a significant shortening of the period of asynchronous, "staggered" axonal regrowth (Al-Majed et al. 2000; Brushart et al. 2002). These beneficial effects were associated with a faster and enhanced upregulation of brain-derived neurotrophic factor (BDNF) and its tyrosine kinase B (TrkB) receptor in motoneurons (Al-Majed et al. 2004; English et al. 2007); in addition, TrkB-dependent expression of the HNK-1 (human natural killer cell antigen-1) glycoepitope was increased in the quadriceps branch of the femoral nerve (Eberhardt et al. 2006). Brief electrical stimulation after sciatic nerve injury also promoted axonal regeneration and attenuates facilitation of spinal motor responses (Vivó et al. 2008). Could this therapy be also successful after facial nerve lesion?

2.2.2.1 Animal Groups and Overview of Experiments

Forty-eight rats were distributed in three groups each of 16 animals. Group 1 consisted of intact rats and groups 2 and 3 consisted of experimental rats that were subjected to unilateral transection and suture of the right facial nerve (FFA; Fig. 2.1a). Rats in group 2 (sham stimulated, SS, Fig. 2.6b) had electrodes placed on the proximal stump after nerve transection, but no electric current was applied. Rats in group 3 were subjected to electrical stimulation of the facial nerve immediately after facial nerve transection but prior to end-to-end suture (Fig. 2.6a).

In groups 2 (SS) and 3 (ES), vibrissal motor performance was evaluated in the same animals at 1, 2, 3, and 4 months after surgery. The degree of axonal branching and pattern of motor endplate reinnervation were determined at the end of the experiment (i.e., 4 months). Vibrissal motor performance during explorative whisking was analyzed using VBMA. Following the last functional analysis 4 months post-surgery, half ($n = 8$) of the animals in all groups were used to investigate the degree of collateral axonal branching by using triple

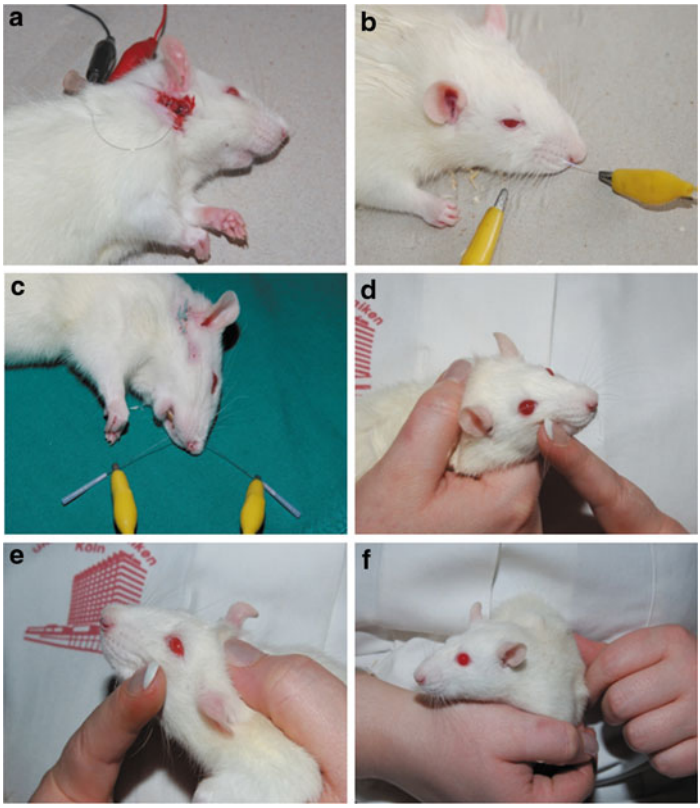

Fig. 2.6 (**a**–**f**) Intraoperative electrical stimulation of the proximal stump of the transected right facial nerve (**a**). Adopted from Skouras et al. (2009). (**b**) Sham stimulation of rats: acupuncture needle electrodes were inserted, but no current was applied to the electrodes (**c**) Postoperative electrical stimulation of the vibrissal muscles. Adopted from Sinis et al. 2009. (**d**) Manual mechanical stimulation of the right, i.e., ipsilateral to the nerve transection and suture (FFA) vibrissae and whisker pad muscles. (**e**) Manual mechanical stimulation of the left, i.e., contralateral to FFA vibrissae and whisker pad muscles. (**f**) Handling of the animals. Adopted from Angelov et al. (2007)

retrograde neuronal labeling. The remaining rats ($n = 8$) were used to determine the proportion of monoinnervated and polyinnervated motor endplates in the ipsilateral levator labii superioris muscle using immunocytochemistry for neuronal class III β-tubulin and histochemistry with alpha-bungarotoxin (see below).

2.2.2.2 Intraoperative Electrical Stimulation

IOES was performed as described by Ahlborn et al. (2007). The right facial nerve was exposed and a Teflon-coated stainless steel wire (50 μm in diameter, bared of

insulation at its tip) was twisted to form a loop around the nerve stump. A second electrode, used as an anode, was fixed to a muscle close to the nerve. In all electrically stimulated rats ($n = 16$), the threshold voltage required to elicit visible contractions of the whisker pad muscles was determined by applying square 0.1 ms pulses at 20 Hz at varying voltage intensities using a pulse generator (Master-8, A.M.P.I., Jerusalem, Israel). Immediately thereafter, the nerve stump was transected with fine scissors about 2 mm distally from the electrode. The proximal nerve stump was then stimulated for 1 h by applying square 0.1 ms pulses at 20 Hz using amplitudes three times above threshold levels (typically 3–4 V; Fig. 2.6a). Thereafter, the electrodes were removed, and the ends of the nerve were sutured with single epineural 11–0 nylon stitches (Ethicon, Norderstedt, Germany). Control sham-stimulated rats were treated similarly to rats subjected to ES except that no current was applied to the electrodes.

2.2.2.3

Analysis of Vibrissae Motor Performance

Analysis of vibrissae motor performance was performed as described (Sect. 2.1.1). At 1–4 months after nerve transection and sham stimulation (Groups 2a–d, Table 2.6), vibrissal motion was poor as compared with intact animals. The mean amplitude and angular velocity of vibrissal movements were reduced to 25–33% and 9–12% of control values, respectively (fourth and fifth column in Table 2.6), and the angle of maximal protraction was increased by more than 50% (third column in Table 2.6).

IOES (Groups 3a–d, Table 2.6) improved neither the amplitude of vibrissal movements nor the angle of maximal protraction as compared with sham stimulation. The angular velocity during protraction was, however, significantly higher (+52–92%) in electrically stimulated rats than in sham-stimulated rats at 1–3, but not at 4 months after surgery. We conclude that IOES does not improve the final outcome of FFA but causes some limited functional advantage in the first three postoperative months.

2.2.2.4

Application of Three Fluorescence Tracers, Fluorescence Microscopy, and Counting

In intact animals, motoneurons with axons entering the zygomatic, buccal, and marginal mandibular ramus were localized in the dorsal, lateral, and intermediate facial subnuclei, respectively (Semba and Egger 1986). No double- or triple-labeled motoneurons were observed because intact motoneurons send only one unbranched axon to one of the facialis rami (Fig. 2.2a). Thus, the index of axonal branching in the facial nerve trunk of intact animals, calculated from the zygomatic motoneurons (sum of the percentages in the third and fourth column of Table 2.7), was 0%.

Table 2.6 Motor recovery after facial nerve lesion and intraoperative electrical stimulation (IOES)

Group of animals	Frequency (in Hz)	Angle at maximal protraction (in degrees)	Amplitude (in degrees)	Angular velocity during protraction (in degrees/s)
1. Intact	7.0 ± 0.8	62.0 ± 13	57 ± 13	1,238 ± 503
2. FFA + SS				
2a. 1 month after FFA	5.8 ± 0.8	102 ± 8.9[#]	15 ± 2.4[#]	107 ± 26[#]
2b. 2 months after FFA-	6.3 ± 0.5	91 ± 12[#]	19 ± 6.1[#]	135 ± 54[#]
2c. 3 months after FFA-	6.1 ± 0.8	101 ± 15[#]	16 ± 4.2[#]	154 ± 38[#]
2d. 4 months after FFA	6.4 ± 0.9	111 ± 11[#]	14 ± 3.1[#]	114 ± 22[#]
3. FFA + IOES				
3a. 1 month after FFA	6.1 ± 1.1	99 ± 10[#]	13 ± 4.2[#]	205 ± 114[*#]
3b. 2 months after FFA	6.3 ± 1.2	80 ± 13[#]	17 ± 9.2[#]	235 ± 74[*#]
3c. 3 months after FFA	6.6 ± 1.1	93 ± 38	18 ± 13[#]	235 ± 53[*#]
3d. 4 months after FFA	6.4 ± 0.9	96 ± 11[#]	11 ± 6.1[#]	136 ± 48[#]

Biometrics of vibrissae motor performance in intact rats (*Intact*), in rats subjected to transection and suture of the facial nerve (FFA) plus 1 h intraoperative sham stimulation (FFA + SS) or 1 h intraoperative electrical stimulation (FFA + IOES) of the proximal stump of the transected facial nerve. All groups consisted of 16 rats. Shown are group mean values ± SD. Asterisks indicate differences between mean values of electrically (ES) and sham-stimulated (SS) animals (group 2a–d) at given postoperative time-point (ANOVA for repeated measurements and post hoc Tukey's test, $p < 0.05$)

[#]Indicate differences in mean values between intact rats and the experimental groups (ANOVA for repeated measurements and post hoc Tukey's test, $p < 0.05$) and show the expected decline in function

Four months after facial nerve cut and suture with sham stimulation (FFA-SS, Group 2), no myotopic organization into subnuclei was observed, i.e., all retrogradely labeled motoneurons were scattered throughout the facial nucleus (Fig. 2.2b). The same labeling pattern was observed when IOES was applied for 1 h prior to end-to-end suture (FFA-ES, Group 3). The lack of myotopy in all groups presumably reflects poor axonal pathfinding and misdirection of the regrowing axons after transection and suture of the facial nerve, a robust feature which could not be overridden by IOES. No fascicular orientation in the zygomatic, buccal, or marginal mandibular branches occurred.

Double and triple labeling was also commonly observed (Fig. 2.2b) and is explained by multiple axonal branches originating from individual perikarya (Shawe 1954) which grow simultaneously into different rami (i.e., zygomaticus, buccalis, and/or marginalis mandibulae); such sprouts retrogradely transported the different fluorescent dyes to their parent motoneurons in the facial nucleus.

Collateral axonal branching after transection of the facial nerve dramatically affected the fiber composition of the different nerve rami (Table 2.7). In intact rats (group 1), the total number of single-labeled (i.e., DiI-only + FG-only + FB-only) cells in the facial nucleus was 2,184 ± 242 but was increased to 3,622 ± 672 at 4 months after FFA plus sham stimulation (group 2) and to 3,233 ± 1,269 at 4 months after FFA + IOES (group 3). The high numbers of single-labeled motoneurons in the

Table 2.7 Degree of collateral axonal branching after facial nerve injury and intraoperative electrical stimulation (IOES)

Group of animals	Neurons projecting only into the zygomatic nerve (DiI-only)	Neurons projecting into the zygomatic and buccal nerves (DiI + FG)	Neurons projecting into the zygomatic and marginal mandibular nerves (DiI + FB)	All DiI labeled neurons projecting into the zygomatic nerve (DiI, DiI + FG, DiI + FB)	Neurons projecting only into the buccal nerve (FG-only)	Neurons projecting only into the mandibular nerve (FB-only)	Total number of single-labeled neurons (DiI-only + FG-only + FB-only)
1. Intact[1]	364 ± 47	–	–	364 ± 47	1441 ± 101	379 ± 94	2184 ± 242
	100%	0%	0%	100%			
2. 4 months	222 ± 35[#]	240 ± 29[#]	258 ± 56[#]	720 ± 120[#]	1911 ± 281[#]	1489 ± 356[#]	3622 ± 672[#]
FFA + SS	31%	33%	36%	100%			
3. 4 months	278 ± 114	161 ± 66[#]	181 ± 66[#]	619 ± 182[#]	1440 ± 709	1515 ± 446[#]	3233 ± 1,269[#]
FFA + IOES	45%	26%	29%	100%			

Number of motoneurons with axons in the zygomatic, buccal, or marginal mandibular branches of the facial nerve in intact rats (Intact), in rats subjected to transection and suture of the facial nerve (FFA) and 1 h intra-operative sham stimulation (FFA + SS) or 1 h electrical stimulation (FFA + IOES) of the proximal stump of the transected facial nerve. Animals were studied 10 days after triple retrograde labeling. At least eight animals were studied per group. Shown are group mean values ± SD. There were no significant differences between the stimulated group (3) and the nonstimulated group (2) (ANOVA, $p > 0.05$)

[#]Indicate significant differences (ANOVA, $p > 0.05$) between intact animals and the experimental group and show the expected increases in numbers of labeled neurons. The percentage values below the absolute numbers in columns 2–5 indicate the portions of motoneurons projecting through the zygomatic nerve with branched (DiI + FG or DiI + FB, column 3 and 4) and unbranched axons (DiI-only, column 2)

[1]Values have been adopted from Table 2.2

experimental groups following labeling of the buccal (FG-only) and marginal mandibular (FB-only), but not the zygomatic, branches (Table 2.7) indicate that other axons must have sprouted and entered these rami. Axons from the two other branches of the facial nerve (posterior auricular and cervical), while not labeled in intact animals, must presumably have sprouted into the zygomatic, buccal, and marginal mandibular rami (Table 2.7). However, the elevation revealed by retrograde tracing does not exceed the normal physiological number of neurons in the rat facial nucleus shown by other techniques [neuron-specific enolase (NSE) immunostaining: 4,066 ± 508 (Angelov et al. 1994); Nissl-staining: 3,835 ± 537 (Guntinas-Lichius et al. 1993); and retrograde labeling with horseradish peroxidase (Angelov et al. 1993; Streppel et al. 1998)]. Similar values are also seen at 1 (4,152 ± 166 facial neurons) and 8 weeks after facial nerve transection and suture (3,753 ± 273 facial neurons; Angelov et al. 1994). On the other hand, cell death after facial nerve axotomy occurs only if (1) rats are newborn (Umemiya et al. 1993; Clatterbuck et al. 1994; Rossiter et al. 1996; Moran and Graeber 2004), (2) the axotomy is followed by resection of approximately 1 cm nerve length which causes permanent deprivation from the target (Tetzlaff et al. 1988a, b), or (3) the facial nerve axotomy was performed in mice rather than in rats (de Bilbao and Dubois-Dauphin 1996; Deckwerth et al. 1996; Raivich et al. 1998, 1999; Moran et al. 2001). Taken together, the data indicate that motoneuron neurogenesis does not occur after facial nerve injury.

Retrograde tracing did not reveal any changes in the total numbers of single-labeled motorneurons (i.e., DiI-only + FG-only + FB-only) in the facial nucleus among the experimental groups (i.e., SS, ES; Table 2.7). The total number of single-labeled cells was 2,184 ± 242 in intact rats (group 1), 3,622 ± 672 after sham stimulation (FFA-SS, group 2), and 3,233 ± 1,269 following ES (FFA + IOES, group 3). Furthermore, the index of axonal branching was 55–69% (sum of the percentages of DiI + FG and DiI + FB retrogradely labeled perikarya in the third and fourth column of Table 2.7). In summary, the complete lack of myotopic organization, and a consistently elevated degree of axonal branching, suggested that IOES did not influence axonal projection patterns.

Pattern of target muscle reinnervation was estimated as described (Sect. 2.1.1).

In intact animals, all motor endplates were monoinnervated (Fig. 2.2d, f). After facial nerve injury, the proportion of polyinnervated motor endplates was 51 ± 10% after sham stimulation (FFA-SS, group 2) and 42 ± 4% after IOES (FFA + IOES, Fig. 2.2c, e; Table 2.8). Thus, IOES failed to improve the quality of muscle reinnervation. However, the total number of motor endplates did not differ either between any of the experimental groups or between the experimental groups and intact animals.

2.2.3 Postoperative Electrical Stimulation of Paralyzed Vibrissal Muscles Did Not Improve Recovery of Function

Another potential intervention is the POES of denervated muscles which, maintaining muscle mass and structural integrity, can counteract loss of muscle

Table 2.8 Quality of target muscle reinnervation after facial nerve injury and intraoperative electrical stimulation (IOES)

Group of animals	Mono-innervated motor end-plates (percent)	Poly-innervated motor end-plates (percent)	Non-innervated motor end-plates (percent)	Total number of motor end-plates examined
1. Intact rats	100 ± 0	0	0	1543 ± 132
2. 4 months after FFA+SS	46 ± 9.5#	51 ± 10#	2.7 ± 1.8#	1362 ± 134
3. 4 months after FFA+IOES	38 ± 7.1#	42 ± 4.1#	20 ± 4.2#	1179 ± 240

Innervation pattern of the levator labii superioris (LLS) motor endplates in intact rats (Intact), in rats subjected to transection and suture of the facial nerve (FFA) and 1 h intraoperative sham stimulation (FFA + SS) or electrical stimulation (FFA + IOES) of the proximal stump of the transected facial nerve. At least eight animals were studied per group. Shown are group mean values ± SD

#Indicate differences in mean values between intact rats and the experimental groups (ANOVA for repeated measurements and post hoc Tukey's test, $p < 0.05$) and show the expected changes in the quality of motor endplate innervation with no changes in their total numbers

excitability and muscle atrophy resulting from disuse (Kern et al. 2005; Salmons et al. 2005; Ashley et al. 2007, 2008; Salmons and Jarvis 2008). However, evidence has yet to be presented as to whether, and to what degree, preservation of a larger muscle mass and better functional properties of denervated muscles would promote functional recovery after facial nerve reconstruction.

2.2.3.1

Animal Groups and Overview of Experiments

Eighty rats were distributed in five groups each of 16 animals. Group 1 consisted of intact rats and groups 2–5 of experimental rats that were subjected to unilateral transection and suture of the right facial nerve (FFA; Fig. 2.1a). Animals in group 3 (Resection) underwent removal of approximately 1-cm nerve length from the three main branches of the facial nerve (see below). Rats in group 4 (operated, but sham stimulated, FFA + SS) had electrodes inserted in the denervated vibrissal muscles, but no electric current was applied (Fig. 2.6b). In group 5, the vibrissal muscles were subjected to ES (Fig. 2.6c).

Vibrissal motor performance during explorative whisking was analyzed in all rats using VBMA. Following the functional analysis at 2 months after operation, half ($n = 8$) of the animals in all groups were used to establish the degree of collateral axonal branching using triple retrograde neuronal labeling. The remaining rats ($n = 8$) were used to determine the proportion of monoinnervated and polyinnervated motor endplates in the m. levator labii superioris (LLS) using immunocytochemistry for neuronal class III β-tubulin, AChE, and histochemistry for alpha-bungarotoxin (see below).

Transection and suture of the facial nerve (FFA) was performed as described (Sect. 2.1.1).

2.2.3.2 Resection of the Facial Nerve

The main trunk of the facial nerve was unilaterally mobilized at its emergence from the stylomastoid foramen, and 8–10 mm length of the temporal, zygomatic, buccal, upper and lower divisions of the marginal mandibular branch were removed. This resection of the facial nerve is a very severe lesion in comparison with crush or transection of the nerve and delivers a permanent separation of the facial motoneurons from their target musculature.

2.2.3.3 Postoperative Electrical Stimulation

Operated rats were subjected to electrical stimulation (ES) of the vibrissal muscles three times a week (Monday, Wednesday and Friday) over 2 months starting on the first day after surgery. Electrical stimulation was delivered three times weekly since animals were required to be anesthetized. Under ketamin/xylazin anesthesia, two acupuncture needle electrodes were inserted toward levator labii superioris LLS, one along the uppermost vibrissal row A and the other in the lowest row D (Arvidsson 1982). The site of electrode placement close to the nose of the animal was thus somewhat distant (approximately 1 cm) to the location where the majority of LLS motor endplates are found, i.e., at the borderline between the cheek and whisker pad. The configuration thus allowed ES of the target muscles, the LLS, and part of the intrinsic vibrissal muscles close to the stimulating electrode, without the risk of direct damage to the motor endplates.

In all electrically stimulated rats ($n = 16$), the threshold voltage required to elicit visible contractions of the whisker pad muscles and movements of the whiskers was initially determined by applying square 0.1 ms pulses at various voltage intensities using an isolated pulse stimulator (Master-8-cp, A.M.P.I., Jerusalem, Israel). The frequency selected (5 Hz) resembled the frequency of normal whisking. The muscles were stimulated for 5 min by applying square 0.1 ms pulses with supra-threshold amplitudes (typically 3.0–5.0 V; Fig. 2.6c). This stimulation was sufficient to depolarize intramuscular axons but not muscle fibers, innervated or denervated, in which action potentials can be elicited only upon much “stronger” stimulation, e.g., pulses of 20 V amplitude and 5 ms duration for normal muscles and higher for denervated muscle fibers (Irintchev et al. 1990; Kern et al. 2002). Efficient muscle stimulation, especially that of denervated muscle fibers, requires delivery of high-voltage current pulses of long duration. This stimulation protocol was not approved by the Animal Welfare Committee in Cologne because of the concern that “strong” stimulation might elicit trigeminal pain. Control sham-stimulated rats were treated identically to rats subjected to ES except that no current was applied to the electrodes (Fig. 2.6b).

2.2.3.4 Analysis of Vibrissae Motor Performance

Analysis of vibrissae motor performance was performed as already described. Compared with intact animals, vibrissal motion was poor in rats receiving sham stimulation (FFA + SS, Group 4) or postoperative POES (FAA + POES; Group 5) of the vibrissal muscles. The mean amplitude was reduced to 16% and 20% of normal (fourth column in Table 2.9) and the angular velocity to 26% and 17% (fifth column in Table 2.9).

We also noted a specific time course of changes in the intensity of muscle contractions throughout the 2-month period of ES in which the stimulation parameters remained unchanged. Muscle contractions and vibrissal movements were readily visible during the first postoperative week. Thereafter they declined to zero (probably due to anterograde Wallerian axonal degeneration) and appeared again as reinnervation of endplates took place after 2–3 weeks. After the third postoperative week, it became increasingly difficult to elicit muscle contractions similar to those observed at the beginning of the treatment period (data not shown).

2.2.3.5 Application of Three Fluorescence Tracers, Fluorescence Microscopy and Counting

Application of three fluorescence tracers, fluorescence microscopy, and counting were performed as described above. Two months after facial nerve cut/anastomosis and sham stimulation (FFA + SS, Group 4), myotopic organization into subnuclei was no longer observed, i.e., all retrogradely labeled motoneurons were scattered throughout the facial nucleus (Fig. 2.2b). The same phenomenon was observed when FFA was combined with POES (Group 5). The lack of myotopy presumably arose because of poor axonal pathfinding and misdirection of the now

Table 2.9 Motor recovery after facial nerve injury and postoperative electrical stimulation (POES)

Group of animals	Frequency (in Hz)	Angle at maximal protraction (in degrees)	Amplitude (in degrees)	Angular velocity during protraction (in degrees/sec)
1. Intact	7.0 ± 0.8	62 ± 13	57 ± 13	1238 ± 503
2. FFA-only	6.3 ± 0.5	91 ± 12	19 ± 6	135 ± 54
3. Resection	7.0 ± 0.8	102 ± 16	16 ± 5	323 ± 170
4. FFA + SS	5.8 ± 0.7	99 ± 11	16 ± 2.4	323 ± 81
5. FFA + POES	5.6 ± 1.1	106 ± 33	20 ± 8	211 ± 93

Biometrics of vibrissae motor performance in intact rats (Intact), in rats subjected to transection and suture of the facial nerve (FFA-only), in rats that underwent removal of 1 cm length from the main branches of the facial nerve (Resection paradigm), in rats subjected to FFA plus postoperative sham stimulation (FFA + SS) or postoperative electrical stimulation (FFA + POES). All groups consisted of 16 rats. Shown are group mean values ± SD. No significant differences between the control group 4 (FFA + SS) and the group with electrically stimulated rats (ANOVA and post hoc Dunnett's test, $p < 0.05$) were detected. Data for groups 1–3 are given as reference and were not included in the analysis

highly branched regenerating axons after transection and suture of the facial nerve. No fascicular orientation in the zygomatic, buccal, or marginal mandibular branches occurred.

Double and triple labeling was also commonly observed (Fig. 2.2a). In addition, robust collateral branching at the lesion site resulted in the retrograde labeling of more motoneuronal perikarya in each of the individual facial nerve branches than in intact animals (Table 2.10). Such increases in axonal numbers, or their branches, in turn lead to hyperinnervation of peripheral muscle targets (Angelov et al. 1996; Streppel et al. 1998).

Retrograde tracing did not reveal any changes in the total numbers of single-labeled motoneurons (i.e., DiI-only + FG-only + FB-only; columns 1, 5, and 6 of Table 2.10) in the facial nucleus. The total number of single-labeled cells was 2,184 ± 242 in intact rats (group 1), 4,281 ± 830 after sham stimulation (FFA + SS, group 4), and 4,731 ± 756 following POES (FFA + POES, group 5).

The index of axonal branching following FFA and either of the treatments (SS or POES) was 57–62% (sum of the percentages of DiI + FG and DiI + FB retrogradely labeled perikarya in the third and fourth column of Table 2.10). In summary, the complete lack of myotopic organization, and a consistently elevated degree of axonal branching, suggested that POES did not influence axonal projection patterns.

Pattern of target muscle reinnervation was estimated as described earlier.

In intact animals, all motor endplates were monoinnervated (Fig. 2.2d, f). After facial nerve injury, the proportion of polyinnervated motor endplates was 49 ± 9.4% after sham stimulation (FFA + SS, Group 4) and 55 ± 14% after POES (FFA + POES, Fig. 2.2c, e; Table 2.11). Thus, POES failed to improve the quality of muscle reinnervation.

A very interesting and novel finding is the massive reduction, compared with other treatments, in the number of motor endplates, identified by the alpha-bungarotoxin-binding AChR, in the LLS at 2 months after ES. The total numbers of motor endplates observed in animals subjected to SS was 1,398 ± 415. Following POES, this number was reduced to approximately 24% of the value in the SS-group.

This observation has several possible explanations. First, many muscle fibers in the electrically stimulated vibrissal muscles have not been innervated, have degenerated, and have disappeared rapidly (Schmalbruch et al. 1991; Dedkov et al. 2001). Alternatively, it is quite possible that the vast majority of muscle fibers in ES muscles persisted, though strongly atrophied, in a denervated state. It has been shown (though in humans) that muscle fibers persist in an atrophic state for several years in denervated muscles before they are replaced by connective tissue (Sunderland 1950; Schwarting et al. 1984). In favor of this possibility was the observation that the diameters of most muscle fibers in FFA + POES rats appeared smaller than in animals subjected to FFA + SS. Finally, it could be that the atrophied fibers seen were actually newly formed, having regenerated in the absence of the nerve and were therefore without endplates. On this basis, POES has promoted regeneration of muscle fibers.

To find more direct evidence for denervated atrophied muscle fibers, we stained representative sections from all electrically stimulated animals with

Table 2.10 Degree of collateral branching after facial nerve injury and postoperative electrical stimulation

Group of animals	Neurons projecting only into the zygomatic nerve (DiI-only)	Neurons projecting into the zygomatic and buccal nerves (DiI + FG)	Neurons projecting into the zygomatic and marginal mandibular nerves (DiI + FB)	All DiI labeled neurons projecting into the zygomatic nerve (DiI, DiI + FG, DiI + FB)	Neurons projecting only into the buccal nerve (FG-only)	Neurons projecting only into the marginal mandibular nerve (FB-only)
1. Intact	364 ± 47 100%	– 0%	– 0%	364 ± 47 100%	1,441 ± 101	379 ± 94
2. FFA-only	213 ± 53 30%	239 ± 52 34%	257 ± 56 36%	709 ± 178 100%	1,908 ± 289	1,488 ± 356
3. Resection	0	0	0	0	0	0
4. FFA + SS	228 ± 165 43%	159 ± 98 30%	138 ± 79 27%	525 ± 342 100%	2,172 ± 256	1,881 ± 409
5. FFA + POES	321 ± 120 38%	237 ± 102 28%	276 ± 83 34%	834 ± 305 100%	2,254 ± 374	2,156 ± 262

Number of motoneurons with axons in the zygomatic, buccal, or marginal mandibular branches of the facial nerve in intact rats (Intact), in rats subjected to transection and suture of the facial nerve (FFA-only), in rats that underwent removal of 1 cm length from the main branches of the facial nerve (Resection paradigm), in rats subjected to FFA plus postoperative sham stimulation (FFA + SS) or postoperative electrical stimulation (FFA + POES). The percentage values below the absolute numbers in columns 2–5 indicate the portions of motoneurons projecting through the zygomatic nerve with branched (DiI + FG or DiI + FB, column 3 and 4) and unbranched axons (DiI-only, column 2). Animals were studied 10 days after triple retrograde labeling. At least eight animals were studied per group. Shown are group mean values ± SD. No significant differences between the control group 4 (FFA + SS) and the group with electrically stimulated rats (ANOVA and post hoc Dunnett's test, $p < 0.05$) were detected. Data for groups 1 and 2 are given as reference and were not included in the analysis

Table 2.11 Quality of target muscle reinnervation after facial nerve injury and postoperative electrical stimulation (POES)

Group of animals	Monoinnervated motor endplates (%)	Polyinnervated motor endplates (%)	Noninnervated motor endplates (%)	Total number of motor endplates in LLS muscle
1. Intact rats	100 ± 0	0	0	1,543 ± 132
2. FFA-only	45 ± 9.6	53 ± 10	2.6 ± 1.8	1,326 ± 413
3. Resection	3.1 ± 0.6	1.6 ± 0.4	95 ± 22	416 ± 113
4. FFA + SS	49 ± 7.7	49 ± 9.4	2.4 ± 0.8	1,398 ± 415
5. FFA + POES	4.4 ± 1.8*	5.5 ± 1.4*	91 ± 25*	346 ± 189*

Innervation pattern of the m. levator labii superioris (LLS) motor endplates in intact rats (Intact), in rats subjected to transection and suture of the facial nerve (FFA-only), in rats that underwent removal of 1 cm length from the main branches of the facial nerve (Resection paradigm), in rats subjected to FFA plus postoperative sham stimulation (FFA + SS) or postoperative electrical stimulation (FFA + POES). At least eight animals were studied per group. Shown are group mean values ± SD. Asterisks indicate difference between groups 4 (FFA + SS) and 5 (FFA + POES) at 2 months after surgery (ANOVA and post hoc Dunnett's test, $p < 0.05$). Data for groups 1–3 are given as reference and were not included in the analysis

both alpha-bungarotoxin and goat anti-AchE (Jevsek et al. 2004). Binding of anti-AchE was visualized by anti-goat IgG CY3 conjugate. We expected to see both innervated (alpha-bungarotoxin- and esterase-positive) endplates and denervated endplates outlined by AChE, an enzyme which can persist, in contrast to the AChRs, for months after denervation of muscles limb and trunk muscles (Lomo and Slater 1980; Decker and Berman 1990). Surprisingly, our analysis showed that postsynaptic AChE was present only in association with postsynaptic nicotinic AChRs. The only explanation for this unexpected result was that endplates in facial muscles, in contrast to limb musculature (Gordon et al. 2007, 2008), lose rapidly, within less than 2 months, both endplate markers, AChE and receptors.

To prove this possibility, we permanently denervated all vibrissal muscles in a group of rats ($n = 16$) by resection of the facial nerve. Two months after the operation, the LLS muscles were indeed completely denervated as indicated by the reduction in the total number of motor endplates and by the absence of beta-tubulin-positive axons.

Altogether, our results show that the POES treatment leads to partial muscle reinnervation after FFA, a procedure normally followed by complete muscle innervation (Angelov et al. 1996).

2.2.4

Manual Stimulation of Paralyzed Vibrissal Muscles Following Facial Nerve Injury Promoted Full Recovery of Whisking

Following denervation and before reinnervation, several changes also occur within the muscle including loss of muscle bulk and circulation; connective

tissue also shrinks and becomes adherent (fibrosis; Eccles 1944; Sunderland 1950; Bardosi et al. 1987). After several months of complete denervation, muscle membrane properties change, becoming relatively nonresponsive to electrical stimulation (Schwarting et al. 1984; Lieber 1992; Stennert et al. 1994). For patients expected to have nerve regrowth after complete denervation, it is important to minimize fibrosis within the muscle connective tissue so that there will be movable muscle structures after muscle reinnervation to allow reacquisition of the contractile proteins that make muscles work (Lömo and Westgaard 1974; Mokrusch et al. 1990; Nix 1990; McCulloch and Nelson 1995). On the basis of clinically established positive benefits of soft tissue massage, supposed to promote muscle blood flow and to keep in optimum condition while awaiting nerve recovery (Hovind and Nielsen 1974; Beurskens 1990; Frach et al. 1992; Coulson 2005), we tested the effect(s) of manual mechanical stimulation of denervated vibrissal muscles after FFA.

2.2.4.1

Animal Groups and Overview of Experiments

One hundred and eight rats were used with one intact control group and six experimental groups (Table 2.12).

Table 2.12 Experimental design chart depicting animal grouping, treatments and parameters investigated

Group of animals	Video-based motion analysis of vibrissae motor performance	Degree of collateral axonal branching as estimated by triple retrograde labeling	Pattern of reinnervation of motor endplates in m. levator labii superioris
1. Intact animals (16 rats)	16	8	8
2. Animals with right FFA (16 rats)	16	8	8
3. Animals with right FFA + EE (16 rats)	16	8	8
4. Animals with right FFA + right MS (32 rats)	32	8	8
5. Animals with right FFA + EE + right MS (16 rats)	16	8	8
6. Animals with right FFA + left MS (six rats)	6	–	6
7. Animals with right FFA + handling (six rats)	6	–	6

Animal grouping and procedures, e.g., facial–facial anastomosis (FFA), dwelling in enriched environment (EE), mechanical stimulation of the vibrissal muscles (MS). In groups 1–5, the animals that underwent video-based motion analysis were subsequently used for estimation the degree of collateral axonal branching. In groups 6 and 7, the animals that were subjected to video-based motion analysis were thereafter used for establishing the pattern of motor endplates reinnervation

Group 1 consisted of 16 intact rats and group 2 of 16 experimental rats which were subjected to unilateral transection and suture of the right facial nerve (FFA) and left to survive for 2 months. In both groups, all rats were used to determine vibrissal motor performance during explorative whisking using VBMA. Thereafter half of these animals were used to establish the degree of collateral axonal branching ipsilaterally by means of retrograde neuronal labeling. Part of the results obtained for group 1 and 2 has already been published (Guntinas-Lichius et al. 2005). The remaining eight rats in both groups were used to determine the proportion of monoinnervated and polyinnervated motor endplates in the ipsilateral levator labii superioris muscle by means of immunocytochemistry for neuronal class III-tubulin and histochemistry with alpha-bungarotoxin (see below).

In groups 3–7, rats underwent unilateral FFA plus subsequent treatments. The animals of group 3 (16 rats) received environmental stimulation for 2 months in an enriched environment (EE). The animals of group 4 (32 rats) received manual stimulation (MS) of the right whisker pad muscles and the animals of group 5 (16 rats) experienced an enriched environment plus manual stimulation of the right whiskers (EE + MS). Vibrissal motor performance, the degree of axonal branching, and patterns of motor endplate reinnervation were then analyzed.

Groups 6 and 7 consisted of six rats each. Animals in group 6 received FFA on the right side and manual stimulation of the intact contralateral (left) whisker pad muscles. Rats in group 7 received no stimulation of the vibrissal muscles but were handled by the experimentor in exactly the same way as occurred during MS except that MS was not used ("handling").

2.2.4.2 Surgery

Transection and end-to-end suture of the right facial nerve (FFA) were performed as described. Animals were kept in different conditions (see below) for 2 months.

2.2.4.3 Standard Housing/Enriched Environment

After surgery, all animals were allowed to recover in individual cages for 24 h. Thereafter, rats from groups 2, 4, 6, and 7 were placed in *standard* cages (425 mm × 266 mm × 185 mm; polycarbonate; Techniplast, Buguggiate, Italy), each cage with two rats.

All 16 rats in group 3 were placed together in specifically designed cages (three cages size 610 mm × 435 mm × 215 mm connected in a row via polycarbonate tunnels; Techniplast, Buguggiate, Italy) where they experienced group living and an enriched environment consisting of horizontal and inclining platforms and various toys (hanging robes, bridges, tunnels, climbing ladders, and balls). Objects and toys were randomly circulated by removing some and adding others during the course of the experiment (cf. van Praag et al. 2000). All 16 rats of group

5 were treated in an identical way, but they received in addition mechanical stimulation of the vibrissal muscles (see below).

2.2.4.4

Mechanical Stimulation of the Vibrissal Muscles

Mechanical stimulation (both, manual as well as environmental) was initiated 1 day after surgery. Rats were daily subjected to gentle rhythmic forward stroking of the right (groups 4 and 5) or left (group 6) vibrissae and whisker pad muscles (Fig. 2.5d, e) 5 days a week. Rats of groups 5 and 6 were manually stimulated for 5 min a day and rats of group 4 were further distributed into four subgroups (4a, 4b, 4c, and 4d) that were stimulated daily for 1 min, 2 min, 5 min, and 10 min, respectively. The pattern of manual stimulation that we selected mimicked the natural active vibrissal movements during whisking, that is, active protraction and passive retraction (Welker 1964; Wineski 1985). Animals rapidly became accustomed to this procedure within 2–3 days and did not show any signs of stress such as freezing or trying to bite, weight loss, or lack of grooming; rather, animals readily cooperated.

2.2.4.5

Handling of the Animals

All six rats of group 7 were subjected to daily "handling". Starting from the first day after FFA, animals were carefully taken by an investigator out of the cage and held as if they were to receive MS for 5 min (Fig. 2.5f). Thereafter, rats were put back in the cages.

Analysis of vibrissae motor performance was performed as described above.

Recovery of vibrissal motion after facial nerve injury (1) alone, i.e., no mechanical stimulation, (2) after mechanical stimulation for 1 and for 2 min only, (3) after stimulation of the contralateral vibrissal muscles, and (4) after postoperative handling was poor most likely due to inadequate muscle function during protraction and retraction (Berg and Kleinfeld 2003): the amplitude of movements and the angular velocity were reduced to less than 40% and 23% of the values in intact animals, respectively (Table 2.13). Frequency of whisking after nerve repair was similar to that in intact rats (see second column in Table 2.13) which may be due to the robust autonomy and capacity of the whisking pattern generator, represented mostly by neurons projecting to the facial nucleus from the brainstem (Popratiloff et al. 2001; Hattox et al. 2002; Veinante and Deschenes 2003).

Manual stimulation of the ipsilateral whiskers for 5 and 10 min daily had a dramatic effect, resulting in a return of normal whisking as indicated by the amplitude of movement (Fig. 2.7a), as well as by the speed during protraction (Table 2.13). Stimulation by an enriched environment did not result in a return of function although combined stimulation (manual and environmental) did (Table 2.13).

Table 2.13 Motor recovery after facial nerve injury and mechanical stimulation

Group of animals	Frequency (in Hz)	Angle at maximal protraction (in degrees)	Amplitude (in degrees)	Angular velocity during protraction (in degrees/s)
1. Intact	7.0 ± 0.8	62.0 ± 13.2*	57 ± 13*	1,238 ± 503*
2. Right FFA[a]	6.3 ± 0.5	91 ± 12[#]	19 ± 6[#]	135 ± 54[#]
3. Right FFA + EE	6.8 ± 0.9	76 ± 6*	26 ± 5[#]	490 ± 187[#]
4a. Right FFA + right MS for 1 min	6.5 ± 0.5	89 ± 6.2	13 ± 4	175 ± 68
4b. Right FFA + right MS for 2 min	6.8 ± 0.9	91 ± 10	14 ± 7	159 ± 127
4c. Right FFA + right MS for 5 min	6.6 ± 0.5	66 ± 15*	51 ± 19*	1,019 ± 408*
4d. Right FFA + right MS for 10 min	6.8 ± 0.8	70 ± 11*	36 ± 18*	781 ± 329*
5. Right FFA + EE + right MS	7.8 ± 2.3	65 ± 16*	55 ± 20*	1,124 ± 358*
6. Right FFA + left MS	6.7 ± 1.0	94 ± 9.5[#]	20 ± 9.5[#]	368 ± 118[#]
7. Right FFA + Handling	6.7 ± 0.8	104 ± 10.1[#]	18 ± 3.4[#]	316 ± 71[#]

Biometrics of vibrissae motor performance in intact rats (*Intact*), in rats after transection and suture of the right facial nerve only (*right FFA-only*), in rats subjected to FFA and postoperative dwelling in enriched environment (*right FFA + EE*), in rats that were subjected to FFA and postoperative mechanical stimulation of the right vibrissal muscles *(right FFA + right MS),* in rats subjected to combined treatment *(right FFA + EE + right MS),* in rats that were subjected to FFA and postoperative mechanical stimulation of the left vibrissal muscles *(right FFA + left MS),* and in rats subjected to FFA and postoperative handling (*right FFA + handling*). Groups 1–3 and 5 consisted of eight animals, group 4 of 32 rats, and groups 6 and 7 of six animals. Shown are group mean values ± SD. Significant differences between group mean values (ANOVA and post hoc Tukey's test, $p < 0.05$): * – from FFA, [#] – from Intact, FFA + MS and FFA + EE + MS
[a]Values adopted from Guntinas-Lichius et al. (2005)

2.2.4.6
Application of Three Fluorescence Tracers, Fluorescence Microscopy and Counting

The estimated index of axonal branching was 70% (Fig. 2.7b). None of the stimulation paradigms, i.e., manual, environmental, or combined, had any significant influence on the projection patterns (Table 2.14). Thus, there was a complete lack of myotopic organization, increased total numbers of projecting motoneurons, and a consistently elevated degree of axonal branching regardless of whether the animals were subjected to any of the stimulation paradigms or not.

2.2.4.7
Pattern of Target Muscle Reinnervation

In intact animals, all motor endplates were monoinnervated (Fig. 2.2d, f). After facial nerve injury and no stimulation, 53% were polyinnervated, i.e., innervated by two or more axons (Fig. 2.2c, e; Table 2.15). However, manual, but not environmental, stimulation significantly reduced the degree of polyinnervated

Table 2.14 Degree of collateral axonal branching after facial nerve injury and mechanical stimulation

Group of animals	Neurons projecting only into the zygomatic nerve (DiI-only)	Neurons projecting into the zygomatic and buccal nerves (DiI + FG)	Neurons projecting into the zygomatic and marginal mandibular nerves	All DiI labeled neurons projecting into the zygomatic nerve (DiI, DiI + FG, DiI + FG)	Neurons projecting only into the buccal nerve (FG-only)	Neurons projecting only into the marginal mandibular nerve (FB-only)
1. Intact[a]	364 ± 47 100%	– 0%	– 0%	364 ± 47 100%	1,441 ± 101	379 ± 94
2. FFA[a]	213 ± 53 30%	239 ± 52$^{\#}$ 34%	257 ± 56$^{\#}$ 36%	709 ± 178$^{\#}$ 100%	1,908 ± 289$^{\#}$	1,488 ± 356$^{\#}$
3. FFA + EE	208 ± 164 45%	140 ± 78$^{\#}$ 30%	117 ± 76$^{\#}$ 25%	465 ± 234 100%	2,871 ± 268$^{*\#}$	2,484 ± 409$^{*\#}$
4. FFA + MS for 5 min daily	276 ± 219 36%	268 ± 149$^{\#}$ 35%	211 ± 105$^{\#}$ 29%	756 ± 251$^{\#}$ 100%	3,162 ± 342$^{*\#}$	2,614 ± 184$^{*\#}$
5. FFA + EE + MS	351 ± 178 43%	286 ± 137$^{\#+}$ 35%	174 ± 113$^{\#}$ 12%	810 ± 256$^{\#}$ 100%	2,790 ± 432$^{*\#}$	1,986 ± 210$^{*\#\S}$

Number of motoneurons with axons in the zygomatic, buccal, or marginal mandibular branches of the facial nerve of intact rats (*Intact*), in rats after transection and suture of the right facial nerve *(FFA-only)*, in rats subjected to postoperative dwelling in enriched environment (*FFA + EE*), in rats that received postoperatve manual stimulation of the vibrissal hairs *(FFA + MS)* and in rats subjected to combined treatment *(FFA + EE + MS)*. The animals were studied 10 days after triple retrograde labeling performed 56 days post-surgery. At least eight animals were studied per group. Shown are group mean values ± SD. Significant differences between group mean values (ANOVA and post hoc Tukey's test, $p < 0.05$): * – from FFA; # – from Intact; + – from FFA+EE; § – from FFA + EE and FFA + MS. The percentage values below the absolute numbers in columns 2–5 indicate the portions of motoneurons projecting through the zygomatic nerve with branched (DiI + FG or DiI + FB, column 3 and 4) and unbranched axons (DiI-only, column 2)

[a]Values adopted from Guntinas-Lichius et al. (2005)

Table 2.15 Quality of target muscle reinnervation after facial nerve injury and mechanical stimulation

Group of animals	Monoinnervated motor endplates (%)	Polyinnervated motor endplates (%)	Noninnervated motor endplates (%)	Total number of motor endplates examined
1. Intact	100 ± 0	0	0	1,543 ± 132
2. Right FFA	45 ± 9.6	53 ± 10	2.6 ± 1.8	1,326 ± 413
3. Right FFA + EE	50 ± 15	41 ± 15	8.9 ± 5.0*	1,411 ± 441
4 d. Right FFA + right MS (5 m daily)	69 ± 7.9*#	22 ± 5.1*#	9.6 ± 3.9*	1,640 ± 338
5. Right FFA + EE + right MS	66 ± 11*	31 ± 10*	2.7 ± 2.0§	1,345 ± 319
6. Right FFA + left MS	38 ± 7	60± 13	2.0 ± 1.6	1,237 ± 249
7. Right FFA + handling	39 ± 6	57 ± 12	5.0 ± 2.1	1,402 ± 235

Reinnervation pattern of the levator m. labii superioris (LLS) motor endplates in intact rats (*Intact*), in rats after transection and suture of the right facial nerve only (*right FFA-only*), in rats subjected to FFA and postoperative dwelling in enriched environment (right *FFA + EE*), in rats subjected to FFA and postoperative manual mechanical stimulation of the right vibrissal muscles *(right FFA + right MS)*, in rats subjected to combined treatment *(right FFA + EE + right MS)*, in rats subjected to FFA and postoperative mechanical stimulation of the left vibrissal muscles *(right FFA + left MS)*, and in rats subjected to FFA and postoperative handling (*right FFA + handling*). Motor endplates were classified as monoinnervated, polyinnervated, or noninnervated according to the number of beta-tubulin-immunoreactive axons that crossed the boundaries of the endplate. Groups 1–5 consisted of eight animals, groups 6 and 7 of six rats. Shown are group mean values ± SD. Significant differences between group mean values (ANOVA and post hoc Turkey's test, $p < 0.05$): * – from FFA; # – from FFA + EE; § – from FFA + EE and FFA-MS. Values for intact rats are given as reference values and not included in the analysis

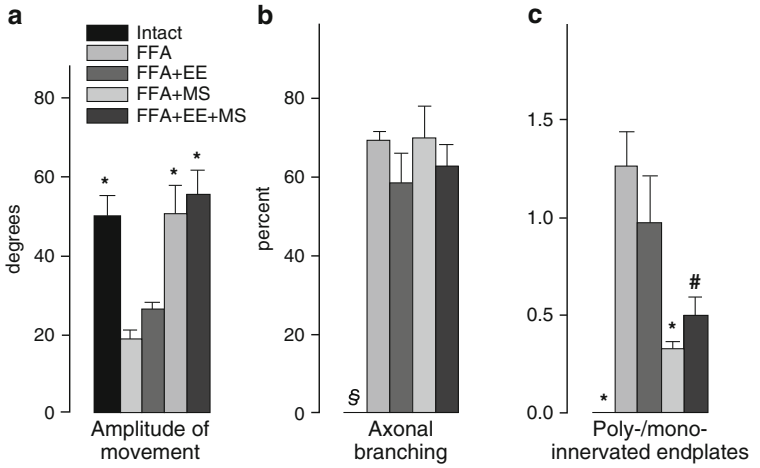

Fig. 2.7 (**a**–**c**) Structural correlates of muscle function. Shown are values of major parameters evaluated in (always from *left* to *right*): intact rats (*Intact*), rats subjected to no mechanical stimulation (*FFA*), enriched environment *(FFA + EE*), mechanical stimulation (*FFA + MS*) or combined treatment (*FFA + EE + MS*) for 2 months after facial–facial anastomosis (FFA). Mechanical stimulation (*FFA + MS*), but not enriched environmental housing (*FFA + EE*), leads to full recovery of the amplitude of vibrissal motion (**a**). The extent of axonal branching in the facial nerve trunk is not influenced by any of the stimulation protocols (**b**). The ratio of polyinnervated to monoinnervated motor endplates is strongly reduced as a result of manual but not of environmental stimulation (**c**). The index of axonal branching represents the ratio of motoneurons projecting branched axons into the zygomatic and the buccal or mandibular branch to motoneurons with unbranched axons innervating the zygomatic branch only. Note that the values of the two structural parameters shown are 0 in intact animals. Values are the mean ± SEM. Groups indicated by symbols are significantly different ($p < 0.05$, ANOVA and Tukey's post hoc test) compared with: * – groups FFA and FFA + EE; # – group FFA; § – all other groups. Adopted from Angelov et al. (2007)

endplates (22% and 41%, respectively), whereas the combination of both had an intermediate effect (31%; Table 2.15). Thus, manual stimulation reduced the ratio of polyinnervated to monoinnervated endplates by a factor of 4 compared with untreated rats and to a level, which did not differ statistically from intact animals (Fig. 2.7c).

2.2.5

Manual Stimulation of Facial Muscles Improved Functional Recovery After Hypoglossal–Facial Anastomosis or Interpositional Nerve Grafting

Encouraged by the improvement in function by using MS after FFA (Angelov et al. 2007), we examined whether the same simple rehabilitation technique would be

also effective following two other common types of facial nerve reconstruction, hypoglossal–facial anastomosis (HFA), and interpositional nerve grafting (IPNG).

2.2.5.1
Animal Groups and Overview of Experiments

One hundred and twelve rats were used with one intact control group and six experimental groups (Table 2.16). Group 1 ($n = 16$) consisted of intact rats and groups 2–4 of experimental rats ($n = 16$ in each group) subjected to unilateral:

- Transection and suture of the right facial nerve (FFA)
- Transection of the right facial and hypoglossal nerves and suture of the proximal hypoglossal stump to the distal facial nerve stump (HFA)
- Interpositional facial nerve grafting (IPNG) with the great auricular nerve

In groups 5–7 ($n = 16$ per group), rats underwent unilateral FFA, HFA, or IPNG followed by manual mechanical stimulation (MS) of the right whisker pad muscles. Estimation of (1) vibrissal motor performance, (2) degree of axonal branching, and (3) pattern of motor endplate reinnervation was undertaken at 2 months in all experimental groups. Data for stimulated animals were compared with nonstimulated ones.

Vibrissal motor performance during explorative whisking was analyzed in all rats using VBMA. Following functional analysis, half ($n = 8$) of the animals in all groups were used to establish the degree of collateral axonal branching using triple retrograde neuronal labeling. The remaining rats ($n = 8$) were used to determine the proportion of monoinnervated and polyinnervated motor endplates in the ipsilateral levator labii superioris muscle using immunocytochemistry for

Table 2.16 Experimental design chart depicting animal grouping and procedures

Group of animals	Video-based motion analysis of vibrissae motor performance	Degree of collateral axonal branching as estimated by triple retrograde labeling	Pattern of reinnervation of the motor endplates in m. levator labii superioris
1 Intact animals (16 rats)[a]	16	8	8
2. Animals with FFA-only (16 rats)[a]	16	8	8
3. Animals with HFA-only (16 rats)	16	8	8
4. Animals with IPNG-only (16 rats)	16	8	8
5. Animals with FFA + MS (16 rats)[a]	16	8	8
6. Animals with HFA + MS (16 rats)	16	8	8
7. Animals with IPNG + MS (16 rats)	16	8	8

Animal grouping and procedures, e.g., facial–facial anastomosis (FFA), hypoglossal–facial anastomosis (HFA), interpositional nerve grafting (IPNG), manual mechanical stimulation of the vibrissal muscles (MS). All animals underwent video-based motion analysis. Thereafter, one half were used for estimation the degree of collateral axonal branching and the other half for establishing the pattern of the motor endplates reinnervation

[a]Data adopted from Angelov et al. (2007)

neuronal class III β-tubulin and histochemistry with alpha-bungarotoxin (see below). Some data, i.e., those obtained for groups 1, 2 and 5, have been published previously (Angelov et al. 2007).

Transection and end-to-end suture of the right facial nerve (FFA) were performed as described above.

2.2.5.2 Hypoglossal–Facial Anastomosis

The hypoglossal nerve was exposed and transected distally to its union with the upper root of the ansa cervicalis but proximally to its bifurcation into medial and lateral branches. The facial nerve was transected at its emergence from the foramen stylomastoideum but distal to its posterior auricular branch. The proximal stump of the hypoglossal nerve was then microsurgically sutured to the distal stump of the facial nerve (Fig. 2.8a).

2.2.5.3 Interpositional Nerve Grafting

The right facial nerve was exposed and transected 2–3 mm distal to its emergence from the stylomastoid foramen. The great auricular nerve *(n. auricularis magnus)* was exposed and a 5–6 mm length removed. The great auricular nerve graft was inserted between the transected ends of the facial nerve and microsurgically sutured to each end (Fig. 2.8c).

Manual mechanical stimulation (MS) and *analysis of vibrissae motor performance* were performed as described above.

Recovery of vibrissal motion after FFA, HFA, or IPNG alone, i.e., with no subsequent mechanical stimulation of vibrissal muscles, was poor as demonstrated by inadequate muscle function during protraction and retraction. Although the frequency of whisking was similar to that in intact animals, the amplitude of movement was reduced to less than 40% and the angular velocity during protraction to about 15% of the values in intact animals (Table 2.17).

Manual stimulation had a beneficial effect on the whisking amplitude, resulting in either complete restoration in animals subjected to FFA (from 19° ± 6° to 51° ± 19°, as reported previously: Angelov et al. 2007) or to its significant increase in animals subjected to HFA (from 21° ± 4° to 30° ± 5°) or to IPNG (from 19° ± 4° to 30° ± 6°).

Application of three fluorescence tracers, fluorescence microscopy, and counting were performed as already described.

After FFA, myotopic organization of the facial nucleus into subnuclei was lost, i.e., all retrogradely labeled motoneurons were scattered throughout the entire facial nucleus (Fig. 2.2b). Double- and triple-labeled motoneurons were commonly observed due to the formation of collateral axon branches innervating two or three facial nerve rami resulting in a branching index of 70% (Table 2.18). Each individual nerve ramus therefore contained axons, or axonal branches, of

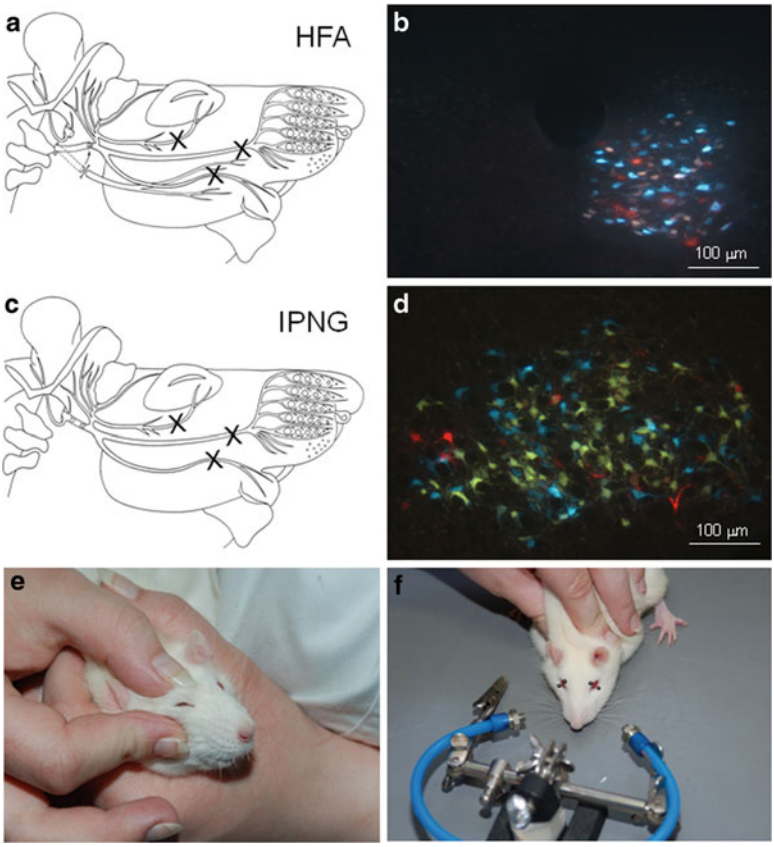

Fig. 2.8 (**a**–**f**) Schematic drawings of the infratemporal portion of the rat facial nerve. Transection of the facial and hypoglossal nerves with subsequent end-to-end suture of the proximal hypoglossal stump to the distal facial fragment indicated by an *arrow* (**a**). Transection of the facial nerve with subsequent end-to-end suture with the interpositional nerve graft (*arrow*) between the proximal and distal facial fragments (**c**). Two months after HFA (**b**) or IPNG (**d**), the myotopic organization is lost irrespective of whether the animals were stimulated or unstimulated. Adopted from Guntinas-Lichius et al. (2007). (**e**) Manual mechanical stimulation of the right, i.e., ipsilateral to the facial nerve transection orbicularis oculi muscle (OOM). (**f**) The blink reflex was evaluated utilizing custom-designed apparatus that delivered a constant 20 ml volume of an air puff to the cornea and periorbital region at a distance of 3 cm. Adopted from Bischoff et al. (2009)

more motoneurons than in intact animals resulting in target hyperinnervation (Rich and Lichtman 1989; Angelov et al. 1996).

After hypoglossal–facial anastomosis and triple retrograde labeling, two major changes, characteristic of aberrant reinnervation of targets, were detected. First, the hypoglossal nucleus lacked somatotopy, i.e., perikarya were not organized into a dorsal subnucleus (with axons projecting into the lateral hypoglossal nerve

Table 2.17 Recovery of whisking function after facial nerve reconstruction and subsequent treatment

Group of animals	Frequency (in Hz)	Angle at maximal protraction (in degrees)	Amplitude (in degrees)	Angular velocity during protraction (in degrees/s)
1. Intact rats[a]	7.0 ± 0.8	62 ± 13	57 ± 13	1,238 ± 503
2. Rats with FFA-only[a]	6.3 ± 0.5	91 ± 12*	19 ± 6.0*	135 ± 54*
3. Rats with HFA-only	6.8 ± 0.6	96 ± 12	21 ± 4.0**	363 ± 177
4. Rats with IPNG-only	7.5 ± 0.8	92 ± 8.2	19 ± 4.0***	406 ± 191
5. Rats with FFA + MS[a]	6.6 ± 0.5	66 ± 15*	51 ± 19*	1,019 ± 408*
6. Rats with HFA + MS	7.6 ± 0.9	91 ± 10	30 ± 5.0**	437 ± 159
7. Rats with IPNG + MS	7.5 ± 0.5	83 ± 16	30 ± 6.0***	382 ± 87

Biometrics of vibrissae motor performance in *intact* animals and in rats that received no postoperative treatment (*FFA-only, HFA-only and IPNG-only*). The other three groups of animals were subjected to daily manual mechanical stimulation (MS) of the vibrissal muscles and hence named FFA + MS, HFA + MS, and IPNG + MS. All groups consisted of 16 animals. Shown are group mean values ± SD. Mean values of a given "stimulated" group (Nr. 5–7) that were significantly different (ANOVA and post hoc Tukey's test, $p < 0.05$) from the respective nonstimulated group (Nr. 2–4) are indicated by *, **, and ***. Values for intact rats are given as reference values and not included in the analysis

[a]Data adopted from Angelov et al. (2007)

branch) and ventral subnucleus (axons projecting into the medial branch of the hypoglossal nerve; Krammer et al. 1979; Uemura-Sumi et al. 1988). Second, the entire hypoglossal nucleus contained double- or triple-labeled motoneuronal perikarya (Fig. 2.8b). Loss of somatotopy was due to transection of the hypoglossal nerve proximally to its bifurcation into its medial and lateral branches and subsequent inaccurate navigation of regrowing neurites into inappropriate branches. Double- and triple-labeled motoneurons arose due to collateral axonal branching at the lesion site. The branching index was 56% (Table 2.18).

Following IPNG and triple retrograde labeling, changes in the facial nucleus were very similar to those observed after FFA: i.e., myotopy was absent and double- and triple-labeled motoneurons were observed throughout (Fig. 2.8c, d). Counts revealed a branching index of 63% (Table 2.18). Following IPNG, the number of retrogradely labeled motoneurons was smaller after applying tracer to the zygomatic (Table 2.18, group 4, fifth column) as compared with the buccal (Table 2.18, group 4, sixth column) and marginal mandibular branches (Table 2.18, group 4, seventh column). The data suggest that IPNG exerts a negative effect on the regrowth of axons into the zygomatic compared with the buccal and marginal mandibular nerves. However, the nature of this possibly mechanical impediment remains unknown.

Mechanical stimulation had no detectable influence on projection patterns after FFA, HFA, and IPNG (Table 2.18). Thus, myotopic organization was completely lacking, the total number of projecting motoneurons was increased (with the exception of ramus zygomaticus after IPNG), and the degree of axonal branching was consistently elevated regardless of whether the animals received MS or not.

Table 2.18 Degree of collateral axonal branching after facial nerve reconstruction and mechanical stimulation

Group of animals	Neurons projecting only into the zygomatic nerve	Neurons projecting into the zygomatic and buccal nerves	Neurons projecting into the zygomatic and marginal mandibular	All DiI labeled neurons projecting into the zygomatic nerve	Neurons projecting only into the buccal nerve	Neurons projecting only into the marginal mandibular nerve
1. Intact[a]	364 ± 47 100%	0 0%	0 0%	364 ± 47 100%	1,441 ± 101	379 ± 94
2. FFA-only[a]	213 ± 53 30%	239 ± 52 34%	257 ± 56 36%	709 ± 178 100%	1,908 ± 289	1,488 ± 356
3. HFA-only	184 ± 125 44%	116 ± 69 28%	116 ± 81 28%	414 ± 211 100%	2,617 ± 623	1,765 ± 1,005
4. IPNG-only	68 ± 28 37%	61 ± 40 33%	56 ± 39 30%	185 ± 100 100%	2,256 ± 376	2,294 ± 519
5. FFA + MS[a]	276 ± 219 36%	268 ± 149 35%	211 ± 105 29%	755 ± 251 100%	1,662 ± 342	1,614 ± 184
6. HFA + MS	231 ± 174 57%	97 ± 40 24%	78 ± 35 19%	406 ± 221 100%	2,224 ± 429	1,743 ± 431
7. IPNG + MS	102 ± 24 48%	62 ± 13 29%	48 ± 21 23%	212 ± 36 100%	2,233 ± 356	2,095 ± 657

Number of motoneurons with axons in the zygomatic, buccal, or marginal mandibular branches of the facial nerve in *intact* animals and in rats that received no postoperative treatment (*FFA-only, HFA-only and IPNG-only*). The other three groups of animals were subjected to daily manual mechanical stimulation of the vibrissal muscles and hence named FFA + MS, HFA + MS, and IPNG + MS. The animals were studied 10 days after triple retrograde labeling performed 56 days post-surgery. The percentage values below the absolute numbers in columns 2–5 indicate the portions of motoneurons projecting through the zygomatic nerve with branched (DiI + FG or DiI + FB, column 3 and 4) and unbranched axons (DiI-only, column 2). All groups consisted of eight animals. Shown are group mean values ± SD. Mean values of a given "stimulated" group (Nr. 5–7) were compared (ANOVA and post hoc Tukey's test, $p < 0.05$) with those of the respective nonstimulated group (Nr. 2–4). No differences were detected. Values for intact rats are given as reference values and not included in the analysis

[a]Data adopted from Angelov et al. (2007)

Table 2.19 Quality of target muscle reinnervation after facial nerve reconstruction and subsequent treatment

Group of animals	Monoinnervated motor endplates (%)	Polyinnervated motor endplates (%)	Noninnervated motor endplates (%)	Total number of motor endplates examined
1. Intact rats[a]	100 ± 0	0	0	1,543 ± 132
2. FFA-only[a]	45 ± 9.6*	53 ± 10*	2.6 ± 1.8	1,326 ± 413
3. HFA-only	68 ± 13**	17 ± 9**	15 ± 6.0	1,524 ± 325
4. IPNG-only	60 ± 11***	22 ± 8***	18 ± 7	1,491 ± 441
5. FFA + MS[a]	66 ± 11*	31 ± 10*	2.7 ± 2.0	1,345 ± 319
6. HFA + MS	79 ± 12**	8 ± 2**	13 ± 5	1,587 ± 402
7. IPNG + MS	76 ± 12***	14 ± 3***	10 ± 3	1,395 ± 312

Reinnervation pattern of the levator labii superioris (LLS) motor endplates in intact rats (*Intact*) and in rats that received no postoperative treatment (*FFA-only, HFA-only and IPNG-only*). The other three groups of animals were subjected to daily manual mechanical stimulation (MS) of the vibrissal muscles and hence named FFA + MS, HFA + MS, and IPNG + MS. Motor endplates were classified as monoinnervated, polyinnervated, or noninnervated according to the number of beta-tubulin-immunoreactive axons that crossed the boundaries of the endplate. All groups consisted of eight animals. Shown are group mean values ± SD. Mean values of a given "stimulated" group (Nr. 5–7) that were significantly different (ANOVA and post hoc Tukey's test, $p < 0.05$) from the respective nonstimulated group (Nr. 2–4) are indicated by *, **, and ***. Values for intact rats are given as reference values and not included in the analysis

[a]Data adopted from Angelov et al. (2007)

Pattern of target muscle reinnervation was estimated as described earlier.

In intact animals, all motor endplates were innervated by one axon and designated as monoinnervated (Fig. 2.2d, f). After FFA, HFA, and IPNG alone (i.e., without stimulation), 53%, 17%, and 22%, respectively, were polyinnervated, i.e., innervated by two or more axons (Fig. 2.2c, e, Table 2.19). Compared with FFA, the decreased degree of polyinnervated motor endplates after HFA and IPNG could be, at least partially, due to more noninnervated endplates after these two types of nerve reconstruction (fourth column of Table 2.19).

Manual stimulation of the vibrissal muscles significantly reduced the proportions of polyinnervated endplates (FFA: 31%, HFA: 8% and IPNG: 14%, respectively; Table 2.19).

2.2.5.4

Manual Stimulation of the Orbicularis Oculi Muscle Improved Eyelid Closure After Facial Nerve Injury in Adult Rats

Following facial nerve injury in humans, soft tissue massage improves blood flow, facial symmetry, and smiling. Together, the findings suggested that interventions that reduced the degree of endplate polyinnervation might also improve functional outcome. We therefore tested the effect of manual stimulation of the vibrissal muscles after facial nerve injury (facial nerve transection and immediate end-to-end anastomosis; FFA) in rat. Minor vibrissal motor performance was first noted at 4–5 weeks after FFA and after two further weeks; recovery was complete

with function being indistinguishable from that in intact animals. Encouraged by the efficacy of manual stimulation in improving function of facial muscles surrounding the mouth, we decided to check whether the same simple rehabilitation technique would also prove effective for another facial muscle, the orbicularis oculi (OOM). This muscle is also innervated solely by the facial nerve and controls eyelid closure and blinking, both of which can be severely compromised by facial nerve injury in humans and with significant consequences.

Thirty rats were used. Group 1 ($n = 10$) consisted of intact rats and groups 2–3 of experimental rats ($n = 10$ in each group) subjected to unilateral transection and suture of the right facial nerve (FFA). Rats in group 2 (handling control) did not receive manual stimulation but were handled daily by an investigator in an equivalent fashion to rats receiving manual stimulation. Those in group 3 received daily manual stimulation of the right OOM after FFA (Fig. 2.6e). We examined (1) the quality of eyelid closure and (2) pattern of motor endplate reinnervation at 2 months -FFA in both experimental groups. Data for stimulated animals were compared with nonstimulated ones.

Transection and end-to-end suture of the right facial nerve (FFA) as well as *handling* (handling control) were performed as already described.

2.2.5.5 Manual Stimulation of the Orbicularis Oculi Muscle

Manual stimulation was initiated 1 day after surgery. All rats in group 3 were subjected to gentle rhythmic manual closure of the right eye (by slightly pushing both eyelids together and then letting go) for 5 min per day, 5 days a week for 2 months (Fig. 2.6e). The pattern of manual stimulation mimicked natural blinking or eyelid closure. Animals became accustomed to this procedure within 2–3 days and did not show any signs of stress such as freezing or trying to bite, weight loss or lack of grooming; rather, animals readily complied.

2.2.5.6 Video-Based Motion Analysis of Eye Closure

Two months after FFA and daily handling or manual stimulation, both eyes of each animal were simultaneously videotaped for blink responses. The blink reflex was evaluated utilizing custom-designed apparatus that, when activated, delivered a single standardized portion of 20 ml air as a "puff" to the cornea and periorbital region bilaterally at a distance of 3 cm (Terrell and Terzis 1994; Thanos and Terzis 1995; Fig. 2.6f). Ten puffs were delivered sequentially over 120 s. Using a digital camcorder, animals were videotaped during air-puff-evoked eyelid closures. Evaluation of the blink was performed using a 2D Manual Advanced Video System (Motus 2005). For calibration reasons, a ruler laid 20 cm below the recorder (i.e., at a constant angle of 180° to it) was videotaped before each trial. Video sequences were inspected on a screen and frames selected when the eyelid closure on the intact left side was maximal, i.e., when the distance between the eyelids was

smallest. A single reference point half-way along the rim of each eye lid was used to measure the mean distance between both eyelids on the left and right side after ten sequential air puffs. Since in intact animals closure of the eyelids is complete, increase in the inter-eyelid distance indicates functional impairment.

In unoperated rats, the curves (Fig. 2.9a) that show the changes in inter-eyelid distance for the left (blue) and right (red) eye over time displayed a strictly parallel course with nearly full closure after each air puff stimulus. Following FFA, the curve for the operated (right) eyelid remained parallel to the *x*-axis indicating no blink reflex, a pattern which we observed immediately after FFA and at 1 month thereafter (Fig. 2.9b). Manual stimulation improved blinking function at 2 months as evidenced by a return in synchrony of the two curves (Fig. 2.9c).

In intact animals, the mean minimum distance between the eyelids was similar on the left and right side (0.4 $\pm$ 0.2 mm and 0.3 $\pm$ 0.1 mm, respectively, Fig. 2.9a).

In both experimental groups, the distance on the unoperated (left) side remained, as expected, unchanged compared with intact animals (group 2, handling control: 1 day, 0.6 $\pm$ 0.4 mm; 1 month, 0.3 $\pm$ 0.1 mm; 2 months, 0.3 $\pm$ 0.1 mm; group 3, manual stimulation: 1 day, 0.3 $\pm$ 0.1; 1 month, 0.4 $\pm$ 0.2; 2 months, 0.2 $\pm$ 0.1).

Eyelid closure was severely impaired 1 day after FFA in both experimental groups as indicated by the large increase, compared with the contralateral side, in the minimum eyelid distance (group 2, control handling: 3.3 $\pm$ 1.8 mm; group 3, manual stimulation: 3.4 $\pm$ 1.2 mm). Thereafter, the degree of eyelid closure proved to be dependant on whether the animals received manual stimulation or not. In group 2 (control handling), the distance between the two eyelids remained unchanged compared with 1 day throughout the observation period (3.2 $\pm$ 1.3 mm and 2.7 $\pm$ 0.4 mm at 1 and 2 months, respectively). No improvement was seen after FFA with manual stimulation at 1 month (2.8 $\pm$ 1.1 mm). However, blink capacity in the manual stimulation group was dramatically improved at 2 months as indicated by the twofold reduction of the minimum eyelid distance compared with handled controls (1.3 $\pm$ 0.5 mm vs. 2.7 $\pm$ 0.4 mm; $p < 0.05$).

2.2.5.7

Pattern of Target Muscle Reinnervation

As previously described, the OOM is situated around the entire circumference of the palpebral fissure, extending for at least 5 mm from the conjunctival margin of the upper and lower eyelids, and 4 mm from both the medial and lateral canthi (Gong et al. 2003). Observations of immunostained frontal sections through the OOM revealed that most motor endplates are located in the region close to the lateral margin of the orbita.

In intact animals, all neuromuscular junctions (100%) were innervated by one axon and designated as monoinnervated (May 1986). After FFA without manual stimulation, the proportion of polyinnervated, i.e., innervated by two or more axons, neuromuscular junctions was 42 $\pm$ 10% (Table 2.20). Daily manual

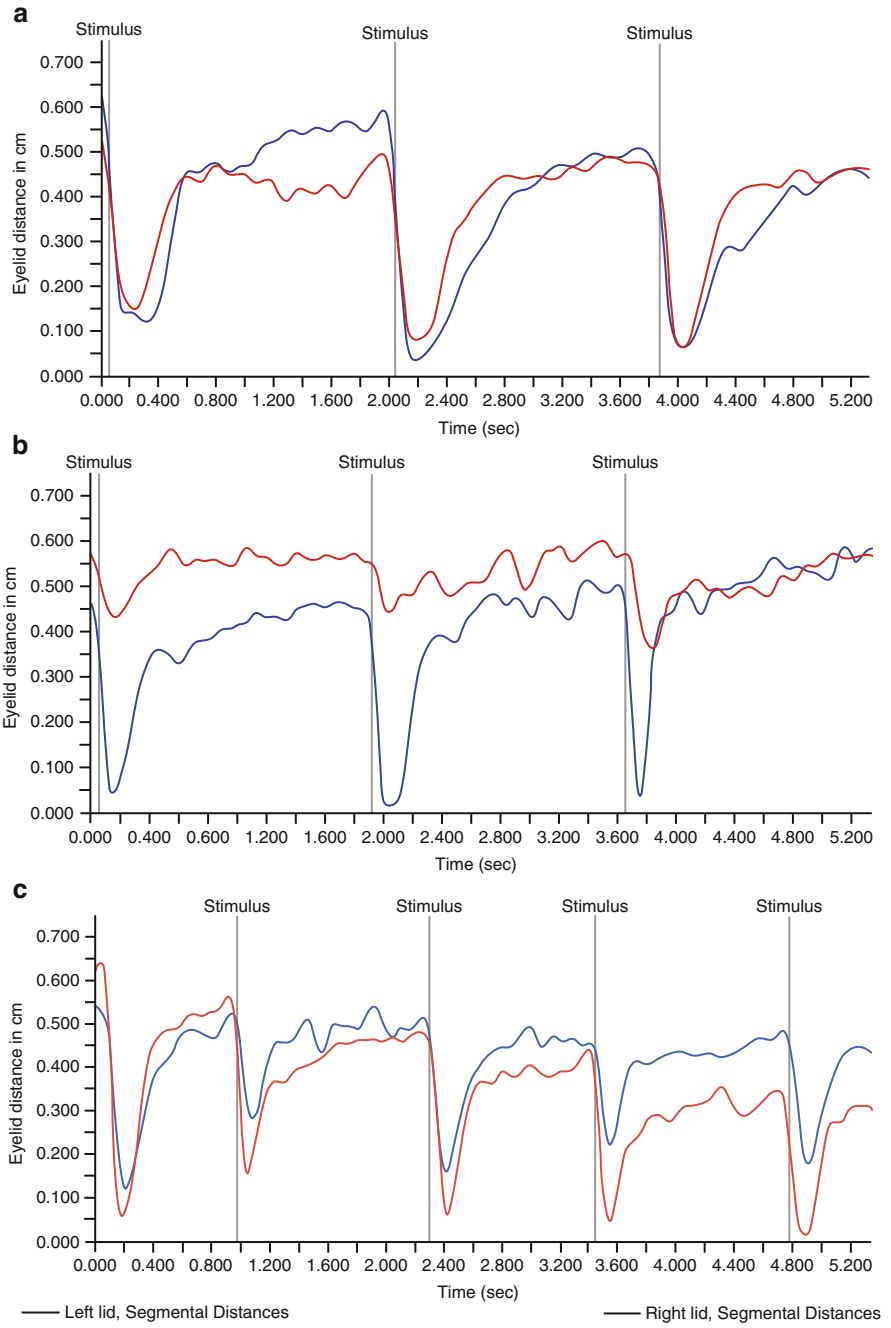

Fig. 2.9 (**a**, **b**) In unoperated rats, both curves, indicating the closure of the eyelids of the left (in *blue*) and right (in *red*) eye, display a parallel course with a very good closure (minimum

Table 2.20 Quality of orbicularis oculi muscle (OOM) reinnervation after facial nerve reconstruction and subsequent treatment

Group of animals	Monoinnervated motor endplates (%)	Polyinnervated motor endplates (%)	Noninnervated motor endplates (%)	Total number of motor endplates examined
1. Intact rats	100 ± 0	0	0	3,943 ± 532
2. FFA-only	55 ± 8.6	42 ± 10*	3.0 ± 1.8	4,267 ± 780
3. FFA plus manual stimulation	76 ± 9.1*	21 ± 10*	3.0 ± 1.0	3,612 ± 991

Reinnervation pattern of the orbicularis oculi muscle (OOM) motor endplates in intact rats (Intact) and in rats that received no postoperative treatment (FFA-only). The animals of the third group were subjected to daily manual mechanical stimulation of OOM. Motor endplates were classified as monoinnervated, polyinnervated, or noninnervated according to the number of beta-tubulin-immunoreactive axons that crossed the boundaries of the endplate. All groups consisted of ten animals. Shown are group mean values ± SD. Mean values of the "stimulated" group (Nr. 3) that were significantly different (ANOVA and post hoc Tukey's test, $p < 0.05$) from the nonstimulated group (Nr. 2) are indicated by *. Values for intact rats are given as reference values and not included in the analysis

stimulation improved the pattern of reinnervation. Two months after FFA, the fraction of polyinnervated neuromuscular junctions was by a factor of 2 lower than in handled controls (21 ± 10%, $p < 0.05$; Table 2.20).

2.2.6

Manual Stimulation of the Suprahyoid–Sublingual Region Diminished Polyinnervation of the Motor Endplates and Improved Recovery of Function After Hypoglossal Nerve Injury in Rats

Studies in experimental animals have shown that mild electrical stimulation of the denervated soleus muscle inhibits intramuscular sprouting and diminishes motor endplate polyinnervation (Love et al. 2003). In addition, soft tissue massage has been shown clinically to have several benefits (Coulson 2005). The findings prompted us to examine the effect of manual stimulation on both functional recovery of vibrissal muscles and the degree of polyinnervation following facial nerve injury. VBMA of vibrissal motor performance showed that manual stimulation resulted in full recovery of whisking which was associated with reduced polyneuronal reinnervation of motor endplates (Angelov et al. 2007). Since manual

Fig. 2.9 (continued) inter-eyelid distance) after each air puff stimulus. (**b**) This is in sharp contrast with the situation in operated rats in which the orbicularis oculi muscle on the operated side is, as indicated by the lack of blink reflex responses, paretic (red curve) even 2 months after FFA and no manual stimulation. (**c**) Definite improvement of the eye closure on the right side (*red* curve almost parallel to the *blue* one) 2 months after FFA and manual stimulation of the orbicularis oculi muscle. Adopted from Bischoff et al. (2009)

stimulation significantly improved functional recovery of whisking after injury to the facial nerve, we asked whether this rehabilitation approach would be also successful after injury to another nerve, namely the hypoglossal nerve. An additional impetus for this study was the recent finding that motor control of human tongue movements can be improved by selected tongue training techniques (Svensson et al. 2003).

2.2.6.1

Animals, Groups, and Overview of Experiments

Seventy-eight rats were divided into two control and four experimental groups (Table 2.21). Groups 1–3 ($n = 16$ per group) were used to study collateral axonal branching at the site of lesion, synaptic input to the hypoglossal motoneurons, and the quality of target reinnervation (*m. hyoglossus*). Group 1 consisted of intact animals. All rats in groups 2 and 3 were subjected to unilateral transection and suture of the right hypoglossal nerve (hypoglossal–hypoglossal anastomosis, HHA). Animals in group 2 received no postoperative treatment, whereas those in group 3 were subjected to manual stimulation (MS) of the extrinsic and intrinsic suprahyoid–sublingual region.

In addition to misdirected reinnervation of muscle targets, insufficient recovery has also been attributed to rearrangement of cortical representations (Sanes et al. 1988; Svensson et al. 2006). Cortical tongue muscle representation volume was therefore examined (groups 4–6; $n = 10$ per group). Animals in group 4 (intact) were subjected to right unilateral HHA and were kept under anesthesia for

Table 2.21 Experimental design chart depicting animal grouping and procedures

Group of animals	Restoration of the tongue position by measuring the deviation angle	Degree of collateral axonal branching as estimated by double retrograde labeling	Extent of synaptic input to hypoglossal motoneurons	Reinnervation pattern of the motor endplates in the hyoglossus muscle	Tongue muscles representation volume (CTMRV)
1. Intact	16	8	8	8	
2. HHA-only	16	8	8	8	
3. HHA + MS	16	8	8	8	
4. Intact	10				10
5. HHA-only	10				10
6. HHA + MS	10				10

Animal grouping and procedures, e.g., hypoglossal–hypoglossal anastomosis (HHA), with or without manual mechanical stimulation of the tongue muscles (MS). All animals from groups 1–3 were subjected to postoperative measurement of the tongue tip deviation from the midline. Thereafter, one half were used for estimation the degree of collateral axonal branching and the other half for establishing the extent of synaptic input to the hypoglossal motoneurons and the pattern of the motor endplates reinnervation. The animals from groups 4–6 served to establish changes in cortical tongue muscles representation volume (CTMRV)

1 h prior to perfusion fixation. Animals from groups 5 and 6 underwent HHA and survived for 2 months; those in group 5 received no postoperative treatment while those in group 6 received MS exactly as those in group 3. After 2 months, the right hypoglossal nerve of all rats in groups 5 and 6 was transected proximally to the earlier lesion kept under anesthesia for 1 h prior to perfusion fixation.

Analyses of (1) deviation angle of the tongue tip from the midline, (2) degree of axonal branching, (3) synaptic input to the hypoglossal motoneurons, (4) pattern of motor endplate reinnervation, and (5) determination of cortical tongue muscle representation volume were performed at 2 months after surgery. Data for rats receiving MS were compared with those that did not.

All animals in groups 1–6 were used to determine the deviation angle of the tongue tip from the midline, a standard procedure for estimating hypoglossal nerve function (Lowe 1981). Thereafter, half the animals ($n = 8$) in groups 1–3 were used to establish the degree of collateral axonal branching by means of double retrograde neuronal labeling (see below). The remaining rats in groups 1–3 ($n = 8$) were used to determine the synaptic input to the hypoglossal motoneurons (using immunocytochemistry for synaptophysin, see below) and the proportion of monoinnervated and polyinnervated motor endplates in the ipsilateral hyoglossus muscle (using immunocytochemistry for neuronal class III β-tubulin and histochemistry with alpha-bungarotoxin, see below). All animals in groups 4–6 (group 4: intact; group 5 HHA no MS; group 6: HHA + MS) were used to determine the deviation angle of the tongue tip from the midline and the cortical tongue muscle representation volume (see below).

2.2.6.2

Surgery

Transection and end-to-end suture of the right hypoglossal nerve (hypoglossal–hypoglossal anastomosis, HHA) were performed after intraperitoneal injection of ketamin/xylazin. The right hypoglossal nerve was exposed and transected proximal to its bifurcation into lateral and medial branches (Fig. 2.10a). End-to-end suture (hypoglossus–hypoglossus anastomosis, HHA) was performed immediately using two 11–0 atraumatic sutures.

2.2.6.3

Manual Stimulation of the Extrinsic and Intrinsic Suprahyoid–Sublingual Region

On the day following surgery, the suprahyoid–sublingual region of all 16 animals from group 3 and 6 were manually stimulated. MS was performed by gently stroking the lower jaw and upper neck to stimulate all three extrinsic (skeletal) muscles of the tongue *(m. styloglossus, m. genoioglossus, m. hyoglossus*) for 5 min a day, 5 days a week for 2 months. The pattern of manual stimulation mimicked the natural active movements during swallowing (Fig. 2.10b). In addition, upon return to the cage, each rat which had received MS also had a drop of honey

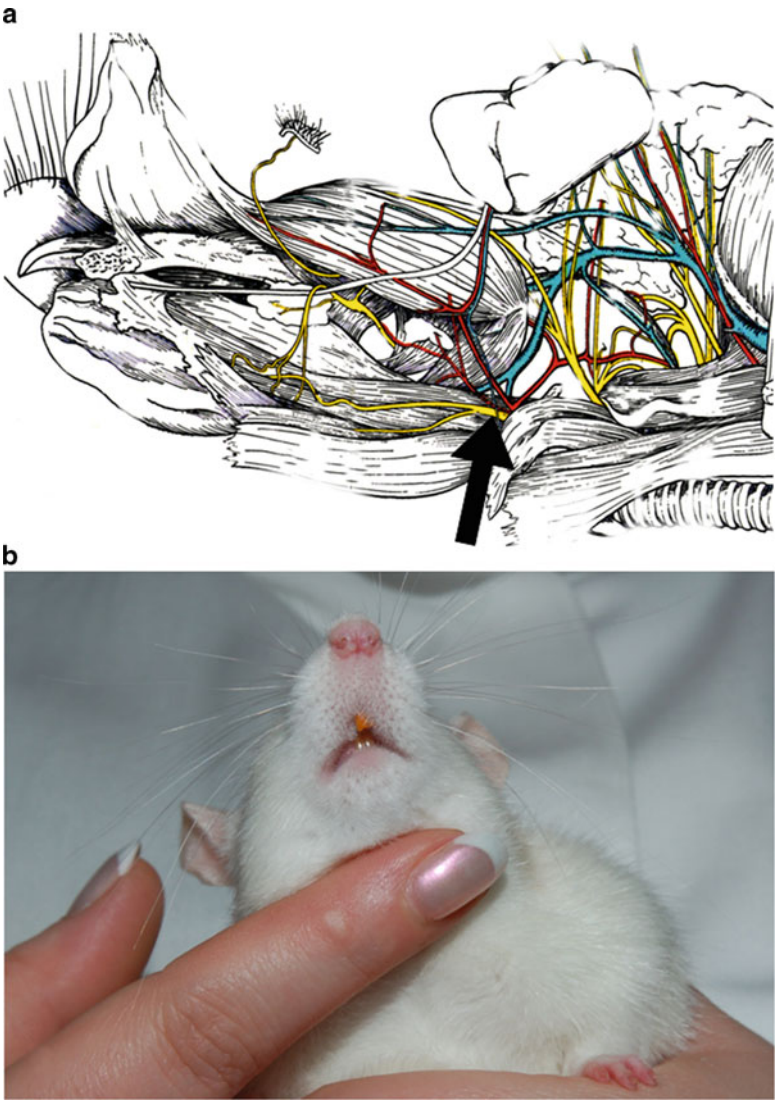

Fig. 2.10 (**a, b**) Surgical procedure and postoperative treatment. (**a**) Schematic drawing of the rat hypoglossal nerve. *Arrow* points at the site of transection and suture. Adopted from Greene (1955). (**b**) Manual "submental" stimulation of the extrinsic suprahyoid–sublingual region. Adopted from Evgenieva et al. (2008)

placed on its back which was accessible to its cage companions. By licking away the honey, cage companions stimulated their intrinsic suprahyoid–sublingual region (*m. longitudinalis sup., m. longitudinalis inf. m. transversus and m. verticalis*) for additional 5–10 min after MS.

2.2.6.4

Restoration of Tongue Position During Protrusion As a Sign for Recovery of Function

Recovery of tongue function was estimated by measuring deviation of the tongue tip from the midline, i.e., the angle between the long axis of the tongue and the median line of the body running between the incisor teeth. Animals were held gently by an experimentator and the upper lip was slightly lifted. Photographs in the frontal plane of all rats were taken from an identical distance (about 20 cm) using the macro-menu of a Nikon 50D digital camera. The very high resolution of the pictures allowed us to readily identify the tip of the tongue, as well as the long axis of the organ. The identical position of each animal when photographed and the short distance between the camera and the head of the rat reduced the possible parallax errors maximally.

In intact rats, tonus of the right and left protruders (the extrinsic *m. genioglossus* and the intrinsic vertical and transverse muscles) is identical, and therefore the tip of the tongue was situated exactly in the midline behind the lower incisors, i.e., the deviation from the midline was 0° (Fig. 2.11a). Following right-sided HHA, malfunction of all right protruders resulted in domination of the opposite (left) muscles which displaced the tongue tip to the right (Wilson et al. 1994), i.e., the long axis of the tongue no longer coincided with the midline (Fig. 2.11b).

Daily MS of the suprahyoid–sublingual region 5 min a day for 2 months improved tongue position after HHA (Fig. 2.11). Deviation of the tongue tip following MS was significantly lower compared with nonstimulated animals (37.4 ± 9.37° vs. 50.1 ± 9.01°; mean ± SD, $n = 26$, Mann–Whitney test, $p = 0.026$).

2.2.6.5

Estimation of Axonal Branching by Double Retrograde Labeling

Previous data (Angelov et al. 1994) after immunostaining of 50-μm-thick vibratome sections for neuron-specific enolase (NSE, i.e., no retrograde labeling performed) showed that the intact hypoglossal nucleus contained 3,576 ± 284 NSE-immunoreactive perikarya; there were no significant changes in these values either at 1 (4,010 ± 245) or 8 weeks after HHA (3,412 ± 348).

2.2.6.6

Application of Fluorescence Tracers

Eight rats from groups 1–3 were used to analyze the degree of collateral axonal branching at the lesion site (HHA). Under Rompun/Ketanest anesthesia, the right hypoglossal nerve was re-exposed distally to the suture site. The medial and lateral branches were transected and instilled with crystals of the retrograde fluorescent dyes Fast Blue and Fluoro-Gold, respectively (Fig. 2.12a). Crystals were left in situ for 30 min after which the application sites were carefully rinsed, dried, and the

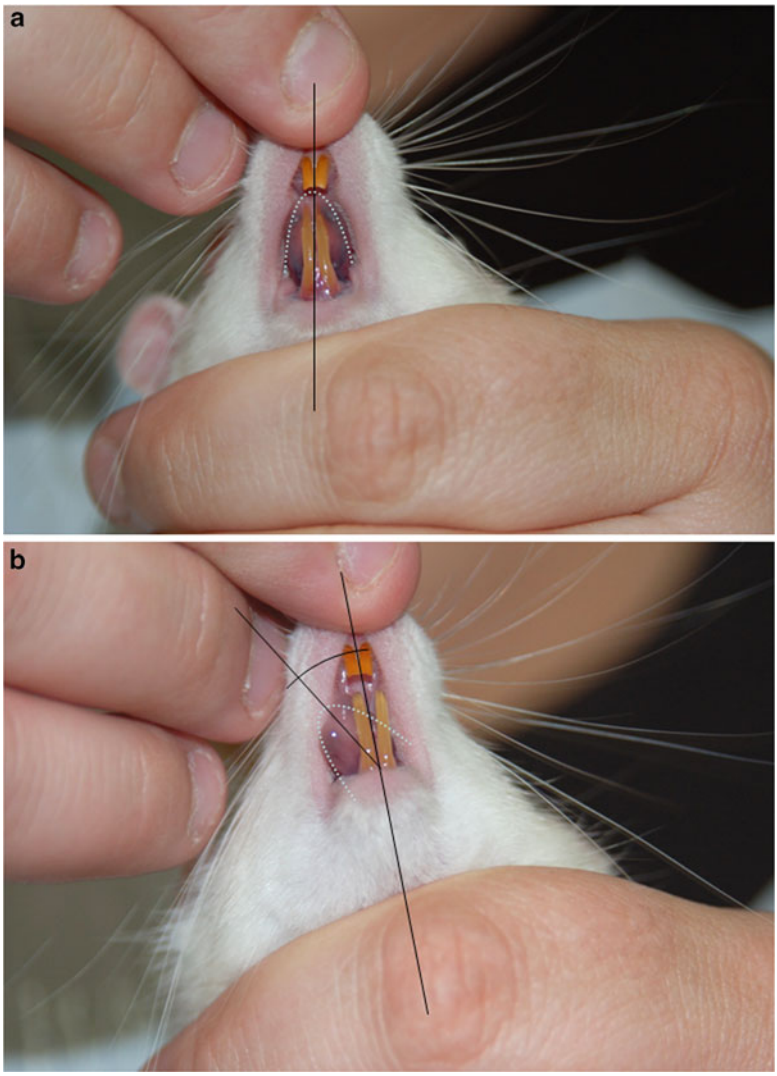

Fig. 2.11 (**a**, **b**) Measurement of tongue tip deviation from the midline, i.e., of the angle between the long axis of the organ and the median line of the body running between the incisor teeth, in representative animals. The edges of the tongue are outlined by a *dotted line*. (**a**) In intact rats, the identical tonus of the right and left protruders and transverse muscles situated the tip of the tongue exactly in the middle behind the lower incisors, i.e., the deviation from the midline was 0°. (**b**) In operated animals, the left protruder dominated and displaced the tongue tip to the right, i.e., the long axis of the organ was no more covering the median line and the angle between them was proportional to the recovery of function. Adopted from Evgenieva et al. (2008)

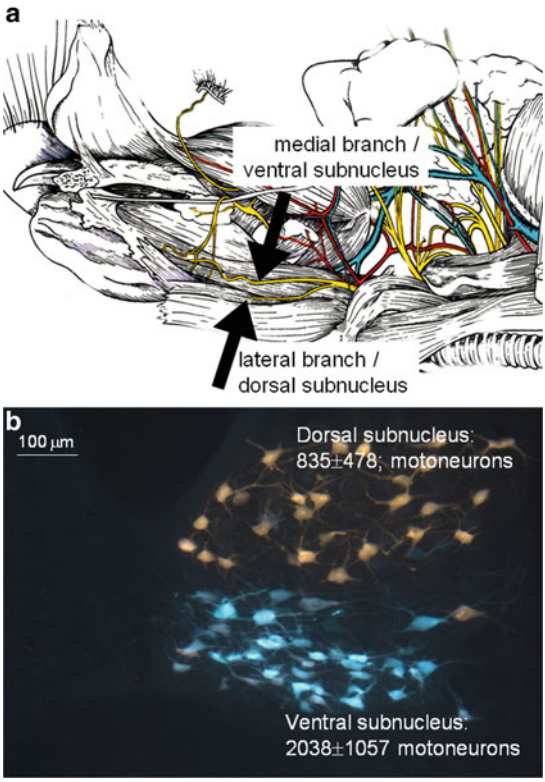

Fig. 2.12 (**a, b**) Retrograde neuronal labeling in intact rats with two fluorescent dyes. (**a**) Schematic drawing of the rat hypoglossal nerve. The *upper arrow* points at the medial branch that was transected and instilled with crystals of FB and the *lower arrow* at the lateral branch of the hypoglossal nerve (transected and labeled with crystals of FG). (**b**) Myotopic organization of the hypoglossal nucleus in intact rats. Application of FB to the transected medial branch labeled perikarya, which were localized in the ventral hypoglossal subnucleus. Likewise application of FG to the transected lateral branch labeled perikarya located in the dorsal hypoglossal subnucleus. No double-labeled perikarya were observed, i.e., the degree of axonal branching was 0%. Adopted from Evgenieva et al. (2008)

wound closed. Ten days later, animals were fixed by perfusion with 4% paraformaldehyde and the brainstems were sectioned coronally at 50 µm.

Under normal physiological conditions, the hypoglossal nerve controls tongue movements by means of its two functionally different nerve branches (Lowe 1981). The medial branch contains the axons of neurons in the ventral hypoglossal subnucleus and innervates muscles that are related to protrusion of the tongue (the extrinsic genioglossus and the intrinsic vertical and transverse muscles). The smaller lateral branch contains the axons of perikarya in the dorsal hypoglossal subnucleus and innervates muscles related to tongue retraction (extrinsic styloglossus and hyoglossus and intrinsic superior and inferior longitudinal). After transection of

the hypoglossal nerve, the regrowing axons navigate poorly and fail to rejoin their original nerve branches (medial or lateral) and to innervate therefore their correct muscle targets. The aim of this procedure was not to determine whether myotopic organization of the hypoglossal nucleus had been preserved or restored, but rather to establish the degree of collateral axonal branching at the lesion site by means of double retrograde labeling and neuronal counts (see below).

2.2.6.7 Fluorescence Microscopy and Counts

In intact rats, retrograde labeling of the medial hypoglossal branch, which innervates the tongue protruders (m. genioglossus) and the intrinsic suprahyoid–sublingual region (vertical and transverse), revealed 2,038 ± 1,057 (mean ± SD; $n = 8$) FB-labeled perikarya localized within the ventral hypoglossal subnucleus. Labeling of the lateral branch revealed 835 ± 478 FG-labeled perikarya located in the dorsal hypoglossal subnucleus (Fig. 2.12b). No double-labeled perikarya were observed, i.e., the index of axonal branching was 0%.

After HHA, two major changes, characteristic of aberrant reinnervation of targets, were detected. First, the hypoglossal nucleus lacked somatotopy, i.e., perikarya were not organized into a dorsal subnucleus (with axons projecting into the lateral hypoglossal nerve branch) and ventral subnucleus (axons projecting into the medial branch of the hypoglossal nerve; Krammer et al. 1979; Uemura-Sumi et al. 1988; Aldes 1995). Loss of somatotopy (Fig. 2.13) was due to transection of the hypoglossal nerve proximally to its bifurcation into its medial and lateral branches and subsequent inaccurate navigation of regrowing neurites into inappropriate branches.

Second, the entire hypoglossal nucleus contained double-labeled (FB + FG) motoneuronal perikarya (*arrows* in Fig. 2.13), which arose due to collateral axonal branching at the lesion site. Following MS, there were 1,234 ± 592 FB_{only}-, 313 ± 460 FG_{only}-, and 1,302 ± 715 FB + FG double-labeled perikarya. In non-stimulated rats, there were 600 ± 364 FB_{only}-, 632 ± 722 FG_{only}-, and 1,616 ± 691 FB + FG double-labeled perikarya (mean ± SD; $n = 8$). The index of collateral axonal branching did not differ between MS and non-MS groups (46% vs. 56%; Mann–Whitney test, $p > 0.05$).

2.2.6.8 Measurement of Motoneuron Soma Sizes

Earlier work has shown that within 1 week after re-injury of chronically axotomized mouse facial motoneurons, their atrophic cell bodies increase in size and expression of growth-related proteins is enhanced (McPhail et al. 2004b). Thus, motoneuron size after a period of recovery from nerve transection and repair followed by a second axotomy is considered to reflect regenerative capacity and thus the functional state of regenerated motoneurons. Similarly, 3 months after femoral nerve transection and repair in mice, the degree of motor recovery

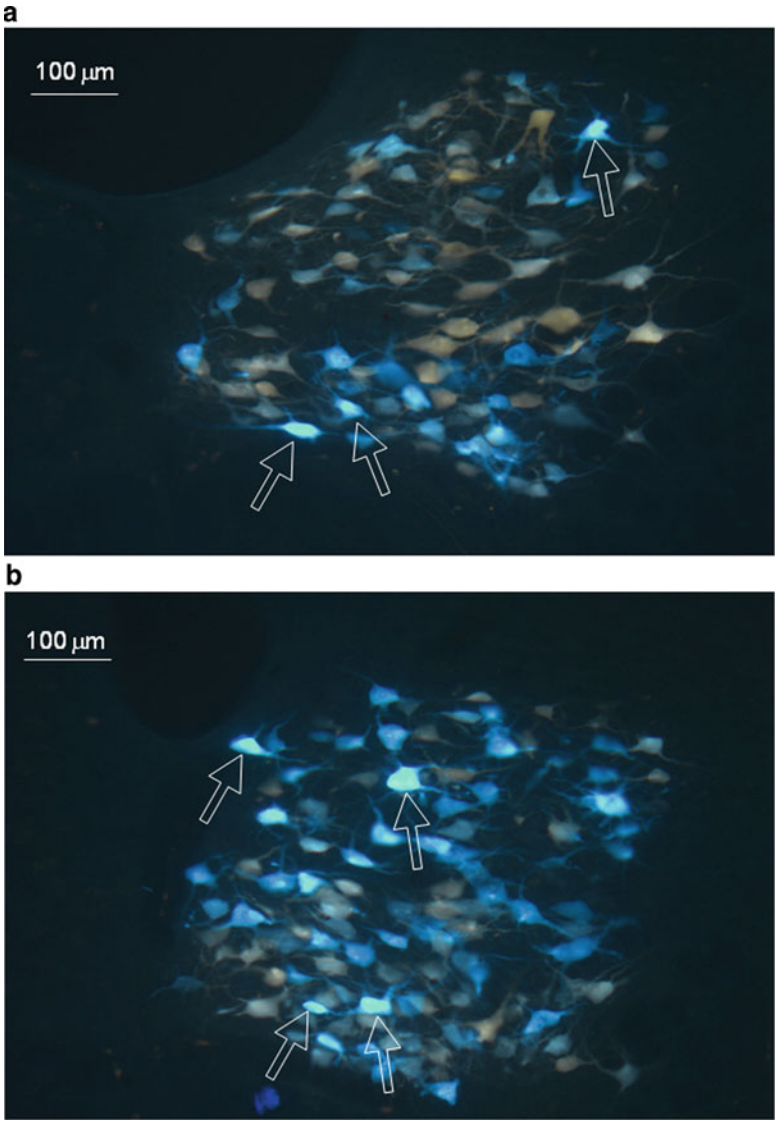

Fig. 2.13 (**a**, **b**) Retrograde neuronal labeling after HHA in nonstimulated (**a**) and stimulated (**b**) rats. The organization of the hypoglossal motoneurons into subnuclei is no longer evident and due to collateral axonal branching there appear double-labeled (FB + FG) neuronal somata (*arrows*). Adopted from Evgenieva et al. (2008)

correlates with soma size of regenerated motoneurons (Simova et al. 2006). We therefore measured hypoglossal motoneuron area following retrograde labeling in rats with and without MS. Labeled hypoglossal motoneurons were photographed with a SPOT-CCD Video Camera System mounted on an Axioplan Zeiss

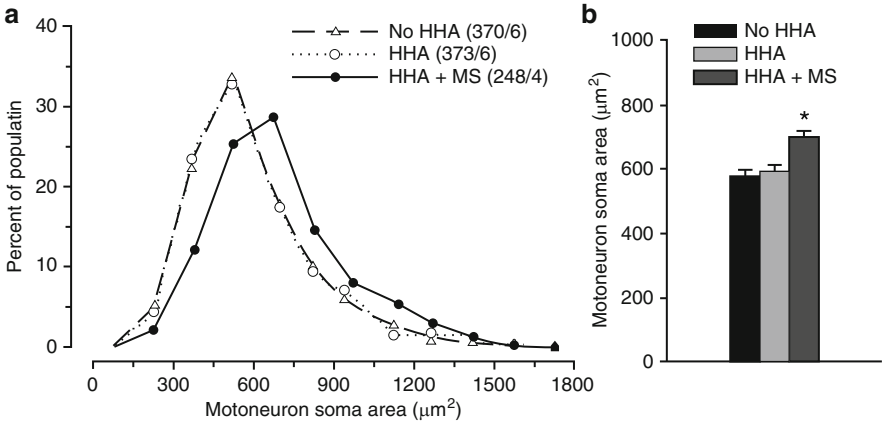

Fig. 2.14 (**a, b**) Motoneuron soma size. (**a**) Normalized frequency distributions of soma areas of back-labeled motoneurons in rats subjected to retrograde labeling only ("No HHA") or to retrograde labeling 2 months after nerve repair and no stimulation ("HHA") or nerve repair and manual stimulation ("HHA + MS"). The distribution in the "HHA + MS" group differs from those in the other two groups ($p < 0.001$, Kolmogorov–Smirnov test). Number of motoneurons/rats studied is indicated in the panel. (**b**) Group mean values + SEM of soma areas of the motoneurons shown in (**a**). *Asterisk* indicates significant difference from both other groups ($p < 0.05$, ANOVA with Tukey's post hoc test). Adopted from Evgenieva et al. (2008)

microscope under ×16 magnification. Images were saved in an uncompressed format (TIFF). Analysis was performed with software ImageJ v. 1.38t (US National Institutes of Health, Bethesda, Maryland, USA, http://rsb.info.nih.gov/ij/). An average of 60 motoneurons per hypoglossal nucleus was randomly selected and outlined semiautomatically using the Multi Cell Outliner plugin (Fig. 2.11). The areas of each perikaryon was automatically measured in μm^2 using the building analysis functions of the software. Measurements were performed by one observer (S. Pavlov) who had no information about the postoperative treatment of the rats.

Two months after transection and suture of the right hypoglossal nerve and 10 days after surgery for retrograde labeling, retrogradely labeled motoneuron perikarya were significantly larger in rats receiving MS than in nonstimulated animals (696 ± 53 μm^2 vs. 594 ± 52 μm^2, group mean values from individual animal mean values, $p < 0.05$, t test). This conclusion was further verified by analysis of the frequency distributions in the two population samples (Fig. 2.14).

2.2.6.9 Analyses of the Synaptic Input to the Hypoglossal Motoneurons

To compare the degree of synaptic input in rats with and without MS, we measured and established the overall intensity of fluorescence in the hypoglossal nucleus after immunostaining for synaptophysin.

Perfusion fixed (4% paraformaldehyde) brainstems were cut coronally in 30-μm-thick vibratome sections. Immunocytochemical staining for synaptophysin (rabbit polyclonal anti-Synaptophysin, Biometra, Cat. No. 100-599) was performed on every fifth section through the hypoglossal nucleus in one incubation batch for all 24 rats. To quantify pixel brightness, images were captured with a slow scan CCD camera (Spot RT, Diagnostic Instruments Inc., USA; ×16 objective) using Image-Pro Plus Software (Version 5.0; Media Cybernetics, Inc., Silver Spring, MD, USA; Fig. 2.15a–d). Black levels were kept constant but gain was manipulated for each group thereby ensuring that only a few pixels were saturated at the 255 pixel gray value. Each pixel therefore contained 8 bits of information encoding brightness ranging in value from 0 to 255. The scale for pixel brightness, or pixel gray value, was constructed so that the higher numbers indicate greater pixel brightness. The use of the collection filter further reduced the number of pixels saturated at 255. Thus the background intensities were identical from image to image around a pixel gray value of 50. Accordingly, the level for measuring pixel number and brightness was set at 51 (Fig. 2.15e).

To assess changes in total synaptic input to the hypoglossal nucleus in the three groups (fourth column in Table 2.21), we quantified synaptophysin expression in ten equidistant sections at ×16 magnification. Immunocytochemical staining with anti-synaptophysin revealed numerous small immunoreactive puncta within the neuropil of the hypoglossal nucleus (Fig. 2.15a–d).

The intensity of synaptophysin immunofluorescence differed significantly between the groups ($n = 8$ rats in each). Although there were no differences in the pixel distribution curves (data not shown), statistical analysis of total pixel numbers (gray values 51–210) revealed that MS restored synaptophysin levels to those in normal intact animals (Fig. 2.15d). Specifically, compared with intact animals (group 1), synaptophysin levels were restored in animals receiving MS (group 3) but remained lower in those without MS (group 2; $p = 0.022$); likewise, following HHA, synaptophysin levels were significantly higher ($p = 0.011$) in animals receiving MS (group 3: HHA + MS) compared with those that did not (group 2: HHA-only).

2.2.6.10

Analysis of Target Muscle Reinnervation

The ratio between monoinnervated versus polyinnervated motor endplates was determined as described previously. We selected the hyoglossus muscle rather than the m. genioglossus and m. styloglossus. The hyoglossus muscle extends as a thin muscle sheet from the hyoid bone and enters the tongue laterally, between the masseter and stylohyoideus muscles, allowing its easy identification and dissection (Fig. 2.16a, b). Analysis of the target muscle reinnervation was performed as already described. “intact rats” and the group “HHA + MS” according to one-way ANOVA with post hoc Bonferroni test.

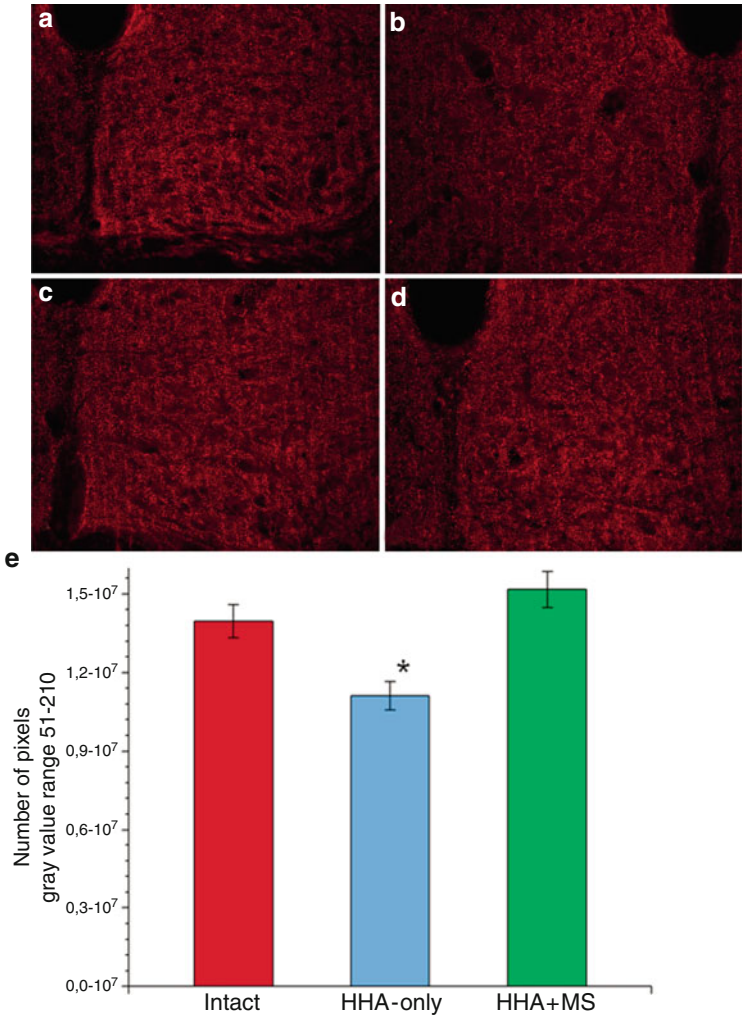

Fig. 2.15 (**a**–**e**) Quantification of synaptic terminals. Measurements were made using 30-μm-thick vibratome sections through the intact (**a**), contralateral to HHA (**b**), and lesioned hypoglossal nucleus either without (**c**) or with MS (**d**). (**e**) Graphical representations of the intensity of fluorescence in the intact and lesioned hypoglossal nucleus after immunostaining for synaptophysin and Cy3 as florescent dye. Sections were photographed at ×16 magnification. Shown are mean values + SD of pixel numbers within the defined range of *gray* values (51–210). Each experimental group comprised of eight rats. *Asterisk* indicates a significant reduction in the number of pixels in group "HHA-only" when compared with those of group "intact rats" and the group "HHA + MS" according to one-way ANOVA with post hoc Bonferroni test. Adopted from Evgenieva et al. (2008)

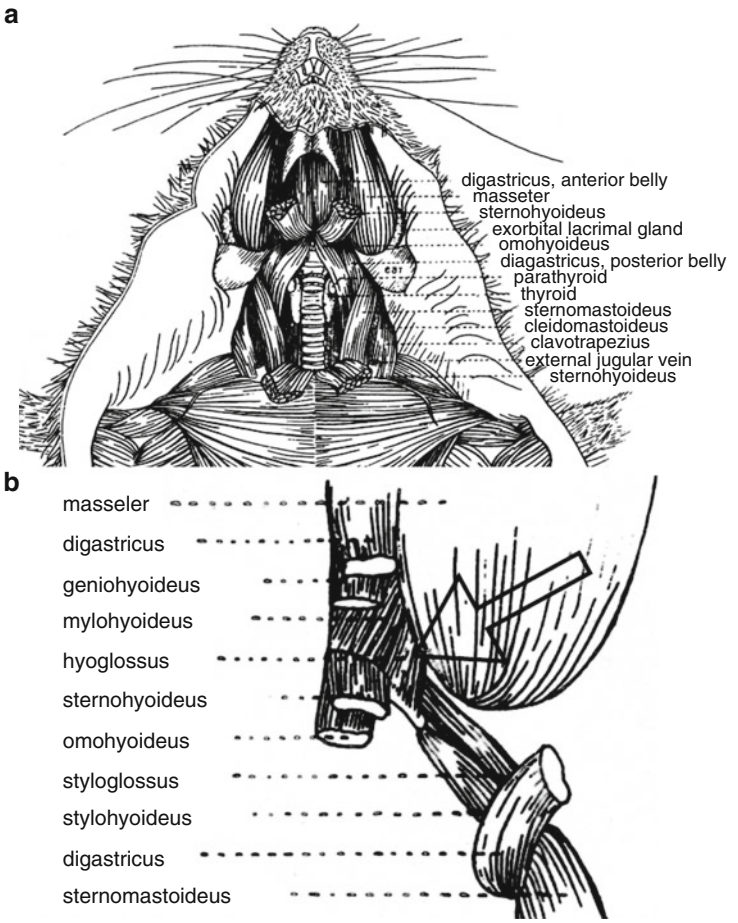

Fig. 2.16 (**a**, **b**) Schematic drawings demonstrating an overview of the supra- and infrahyoid musculature of the rat (**a**) and the detailed localization of the hyoglossus muscle (**b**). While a differentiation among m. geniohyoideus, m. mylohyoideus, m. sternohyoideus, and m. omohyoideus is sometimes hard to achieve, this thin muscle sheet (*arrow*) extends unvariably from the hyoid bone and enters the tongue laterally between the masseter and stylohyoideus muscles. Adopted from Evgenieva et al. 2008

The number of polyinnervated and monoinnervated motor endplates in the hyoglossus muscle of rats receiving MS was, respectively, 327 ± 126 and $1{,}464 \pm 289$; in nonstimulated rats, numbers were 375 ± 151 and 803 ± 329. The number of polyinnervated endplates was significantly smaller in rats receiving MS than in nonstimulated animals (18% vs. 32%; ANOVA and post hoc Bonferroni test, $p < 0.0001$).

2.2.6.11

Estimation of Cortical Tongue Muscle Representation Volume

Cortical motor representation of musculature has been visualized previously using c-Fos immunoreactivity that is upregulated after axotomy and is a marker for *trans*-synaptic neuronal activation (Bisler et al. 2002). In both intact and operated animals, the hypoglossal nerve was transected and animals perfused with fixative 1 h later. The clearly visible ventral rhinal fissure (bregma 5.0 mm; Fig. 2.17a, b) was selected as the rostral border of the cortical region containing the tongue muscle motor area. The brain was placed in a rat brain matrix (RBMS-300C, World Precision Instruments, Berlin, Germany; Fig. 2.17c), allowing identical slices to be cut through the telencephalon with a razor blade in each animal. A demarcation of the side contralateral to HHA (left) was made using a canule perforation in the caudoputamen (Fig. 2.17d). The cryoprotected (sucrose-infiltrated) slice was cut coronally (100 sections; 50 μm thick).

c-Fos was detected using rabbit anti-human cFos-Ab-5 (1:5,000; PC38, Merck Biosciences, Nottingham, UK), biotinylated anti-rabbit IgG (DakoCytomation, Hamburg, Germany), and streptavidin–HRP conjugate (1:100; Amersham, Freiburg, Germany). All sections used to compare CTMRV between stimulated and nonstimulated rats were incubated simultaneously using identical solutions (Fig. 2.17e, f).

Using the fractionator sampling strategy (Gundersen et al. 1988), each tenth coronal section (a total of at least ten equidistant sections through the brain) was used for immunocytochemistry of c-Fos. A Zeiss microscope equipped with a CCD Video Camera System (Optronics Engineering Model DEI-470, Goleta, CA, supplied by Visitron Systems, Puchheim, Germany) combined with Image-Pro Plus 5.0 software (Media Cybernetics, Silver Spring, MD, USA) was used to quantify the projection areas (μm^2) containing c-Fos-positive neurons in each section at a primary magnification of $\times 2.5$. Cortical tongue muscle representation volume was calculated according to the Cavalieri method (Gundersen et al. 1988). Measurements were performed by three observers (P. Schweigert, S.K. Angelova, and D.N. Angelov) who had no information about treatment of the rats.

One hour after transection of the right *intact hypoglossal nerve* (group 4), c-Fos immunopositive nerve cells were seen in the tongue muscle projection area in both the left and right anterior-lateral neocortex (Fig. 2.17), our findings being in agreement with previous studies (Rodel et al. 2004; Donoghue and Wise 1982; Neafsey et al. 1986). Right and left cortical tongue muscle representation volumes did not differ and were 0.063 ± 0.02 and 0.052 ± 0.02 mm^3 ($p < 0.05$).

At 2 months after HHA, we re-transected the right hypoglossal nerve trunk in groups 5 and 6 inducing acute, within an hour, *trans*-synaptic upregulation of c-Fos expression in the motor cerebral cortex (Bisler et al. 2002; Narita et al. 2003; Peeva et al. 2006). As for intact animals, left and right cortical tongue muscle representation volumes did not differ in either MS (left: 0.07 ± 0.03 mm^3; right: 0.08 ± 0.04 mm^3; $p > 0.05$) or nonstimulated (left: 0.12 ± 0.06 mm^3; right:

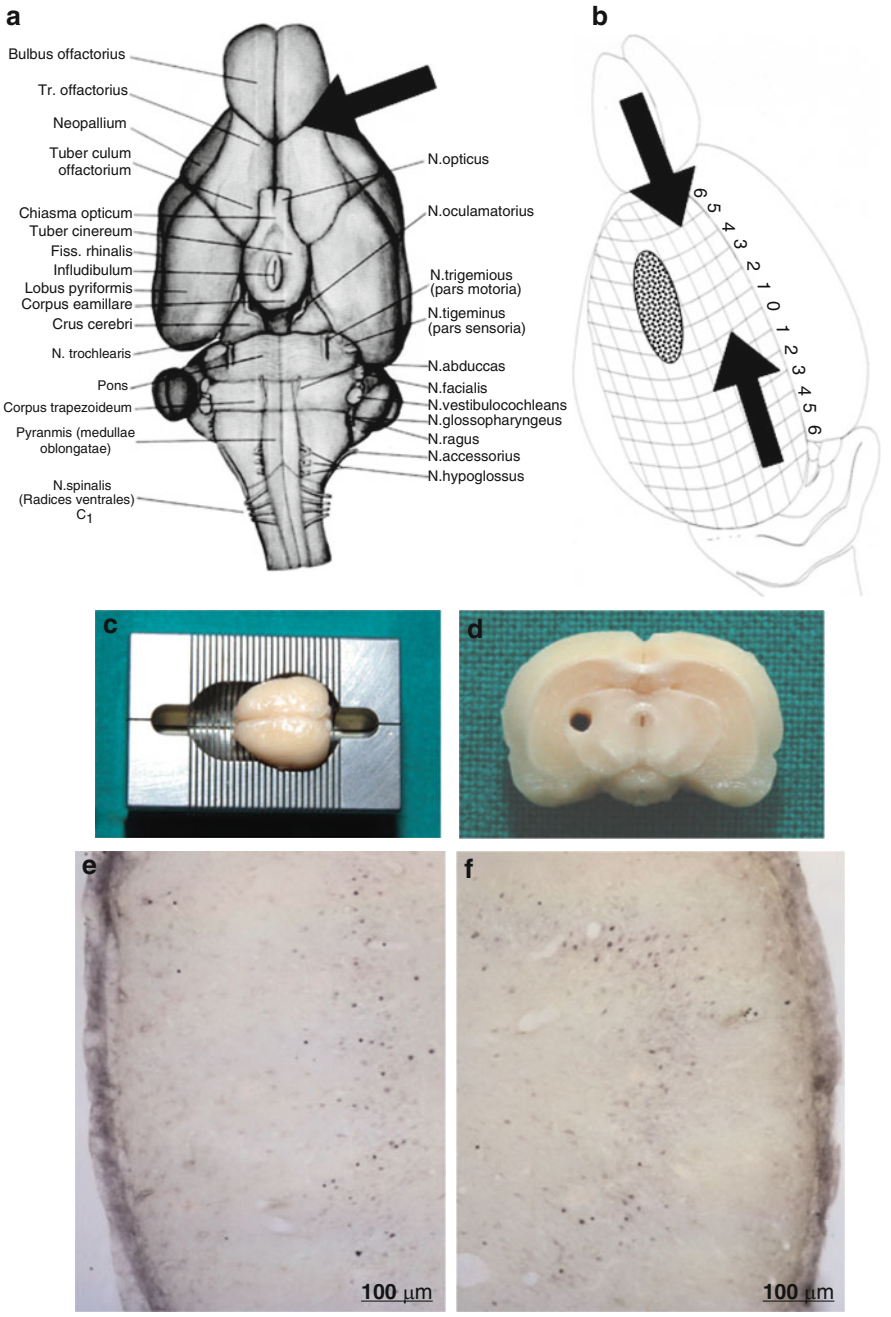

Fig. 2.17 (**a**–**f**) Quantification of cortical tongue muscle representation volume. (**a**) Ventral aspect of the rat cerebrum with depicted rostral borderline of the brain slice, i.e., the rhinal

0.12 ± 0.05 mm^3; $p > 0.05$). Furthermore, compared with intact rats, values did not differ following MS or in the nonstimulated animals.

2.2.7 Manual Stimulation of Forearm Muscles Did Not Improve Recovery of Motor Function After Injury to a Mixed Peripheral Nerve

It has been recently shown that brief manual stimulation of the whisker pad muscles restored normal whisking function by re-instating monoinnervation of the motor endplates rather than by reducing sprouting at the injury site or restoring myotopy (Angelov et al. 2007; Guntinas-Lichius et al. 2007). Given the effectiveness of manual stimulation following transection and re-anastomosis of a purely motor nerve, we asked to what extent this treatment would influence the outcome after injury to a mixed motor and sensory nerve, namely the median nerve in rats.

2.2.7.1 Animal Groups and Overview of Experiments

Forty-eight rats were divided into four groups (1–4) each consisting of 12 animals (Table 2.22).

Group 1 consisted of 12 intact animals. All rats in groups 2–4 were subjected to unilateral transection and suture of the right median nerve (medianus–medianus anastomosis (MMA)). Animals in group 2 received no postoperative treatment. Animals in group 3 were subjected to manual stimulation (MS) of the forearm whereby the skin and muscles were gently stroked for 5 min a day for 3 months. The protocol was aimed at manually stimulating the muscles within the antebrachium which contains the flexors of the fingers and which are responsible for grip strength (see below III. Surgery). We thus limited MS to the forearm and did not stimulate the skin on the palmar side of the paw which receives primarily sensory innervation from the median nerve (Greene 1955). To control for handling effects, animals in group 4 were only held in hand by the experimentator for 5 min in each session (handling paradigm).

Fig. 2.17 (continued) fissure (bregma 5.0 mm). (**b**) Schematic drawing of the rat brain indicating the dimensions of the slice containing the tongue motor area. The entire brain was placed in a rat brain matrix (RBMS-300C, World Precision Instruments) (**c**) which allowed cutting of identical slices through the telencephalon of all animals. A demarcation of the side contralateral to HHA (*left*) was made using a canule perforation in the caudoputamen (**d**). The cortical representation of the suprahyoid–sublingual region (intact or reinnervated) is in the anterior-lateral neocortex TM1 of both cerebral hemispheres (**e**, **f**) as identified by c-Fos immunoreactive neurons (with nuclear localization of the DAB-HRP immunoreaction product) 1 h after transection of the right hypoglossal nerve. The portions containing reactive cortical motoneurons were delineated, their areas calculated, and the volume determined according to the Cavalieri principle. Adopted from Evgenieva et al. (2008)

Table 2.22 Experimental design chart depicting animal grouping and procedures

Group of animals	Restoration of grasping force	Degree of collateral axonal branching as estimated by double retrograde labeling	Pattern of reinnervation of the motor endplates in the flexor digitorum profundus muscle
1. Intact animals	12	6	6
2. Rats with MMA-only	12	6	6
3. Rats with MMA + MS	12	6	6
4. Rats with MMA + handling	12	6	6

Animal grouping and procedures, e.g., medianus–medianus anastomosis (MMA), with or without manual mechanical stimulation of the forearm muscles (MS). All animals were subjected to measurement of the grasping force. Thereafter, one half were used for estimation the degree of collateral axonal branching and the other half for establishing the pattern of the motor endplates reinnervation

All animals were used to determine grip force, a standard procedure for estimating motor function of forearm and hand flexors (Bertelli and Mira 1995). Thereafter, half the animals ($n = 6$) were used to establish the degree of collateral axonal branching by means of double retrograde neuronal labeling (see below). The remaining six rats in each group were used to determine the proportion of monoinnervated and polyinnervated motor endplates in the forearm *(m. flexor digitorum sublimis)* using immunocytochemistry for neuronal class III β-tubulin and histochemistry with alpha-bungarotoxin (see below).

2.2.7.2

Anatomy

The rat median nerve runs together with the axillary artery and the radial (musculospiral) nerve to the brachium. At this point, it does not branch, but in the hollow of the elbow two branches arise, one medial and one lateral. The medial branch supplies the *m. flexor digitorum sublimis* and the *m. palmaris longus*; the lateral branch innervates the *m. flexor digitorum profundus* and the *m. pronator quadratus*. Continuing through the antebrachium, the medial branch divides just above the transverse carpal ligament into three common volar digital nerves to the first, second, and third interdigital spaces. Each of these divides into two proper volar digital nerves to the adjacent sides of the first and second, second and third, and third and fourth digits (Greene 1935).

2.2.7.3

Surgery

The right median nerve was exposed in the brachium and transected proximal to its bifurcation into lateral and medial branches (Fig. 2.18a). End-to-end suture (MMA) was performed immediately.

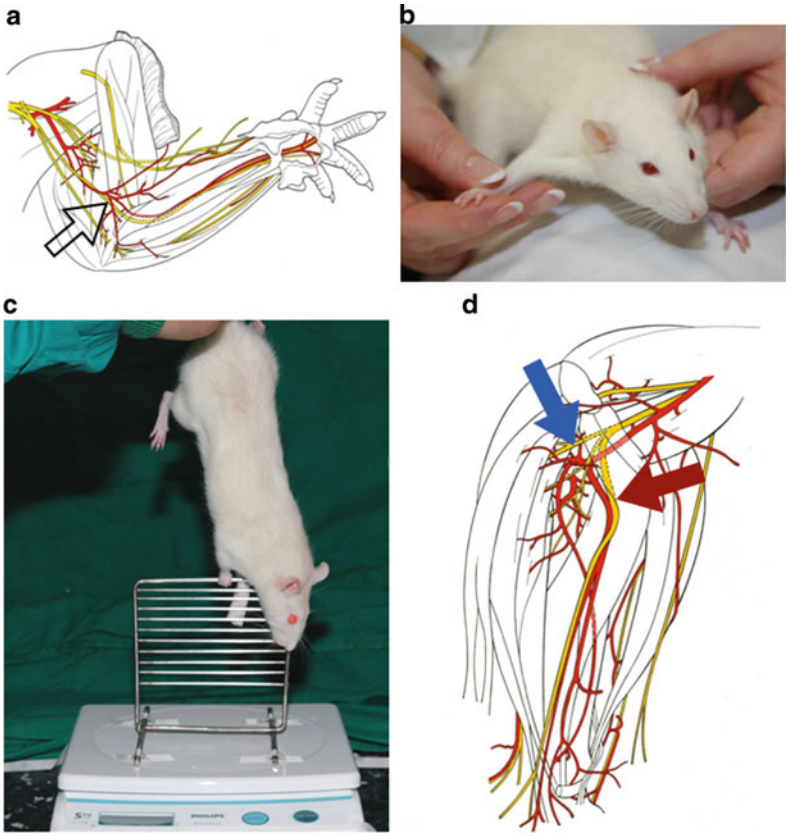

Fig. 2.18 (**a**) Schematic drawing of the rat median nerve. *Arrow* points at the site of transection and suture. (**b**) Manual mechanical stimulation of the forearm flexor muscles. (**c**) Measuring the grip force by means of a wire grid taped onto an electronic balance. (**d**) Schematic drawing of the rat median nerve to depict the retrograde neuronal labeling with two fluorescent dyes. The *blue arrow* points at the medial branch that was transected and instilled with crystals of FB and the *red arrow* at the lateral branch of the median nerve (transected and labeled with crystals of FG). Adopted from Sinis et al. (2008)

2.2.7.4

Manual Stimulation of the Forearm Muscles

On the day following surgery, the right forearms of all 12 animals from group 3 were manually stimulated by stroking all anterior forearm muscles (m. palmaris longus, m. flexor digitorum sublimis, m. flexor digitorum profundus, m. pronator quadratus) that lie just under the skin and the very thin fascia antebrachii. This massage was performed for 5 min daily in a very gentle way, a procedure which avoided postoperative rupture of the coaptation (Fig. 2.18b).

2.2.7.5

Restoration of Grip Force as a Sign for Recovery of Function

The grip test was used to assess functional regeneration. The test is based on denervation of the flexor muscle group which results in a loss of finger flexion after injury to the median nerve. After successful regeneration, the ability to flex the digits and grasp (gripping ability) is regained (Bertelli and Mira 1995; Bontioti et al. 2003; Papalia et al. 2003; Blanco et al. 2007). Grip force was measured using a wire grid (8 × 14 cm) taped to an electronic balance. Normally, rats grasp for the grid when held over it by the tail. When the rats are gently lifted by the tail with increasing strength, they will lose their grip when the maximum grip force is exceeded. The corresponding value displayed on the balance reflects the maximum grip force (Fig. 2.18c). Animals were first given the grip test when active finger flexion was observed by the examiner. Each assessment comprised three grasping attempts and the highest value was recorded. The test was performed weekly for 3 months. To avoid grasping via the left (intact) paw, fingers were covered by a piece of adhesive textile tape. Examiners (D. Bösel and D. Felder) were blinded as to treatment group.

Daily observations of the animals revealed no deviations from their normal behavior, gait, or walking patterns. Despite paresis of the right forepaw finger flexors, rats were able to stand and feed normally.

Daily MS of the forearm muscles 5 min a day for 3 months did not improve recovery of grip function after MMA. Throughout the entire postoperative period, the grip force following MS was not significantly higher compared with nonstimulated animals or to rats subjected only to "handling" (Table 2.23; mean ± SD, $n = 12$, Mann–Whitney test).

2.2.7.6

Estimation of Axonal Branching by Double Retrograde Labeling

Six rats from each group were used to determine the degree of collateral axonal branching at the lesion site (MMA). Under Rompun/Ketanest anesthesia, the right median nerve was re-exposed distally to the suture site. The medial and lateral branches were transected and instilled with crystals of the retrograde fluorescent dyes Fast Blue and DiI, respectively (Fig. 2.18d). Crystals were left in situ for 30 min after which the application sites were carefully rinsed, dried, and the wound closed. Ten days later, animals were fixed by perfusion with 4% paraformaldehyde. The spinal cord and the dorsal root ganglia (DRG) C_5 – Th_1 were cut into 50-μm-thick longitudinal sections.

Sections were observed with an epifluorescence microscope (Zeiss Axioskop 50, Oberkochen, Germany) using a custom-made band pass-filter set combination which maximally limits fluorescence crosstalk between the tracers. Separate color images of retrogradely labeled motoneurons and dorsal root ganglion (DRG) cells were visualized through the different filter sets using a CCD

Table 2.23 Time course of restoration of the grasping force in grams

Group of animals	2 weeks after MMA	4 weeks after MMA	6 weeks after MMA	8 weeks after MMA	12 weeks after MMA
1. Intact animals	264 ± 25	289 ± 33	280 ± 37	293 ± 34	320 ± 43
2. Rats with MMA-only	31 ± 16	60 ± 30	100 ± 36	180 ± 63	218 ± 67
3. Rats with MMA + MS	33 ± 11	48 ± 27	80 ± 45	164 ± 27	232 ± 39
4. Rats with MMA + handling	23 ± 9	50 ± 23	105 ± 49	204 ± 50	239 ± 35

All groups consisted of 12 animals. Shown are group mean values ± SD. Mean values of a given "stimulated" group (Nr. 3, 4) were compared (ANOVA and post hoc Tukey's test, $p < 0.05$) with those of the nonstimulated group (Nr. 2). No differences were detected. Values for intact rats are given as reference values and not included in the analysis

Video Camera System described above. All cells stained by FB_{only}, DiI_{only}, as well as all double-labeled (FB + DiI) cells (Fig. 2.20) were identified and manually counted on the computer screen (Dohm et al. 2000). We quantified the degree (index) of axonal branching (sum of the percentages given in the third and fourth column in Tables 2.24 and 2.25). In rats with an intact median nerve trunk that had been subjected only to surgery for tracer application, the index of axonal branching was 0% (Fig. 2.19).

Counts of all perikarya labeled with FB, DiI, and FB + DiI (Figs. 2.19 and 2.20) were undertaken using the fractionator principle (Gundersen 1986) examining every third section through the spinal cord and spinal ganglion. Details have been described previously (Neiss et al. 1992; see also Valero-Cabre et al. 2004). Counting was performed blindly with respect to treatment.

In intact rats, application of crystals of the fluorescent tracer DiI to the lateral branch of the median nerve (supplying the *flexor digitorum profundus* and *pronator quadratus*) retrogradely labeled 889 ± 61 DRG cells (Fig. 2.19a) and 665 ± 42 motoneurons (mean ± SD; $n = 6$) in the ventral horn of the spinal cord (Fig. 2.19d; Tables 2.24 and 2.25).

Likewise, application of the retrograde fluorescent dye Fast Blue to the medial branch (supplying *flexor digitorum sublimis* and *palmaris longus*) retrogradely labeled 542 ± 93 DRG cells (Fig. 2.19b) and 397 ± 55 motoneurons (Fig. 2.19e; Tables 2.24 and 2.25). No double-labeled neuronal somata were observed either in the DRG (Fig. 2.19c) or in the ventral horn of the spinal cord (Fig. 2.19f). Thus, the index of collateral axonal branching for both sensory and motor neurons was 0%.

Neither MS nor handling changed the degree of postoperative collateral axonal branching. After MMA, double-labeled (DiI + FB) neurons were seen, regardless of the postoperative treatments (Fig. 2.20c, f). In nonstimulated rats (group 2), there were 174 ± 57 (12%) double-labeled DRG cells and 143 ± 21 (16%) motoneurons. A similar index of collateral axonal branching (12–20%) was observed following MS (group 3) or handling (group 4) (Tables 2.24 and 2.25).

Table 2.24 Peripheral projection pattern of sensory (DRG) neurons after median nerve reconstruction and subsequent treatment

Group of animals	Neurons projecting only through the lateral branch (DiI-only)	Neurons projecting only through the medial branch (FB-only)	Neurons projecting through the lateral and medial branches (DiI + FB)	All labeled neurons projecting through the median nerve (DiI, FB, DiI + FB)
1. Intact animals	889 ± 61	542 ± 93	0 0%	1,431 ± 102 100%
2. Rats with MMA-only	613 ± 180	642 ± 121	174 ± 57 12%	1,428 ± 288 100%
3. Rats with MMA + MS	649 ± 229	606 ± 246	254 ± 115 17%	1,509 ± 452 100%
4. Rats with MMA + handling	844 ± 158	591 ± 184	262 ± 57 15%	1,696 ± 217 100%

Number of pseudounipolar neurons (dorsal root ganglion cells) with peripheral processes in the lateral or medial branches of the median nerve in *intact* animals and in rats that received no postoperative treatment (*MMA only*). The animals from the third group were subjected to daily manual mechanical stimulation of the forearm muscles (*MMA + MS*) and those from the fourth group received daily "handling" (*MMA + handling*). The animals were studied 10 days after double retrograde labeling performed 3 months post-surgery. The percentage values below the absolute numbers in column 4 indicate the portions of neurons (DiI + FB) projecting through the median nerve with branched peripheral processes. All groups consisted of six animals. Shown are group mean values ± SD. Mean values of a given "stimulated" group (Nr. 3, 4) were compared (ANOVA and post hoc Tukey's test, $p < 0.05$) to those of the nonstimulated group (Nr. 2). No differences were detected. Values for intact rats are given as reference values and not included in the analysis

2.2.7.7

Measurement of Motoneuron Soma Sizes

Measurement of motoneuron soma sizes was performed as already described. Three months after transection and suture of the right median nerve and 10 days after surgery for retrograde labeling, back-labeled motoneuron perikarya in manually stimulated rats were not significantly larger than in nonstimulated animals subjected to handling only (576 ± 46 μm^2 vs. 586 ± 34 μm^2, group mean values from individual animal mean values, $p > 0.05$, *t* test). This conclusion was further verified by analysis of the frequency distributions in the two population samples (Fig. 2.21).

2.2.7.8

Analysis of Target Muscle Reinnervation

The ratio between monoinnervated versus polyinnervated motor endplates was calculated as described previously. We selected the superficial head of the *m.*

Table 2.25 Projection pattern of motoneurons after median nerve reconstruction and subsequent treatment

Group of animals	Neurons projecting only through the lateral branch (DiI-only)	Neurons projecting only through the medial branch (FB-only)	Neurons projecting through the lateral and medial branches (DiI + FB)	All labeled neurons projecting through the median nerve (DiI, FB, DiI + FB)
1. Intact animals	665 ± 42	397 ± 55	0 0%	1,062 ± 58 100%
2. Rats with MMA-only	328 ± 68	396 ± 131	143 ± 21 16%	866 ± 165 100%
3. Rats with MMA + MS	302 ± 104	434 ± 105	185 ± 34 20%	921 ± 163 100%
4. Rats with MMA + handling	302 ± 111	409 ± 69	170 ± 56 19%	881 ± 199 100%

Number of motoneuronal perikarya projecting through the lateral or medial branches of the median nerve in *intact* animals and in rats that received no postoperative treatment (*MMA-only*). The animals from the third group were subjected to daily manual mechanical stimulation of the forearm muscles (*MMA + MS*) and those from the fourth group received daily "handling" (*MMA + handling*). The animals were studied 10 days after double retrograde labeling performed 3 months post-surgery. The percentage values below the absolute numbers in column 4 indicate the portions of neurons (DiI + FB) projecting through the median nerve with branched axons. All groups consisted of six animals. Shown are group mean values ± SD. Mean values of a given "stimulated" group (Nr. 3, 4) were compared (ANOVA and post hoc Tukey's test, $p < 0.05$) with those of the nonstimulated group (Nr. 2). No differences were detected. Values for intact rats are given as reference values and not included in the analysis

flexor digitorum sublimis (FDS) muscle because of its easy identification and reliable dissection.

The overall number of motor endplates in the *flexor digitorum profundus* muscle did not differ between the groups (Table 2.26). The proportion of polyinnervated endplates (Fig. 2.2c, e) also did not differ between groups being 10 ± 2% in nonstimulated rats (group 2), 14 ± 4% following MS (group 3) (MS), and 13 ± 8% following handling (group 4).

2.2.8

Manually Stimulated Recovery of Motor Function After Facial Nerve Repair Requires Intact Sensory Input

Both clinical and experimental data show that recovery of function is better following damage of a purely motor nerve compared with mixed peripheral nerves possessing both motor and sensory axons such as the median nerve (Mackinnon et al. 1985; Terzis and Papakonstantinou 2000; Bontioti et al. 2005; Sinis et al. 2005; Kelly et al. 2007). Nerve supply to facial muscles has the distinct advantage

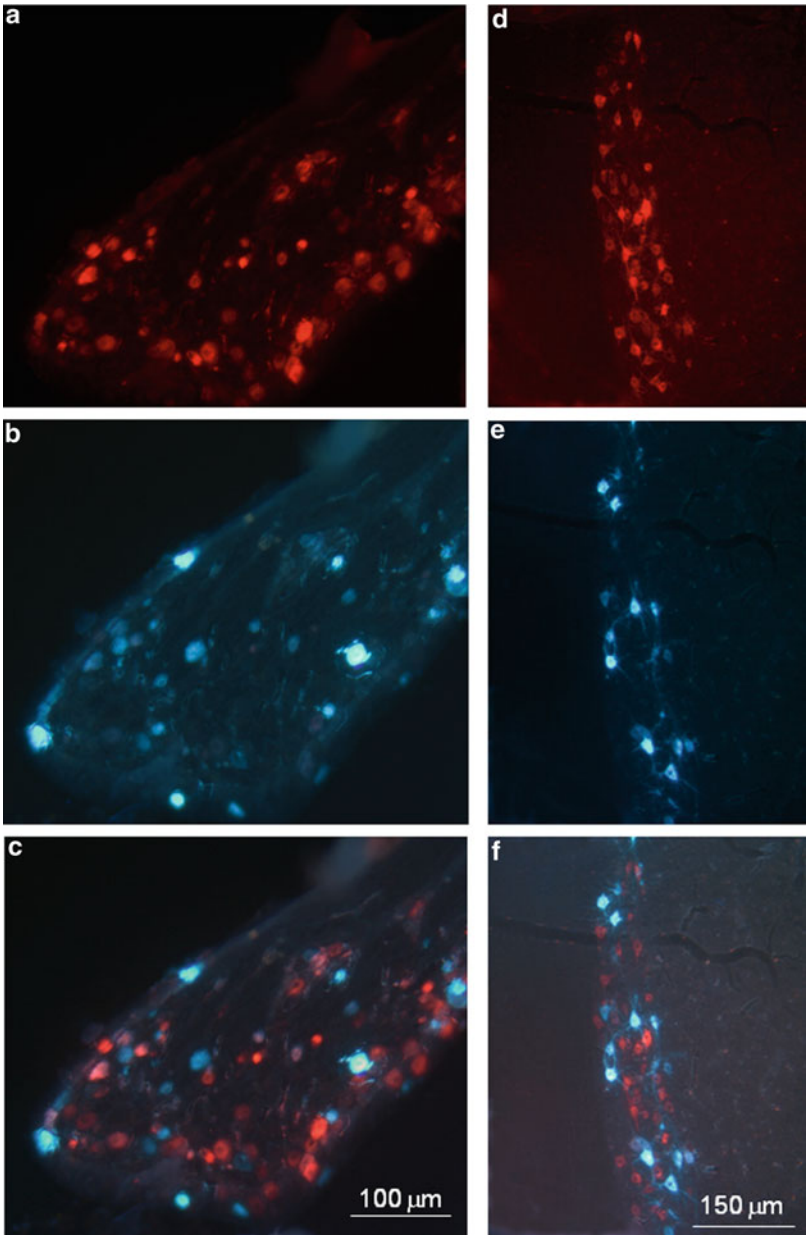

Fig. 2.19 (**a**–**f**) Representative cryosection from an intact rat. Application of DiI and FB to the transected lateral and medial branches labeled perikarya, which were localized in the DRG (**a**, **b**) and in the ventral column of the spinal cord (**d**, **f**). No double-labeled perikarya were observed (**c**, **F**), i.e., the degree of axonal branching was 0%. Adopted from Sinis et al. (2008)

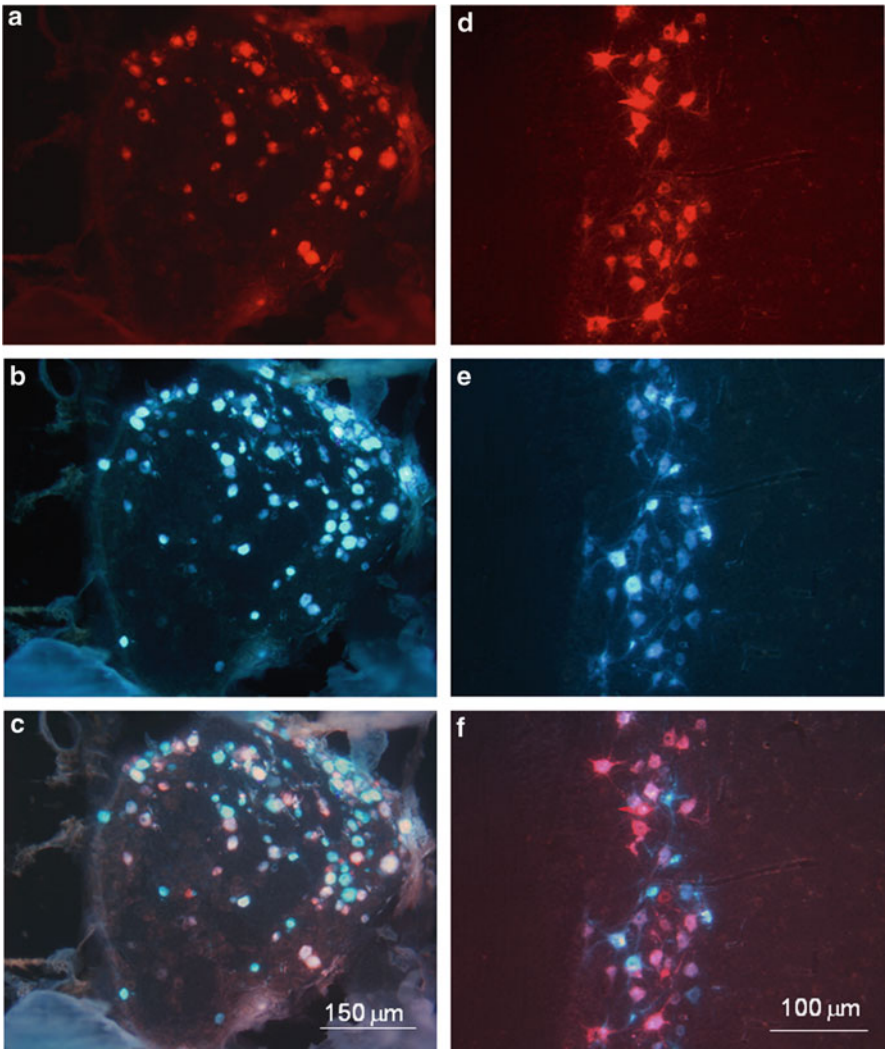

Fig. 2.20 (**a, f**) Representative cryosection from an operated rat. Application of DiI and FB to the transected lateral and medial branches labeled perikarya, which were localized in the DRG (**a**, **b**) and in the ventral column of the spinal cord (**d**, **f**). Numerous double-labeled perikarya were observed (**c**, **f**), i.e., the degree of axonal branching was 12–20%. Adopted from Sinis et al. (2008)

that the motor and sensory supplies are separate (Moller and Jannetta 1986; Valls-Sole and Tolosa 1989). In the case of the facial nerve, sensory feed back occurs via the trigeminal nerve with direct ipsilateral connections between the trigeminal and the facial nucleus in the brainstem (Kimura and Lyon 1972; Erzurumlu and

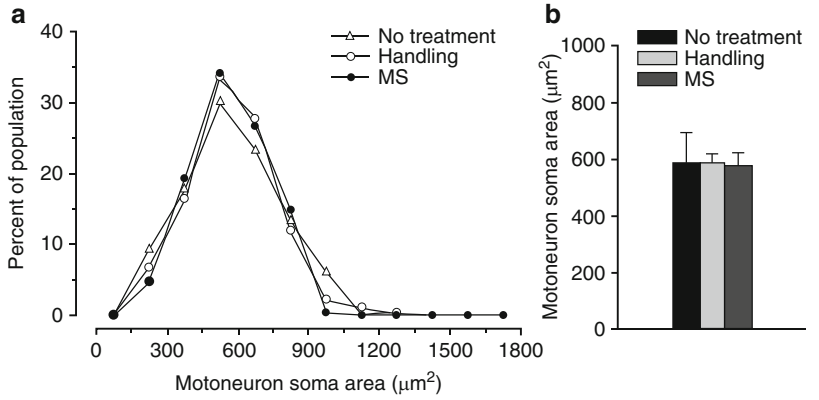

Fig. 2.21 (**a**, **b**) Motoneuron soma size. (**a**) Normalized frequency distributions of soma areas of back-labeled motoneurons in rats subjected to retrograde labeling only ("No treatment") or to retrograde labeling 3 months after nerve repair and handling only ("Handling") or nerve repair and manual stimulation ("MS"). The distribution in the "MS" group does not differ from those in the other two groups ($p < 0.001$, Kolmogorov–Smirnov test). (**b**) Group mean values + SEM of soma areas of the motoneurons shown in **a**. No significant differences between MS and the other two groups ($p < 0.05$, ANOVA with Tukey's post hoc test). Adopted from Sinis et al. (2008)

Table 2.26 Quality of target muscle reinnervation after median nerve reconstruction and subsequent treatment

Group of animals	Monoinnervated motor endplates (%)	Polyinnervated motor endplates (%)	Noninnervated motor endplates (%)	Total number of motor endplates examined
1. Intact animals	100 ± 0	0	0	5,433 ± 1,032
2. Rats with MMA-only	80 ± 10	10 ± 2	5 ± 2	5,962 ± 1,326
3. Rats with MMA + MS	79 ± 13	14 ± 4	7 ± 3	4,865 ± 1,088
4. Rats with MMA + handling	81 ± 11	13 ± 8	6 ± 1	5,362 ± 635

Reinnervation pattern of the flexor digitorum profundus (FDP) motor endplates in intact rats (*Intact*) and in rats that received no postoperative treatment (*MMA-only*). The animals from the third group were subjected to daily manual mechanical stimulation (MS) of the forearm muscles (*MMA + MS*) and those from the fourth group received daily "handling" (*MMA + handling*). Motor endplates were classified as monoinnervated, polyinnervated, or noninnervated according to the number of beta-tubulin-immunoreactive axons that crossed the boundaries of the endplate. All groups consisted of six animals. Shown are group mean values ± SD. Mean values of a given "stimulated" group (Nr. 3, 4) were compared (ANOVA and post hoc Tukey's test, $p < 0.05$) with those of the nonstimulated group (Nr. 2). No differences were detected. Values for intact rats are given as reference values and not included in the analysis

Killackey 1979; Stennert and Limberg 1982; Hinrichsen and Watson 1983; Travers and Norgren 1983; Isokawa-Akesson and Komisaruk 1987; Sharp et al. 1988). We took a two-step approach to examine the role of afferent

inputs. First, we estimated, using synaptophysin immunohistochemistry, the influence of manual stimulation on the afferent synaptic input to the facial nucleus. In addition, we tested the influence of the trigeminal sensory input by extirpating one of its branches, the infraorbital nerve (ION). The procedure ablates sensory input from the vibrissal muscle pads to facial motoneurons.

2.2.8.1

Animal Groups and Overview of Experiments

Seventy-eight rats were used in two studies (A, B; Table 2.27)

Study A: To examine synaptic input to facial motorneurons, we used three groups of rats ($n = 6$ in each), namely intact animals, rats with FFA (FFA only), and rats with FFA plus MS (FFA + MS).

Study B: To examine the role of trigeminal afferents (ION) which provide exclusive sensory innervation to the vibrissal muscles (Jacquin et al. 1993; Munger and Renehan 1989; Rice et al. 1993), we used five groups namely intact rats, those with FFA (FFA only), FFA plus MS (FFA + MS), FFA plus excision of the ipsilateral infraorbital nerve (IONex) (FAA + IONex), and those with FFA plus IONex but followed by MS (FFA + IONex + MS). Vibrissal motor performance and the pattern of motor endplate reinnervation were studied at 2 months. Data for animals receiving MS were compared with those lacking MS. Data for intact animals, those with FFA and those with FFA + MS, have been published previously (Angelov et al. 2007).

Table 2.27 Experimental design chart depicting animal grouping, procedures, and investigation mode

Surgery	Motion analysis of vibrissae whisking	Pattern of NMJ reinnervation	Synaptic input to facial motorneurons
Study A			
1. Intact			6
2. FFA only			6
3. FFA + MS			6
Study B			
1. Intact rats[a]	16	8	
2. FFA-only[a]	16	8	
3. FFA + MS[a]	16	8	
4. FFA + IONex	6	6	
5. FFA + IONex + MS	6	6	

Animal grouping, procedures, and investigation mode, e.g., facial–facial anastomosis (FFA), excision of the ipsilateral infraorbital nerve (IONex), manual stimulation of the vibrissal muscles (MS), video-based motion analysis (VBMA), pattern of reinnervation of the neuro-muscular junctions (NMJ), estimation of the synaptic covering of the facial motoneurons after quantitative immunocytochemistry for synaptophysin

[a]Data adopted from Angelov et al., Neurobiol Disease (2007)

2.2.8.2

Surgery

Transection and end-to-end suture of the right facial nerve (FFA) were performed as described. Excision of the ipsilateral ION was performed after FFA. While under ketamin/xylazin narcosis, the ipsilateral ION was transected at its exit from the infraorbital foramen (Fig. 2.4a, b) and all its peripheral fascicles were removed.

2.2.8.3

Manual Stimulation (MS) of Vibrissal Muscles and Analysis of Vibrissae Motor Performance

Manual stimulation (MS) of vibrissal muscles and analysis of vibrissae motor performance were performed as described. Following *FFA alone*, recovery was poor. Although whisking frequency was similar compared with intact animals, both amplitude and angular velocity during protraction were reduced, respectively, to approximately 40% and 15% of values in intact animals (Table 2.28).

However, *MS after FFA* restored the amplitude of vibrissal whisking from 19° ± 6° to 51° ± 19°, that is, within the range for intact animals (Angelov et al. 2007).

By contrast, MS failed to restore vibrissal function in animals which had facial nerve injury, as well as elimination of sensory input *(FFA±IONex±MS)*. Indeed, MS led to a worsening of function with a reduction of whisking amplitude in animals that received MS (FFA + IONex + MS: 14° ± 5.5°) compared with those that did not (FFA + IONex: 22° ± 3.4°; Table 2.28).

Table 2.28 Motor recovery after facial nerve reconstruction and subsequent treatment

Group of animals	Frequency (in Hz)	Angle at maximal protraction (in degrees)	Amplitude (in degrees)	Angular velocity during protraction (in degrees/s)
1. Intact rats[a]	7.0 ± 0.8	62 ± 13	57 ± 13	1,238 ± 503
2. FFA-only[a]	6.3 ± 0.5	91 ± 12*	19 ± 6.0*	135 ± 54*
3. FFA + MS[a]	6.6 ± 0.5	66 ± 15*	51 ± 19*	1,019 ± 408*
4. FFA + IONex	6.0 ± 0.8	76 ± 10	22 ± 3.4	469 ± 400
5. FFA + IONex + MS	6.0 ± 1.2	87 ± 18	14 ± 5.5**	148 ± 68**

Biometrics of vibrissae motor performance in intact animals, in rats that received no postoperative treatment (FFA-only) and in animals that were subjected to FFA plus excision of the ipsilateral infraorbital nerve (FFA + IONex). Groups FFA + MS and FFA + IONex + MS received daily manual stimulation (MS) of the vibrissal muscles. The first three groups consisted of 16 animals and the last two groups of six rats. Shown are group mean values ± SD. Mean values of a given "stimulated" group that were significantly different (ANOVA and post hoc Tukey's test, $p < 0.05$) from the respective nonstimulated group are indicated by * and **. Values for intact rats are given as reference values and not included in the analysis

[a]Data adopted from Angelov et al. (2007)

2.2.8.4

Determining the Synaptic Input to the Facial Motoneurons

Determining the synaptic input to the facial motoneurons was performed as already described. To assess the synaptic input to the facial nucleus in intact rats and rats subjected to FFA with or without subsequent MS (Table 2.27), we

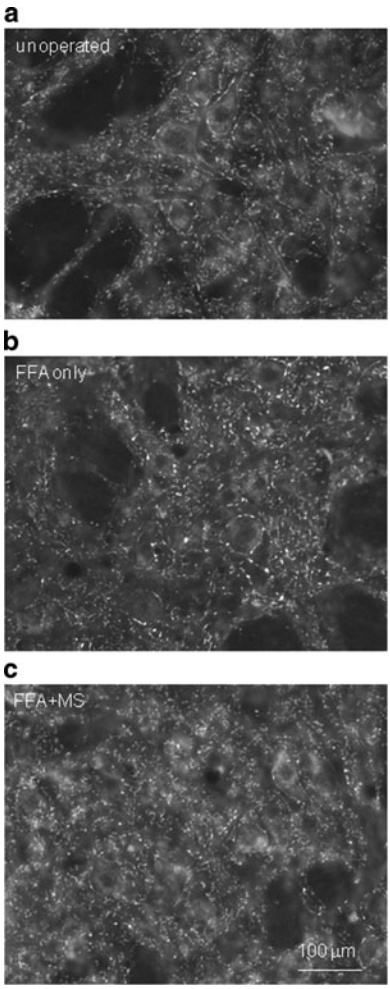

Fig. 2.22 (**a**–**c**) Immunostaining for synaptophysin in 30-µm-thick vibratome sections from the facial nucleus in intact rats (**a**), in rats 2 months after facial–facial anastomosis and no further treatment (FFA-only; **b**), and in rats which received MS of the vibrissal muscles after FFA (FFA + MS; **c**). Note the clearly discernible numerous puncta within the neuropil and around motoneuronal cell bodies in the facial nucleus representing synaptic terminals. Adopted from Pavlov et al. (2008)

quantified levels of synaptophysin according to Calhoun et al. (1996) and Marques et al. (2006). Images were obtained on an epi-fluorescence microscope from sections stained with a highly diluted (1:4,000) anti-synaptophysin antibody. This protocol allowed us to obtain photo images in which, comparable with thin confocal optical sections, numerous puncta within the neuropil and around motoneuronal cell bodies in the facial nucleus were clearly discernible (Fig. 2.22).

Analyses of the frequency distributions of pixel intensities revealed no differences among the three groups (data not shown) indicating similar overall intensities of the immunofluorescence staining. The background intensities were identical from image to image around a pixel gray value of 30. Therefore, we used the total number of pixels per frame within the range (gray values 30–129) as an estimate of axon terminal density.

In animals with FFA and no MS, the mean total number of pixels was significantly lower compared with intact animals ($29.2 \times 10^6 \pm 1.8 \times 10^6$ vs. $34.3 \times 10^6 \pm 2.3 \times 10^6$; $p = 0.036$, ANOVA with Bonferroni post hoc test). In animals receiving MS after FFA, the mean pixel number was similar to intact animals ($33 \times 10^6 \pm 2.6 \times 10^6$) but higher than in the control FFA group ($p = 0.007$). These results indicate that the synaptic input after FFA alone is reduced compared with normal and this loss is counteracted by MS.

2.2.8.5

Quality of Target Muscle Reinnervation

Quality of target muscle reinnervation was evaluated in m. levator labii superioris, an extrinsic vibrissal muscle which, like the intrinsic vibrissal muscles, is

Table 2.29 Quality of target muscle reinnervation after facial nerve injury and trigeminal depletion

Group of animals	Monoinnervated motor endplates (percent)	Polyinnervated motor endplates (percent)	Noninnervated motor endplates (percent)	Total number of motor endplates examined
1. Intact rats[#]	100 ± 0	0	0	1543 ± 132
2. FFA only[#]	45 ± 9.6	53 ± 10	2.6 ± 1.8	1326 ± 413
3. FFA + MS[#]	69 ± 7.9*	22 ± 5.1*	9.6 ± 3.9*	1640 ± 338
4. FFA + IONex	51 ± 8.6	43.3 ± 9.4	5.7 ± 2.8	1495 ± 435
5. FFA + IONex + MS	41 ± 6.1	50.7 ± 10	8.3 ± 3.6	1579 ± 443

Innervation pattern of the m. levator labii superioris (LLS) motor-endplates in intact animals, in rats that received no postoperative treatment (FFA-only) and in animals that were subjected to FFA plus excisiion of the ipsilateral infraorbital nerve (FFA + IONex). Groups FFA + MS and FFA + IONex + MS received daily manual stimulation (MS) of the vibrissal muscles. The first three groups consisted of eight animals and the last two groups of six rats. Shown are group mean values ± SD. Mean values of a given "stimulated" group that were significantly different (ANOVA and post hoc Tukey's test, $p < 0.05$) from the respective nonstimulated group are indicated by *. Values for intact rats are given as reference values and not included in the analysis

[#]Data adopted from Angelov et al. (2007)

innervated by six longitudinal branches of the buccal branch of the facial nerve (the short common trunk of the fused ramus buccolabialis superior and ramus buccolabialis inferior; Dörfl 1985). There are no proprioceptors in the mystacial musculature (Stal et al. 1987, 1990; Welt and Abbs 1990; Rice et al. 1997; McComas 1998; Whitehead et al. 2005).

Qualitative examination revealed two major features of the m. levator labii superioris. Compared with rats that received FFA + MS, the incidence of intramuscular axonal branches was higher and diameters of muscle fibers were smaller in rats with FFA only, FFA + IONex, as well as FFA + IONex + MS.

Our qualitative observations were matched by quantitative assessments of vibrissal function and the degree of polyinnervation. Thus, rats with FFA, FFA + IONex, and FFA + IONex + MS consistently had poor function and a high percentage of polyinnervated endplates (53 $\pm$ 10%, 43 $\pm$ 9.4% and 51 $\pm$ 10% respectively; Table 2.29). By contrast, rats with FFA + MS had normal vibrissal function and the degree of polyinnervation endplates was significantly smaller (22 $\pm$ 5%).

http://www.springer.com/978-3-642-18119-1

Physical Rehabilitation of Paralysed Facial Muscles:
Functional and Morphological Correlates
Angelov, D.N.
2011, XII, 144 p. 22 illus., 14 illus. in color., Softcover
ISBN: 978-3-642-18119-1